FBC DETAILED FLOOD MAPPING STUDY

Frequency-Magnitude Relationship for the Coldwater River

DRAFT
May 20, 2022

BGC Project No.:
0511009.05.04

Prepared by BGC Engineering Inc. for:
Fraser Basin Council

BGC ENGINEERING INC.
AN APPLIED EARTH SCIENCES COMPANY
Suite 500 - 980 Howe Street
Vancouver, BC Canada V6Z 0C8
Telephone (604) 684-5900
Fax (604) 684-5909

May 20, 2022
Project No.: 0511009.05.04

Terry Robert, M.Ed.
Director, Interior Regional Programs
Fraser Basin Council
200A – 1383 McGill Road
Kamloops, BC V2C 6K7

Dear Mr. Robert,

Re: Frequency-Magnitude Relationship for the Coldwater River - Draft

Please find attached the above referenced report. Should you have any further questions, please do not hesitate to contact the undersigned. We appreciate the opportunity to collaborate with you on this challenging and interesting study.

Yours sincerely,

BGC ENGINEERING INC.
per:

Kris Holm, M.Sc., P.Geo.
Principal Geoscientist

EXECUTIVE SUMMARY

Landfalling of an atmospheric river (AR) brought two days of intense rainfall to southwestern British Columbia (BC) on November 14, 2021. This rainfall resulted in extreme streamflow on November 15, 2021 and extensive flooding and river planform changes in watersheds across numerous rivers in the lower Fraser River watershed, including the Coldwater River at Merritt. Numerous infrastructures, notably roads and bridges were destroyed or inoperable. This destruction led to a near complete isolation of the Lower Mainland from road and rail access.

ARs are long, conveyor belts of warm, moist air typically during the late fall and early winter. AR-related floods are typically larger than non-AR-related floods in coastal watersheds in BC. During the November 14, 2021 AR, the streamflow generated by rainfall was augmented by melting snow, associated with a rapid rise in temperature.

Following the November 15, 2021 flood, an urgent need emerged to estimate the peak flow of the Coldwater River to inform long-term reconstruction and mitigation efforts. The flood event was recorded at the *Coldwater River at Brookmere* (08LG048) (upstream) and *Coldwater River at Merritt* (08LG010) (downstream) hydrometric stations, which are both maintained by the Water Survey of Canada (WSC). However, the event estimates recorded at these stations were deemed unreliable by the Water Survey of Canada (WSC).

In support of ongoing programs and recovery from November 15, 2021 flood, BGC Engineering Inc. (BGC) was retained by several interested parties to complete hydrotechnical hazard and risk assessments and flood hazard mapping in the Coldwater River and Nicola River watersheds. To support this effort, BGC has estimated the magnitude of the November 15, 2021 flood to be 400 m^3/s (independent of ongoing WSC efforts) based on a two-dimensional (2D) HEC-RAS (version 6.2) model. The work was completed for Fraser Basin Council (FBC) on behalf of the Town of Merritt (BGC, June 4, 2021) using pre-event terrain (GeoBC) and high-water marks (HWMs) collected by Ecoscape Environmental Consultants Ltd (Ecoscape), FLNRORD, and BGC Engineering Inc. (BGC).

BGC subsequently developed an updated (post-flood) flood frequency-magnitude relationship for the Coldwater River at Merritt by combining models for AR-related and snowmelt-related peak flows. The frequency analysis was based on the maximum value for each of the snowmelt- and AR-related peak flows by splitting the year (January to December) in half forming the Dual Maximum Series (DMS). Various statistical distribution were compared given the uncertainty in the return period (% AEP) of large magnitude events. An ensemble of the three distributions was selected to span the range of tail behaviours of the AR-related peak flows (Generalised Extreme Value [GEV], the Log Normal, and the Pearson Type III). BGC's current best estimate of the 200-year (0.5% AEP) flood event is 445 m^3/s (90% confidence interval 240 m^3/s to 980 m^3/s).

For comparison, a frequency-magnitude relationship based on a standard approach to frequency analysis using the Annual Maximum Series (AMS) and including the November 15, 2021 flood results in a 200-year (0.5% AEP) of 295 m^3/s (160 m^3/s to 550 m^3/s for the 90% confidence interval). The 200-year (0.5% AEP) based on the combined model lies within the confidence interval of the standard approach. The 200-year (0.5% AEP) based on the combined approach excluding the November 15, 2021 flood and ignoring the effects of climate change is 325 m^3/s.

To account for climate change, the peak flow distributions (AR-related and snowmelt-related) in the Coldwater River were scaled to account for the trends in rainfall-related (AR and non-AR) and snowmelt-related peak flows as projected by PCIC's six Global Circulation Models (GCM)-run Variable Infiltration Capacity (VIC-GL) hydrological model simulations (based on Coupled Model Intercomparison Project 5 [CMIP5] models) at the *Coquihalla River above Alexander Creek* (08MF068). The climate-adjusted 200-year (0.5% AEP) flood event was estimated to be 730 m^3/s (400 m^3/s to 1600 m^3/s for the 90% confidence interval). This corresponds to a 64% increase compared to the stationary case (445 m^3/s).

The primary objective of this work was to provide a baseline estimate of the frequency-magnitude relationship for the Coldwater River at Merritt. The analysis is based on current data and methods. The frequency-magnitude relationship is summarized in Table ES-1 over a range of return periods (% AEPs).

Table ES-1. Comparison of frequency-magnitude relationships over a range of return periods (%AEPs) in the Coldwater River at Merritt, BC, including the 90% confidence intervals.

Return Period (%AEP)	Standard Approach[1] with November 15, 2021 (m^3/s)			Combined Approach[2] with November 15, 2021 (m^3/s)			Combined Approach with November 15, 2021, Climate-adjusted[3] (m^3/s)			Combined Approach excluding November 15, 2021 (m^3/s)		
	Estimate	Lower CI	Upper CI	Estimate	Lower CI	Upper CI	Estimate	Lower CI	Upper CI	Estimate	Lower CI	Upper CI
2 (50% AEP)	70	65	75	70	65	75	65[4]	60	75	70	65	75
5 (20% AEP)	95	85	110	90	80	100	115	90	145	90	80	95
10 (10% AEP)	120	100	145	115	95	155	180	130	235	105	90	130
20 (5% AEP)	150	115	200	165	115	230	265	170	370	145	105	185
50 (2% AEP)	195	130	295	245	155	380	400	245	620	205	135	285
100 (1% AEP)	240	150	400	330	195	580	540	320	930	260	170	390
200 (0.5 % AEP)	295	160	545	445	240	980	730	400	1600	325	210	560
500 (0.2 % AEP)	385	185	830	680	315	2190	1110	540	3525	450	265	1060

Notes:

1. The updated (post-event) analysis based on a standard approach to frequency analysis (AMS) assumes the GEV distribution and the maximum likelihood estimate (MLE) method of inference for parameter estimation.
2. The updated (post-event) analysis is based on a combined approach (ensemble of DMS models [GEV, Log Normal, and Pearson Type III]). The MLE was used to estimate the parameters of the GEV and Log Normal distributions. The maximum goodness-of-fit estimates (MGE) method of inference was used instead to fit the Pearson Type III distribution due to convergence issues with the MLE.
3. The rainfall-related (AR and non-AR) and snowmelt-related peak flow distributions in the Coldwater River at Merritt were scaled to account for the trends as projected by PCIC using the six GCM-run VIC-GL model at the *Coquihalla River above Alexander Creek* (08MF068) hydrometric station.
4. The climate-adjusted 2-year (50% AEP) is 65 m^3/s which is lower than the stationary 2-year (50% AEP). This reduction is because the AR-related peak flow distribution that is being scaled every year into the future has 24% of its smallest values as “zero” because AR-related peak flows do not occur every year.

GLOSSARY

Acronym	Definition	Description
ADC	Anderson-Darling Criterion	A statistical test that gives more weight to the tails of distributions.
AEP	Annual Exceedance Probability	Annual probability that a flood of a given magnitude will be exceeded in any one year.
AIC	Akaike Information Criterion	A measure to assess the relative fit of models to data. Based on the log-likelihood with a penalizing term for the number of variables.
AMS	Annual Maximum Series	A data series containing the largest instantaneous flow rates per calendar year.
API	Antecedent Precipitation Index	A running measurement of the wetness of a watershed based on the rainfall that occurred over the previous days.
ASWS	Automated Snow Weather Station	Automated weather monitoring station network in British Columbia.
AR	Atmospheric River	A narrow band of air carrying large amounts of moisture which can result in torrential precipitation, measured by the Integrated Vapour Transport.
BIC	Bayesian Information Criterion	A measure to assess the relative fit of models to data. Based on the log-likelihood with a larger penalizing term (compared to the AIC) for the number of variables.
CaPA	Canadian Precipitation Analysis	A gridded dataset which combines available surface observations with numerical weather predictions to produce estimates of precipitation on a 2.5-km grid at each synoptic hour.
CV	Coefficient of Variation	Statistical parameter measuring the dispersion of data around a mean.
DMS	Dual Maximum Series	A data series containing two instantaneous flow rates per calendar year, the largest flow rate caused by a snowmelt driven flood and an AR-driven flood.
EV1	Gumbel Distribution	Statistical distribution used in the prediction of floods generated by mixed processes.
EV2	Freshet Distribution	Statistical distribution used in the prediction of freshet (snowmelt) floods.
GCM	General Circulation Models	A global circulation model constructed from circulatory air patterns.
GEV	Generalized Extreme Values	Statistical distribution for extreme values from a dataset.
HWM	High Water Mark	Physical marks displaying the maximum water surface elevation during a flood event.

Acronym	Definition	Description
IVT	Integrated Vapour Transfer	Moisture transport in the atmosphere characterized by the vertically integrated horizontal water transport at specific levels.
MAP	Mean Annual Precipitation	Average depth of rainfall that occurs across a watershed each calendar year.
MGE	Maximum Goodness of Fit Estimate	Statistical test to determine distribution parameters. Requires a relatively small sample size for convergence.
MLE	Maximum Likelihood Estimate	Statistical test to determine distribution parameters. Requires a relatively large sample size for convergence.
PCIC	Pacific Climate Impacts Consortium	Climate service centre at the University of Victoria providing climate change data.
RCP	Representative Concentration Pathway	Forecasted climate scenarios based off expected greenhouse gas emissions.
SWE	Snow Water Equivalent	Volume of liquid water contained in a snowpack.
VIC	Variable Infiltration Capacity	Large scale surface water models.
WSC	Water Survey of Canada	Federal authority monitoring and collecting water resource information in Canada.
WSE	Water Surface Elevation	Height of floods in relation to sea level.

TABLE OF CONTENTS

LIST OF TABLES

LIST OF FIGURES

LIST OF APPENDICES

LIST OF DRAWINGS

TABLE OF REVISIONS

ISSUE	DATE	REV	REMARKS
DRAFT	May 20, 2022		Original issue

CREDITS AND ACKNOWLEDGEMENTS

BGC Engineering Inc. (BGC) would like to express gratitude to the Fraser Basin Council (FBC) for its leadership in sharing this work broadly to all stakeholders.

Contributors to this report are listed below including primary authors and reviewers:

- Melissa Hairabedian, M.Sc., P.Geo., Senior Hydrologist
- Patrick Grover, Ph.D., P.Eng., Principal Hydrotechnical Engineer
- Hamish Weatherly, M.Sc., P.Geo., Principal Hydrologist
- Rob Millar, Ph.D., P.Geo., P.Eng., Principal Hydrotechnical Engineer
- Matthias Jakob, P.Geo., P.L. Eng., Principal Geoscientist
- Kenneth Lockwood, Ph.D., EIT, Intermediate Hydrotechnical Engineer
- Kathleen Horita, M.Sc., P.Eng., Intermediate Hydrotechnical Engineer
- Pascal Szeftel, Ph.D., P.Eng., Senior Hydrotechnical Engineer
- Elisa Scordo, M.Sc., P.Geo., Senior Hydrologist
- Kris Holm, M.Sc., P.Geo., Principal Geoscientist

BGC is grateful for the technical guidance and statistical expertise provided by:

- Dr. Vincenzo Coia, Statistician, University of British Columbia, Department of Statistics.

BGC is grateful for the support and input provided by external reviewers including:

- Dr. Tricia Stadnyk, P.Eng., Principal Researcher, HydroS Engineering Ltd.
- Dr. Michael Church, Professor Emeritus, Department of Geography, University of British Columbia.

LIMITATIONS

BGC Engineering Inc. (BGC) prepared this document for the account of Fraser Basin Council (FBC). The material in it reflects the judgment of BGC staff in light of the information available to BGC at the time of document preparation. Any use which a third party makes of this document or any reliance on decisions to be based on it is the responsibility of such third parties. BGC accepts no responsibility for damages, if any, suffered by any third party as a result of decisions made or actions based on this document.

As a mutual protection to our client, the public, and ourselves all documents and drawings are submitted for the confidential information of our client for a specific project. BGC authorizes FBC to disclose this document to government and First Nations authorities and for download via FBC's website. Authorization for any other use and/or publication of this document or any data, statements, conclusions or abstracts from or regarding our documents and drawings, through any form of print or electronic media, including without limitation, posting or reproduction of same on any website, is reserved pending BGC's written approval. A record copy of this document is on file at BGC. That copy takes precedence over any other copy or reproduction of this document.

1.0 INTRODUCTION

On November 14, 2021, landfalling of an atmospheric river (AR) brought two days of intense precipitation to southwestern British Columbia (BC). This precipitation resulted in extreme streamflow and extensive geomorphic change in watersheds across a large spatial extent in the lower Fraser River watershed, including the Coldwater River. This extreme event resulted in landslides, washouts, bank erosion, and avulsions that caused extensive damage to highways (e.g., Highway 5 and Highway 8), railways (e.g., Canadian Pacific), bridges (e.g., Middlesborough bridge in Merritt, BC), and pipeline watercourse crossings for several operators (e.g., Enbridge Westcoast, FortisBC, and Trans Mountain). It can therefore be classified as a debris flood as per a definition by Church and Jakob (2020) and hazard analyses conducted for such streams should acknowledge this unique behaviour associated with debris floods (Jakob et al., 2022).

ARs are synoptic-scale processes that impact the Pacific coast of North America. They are made of long and narrow contiguous filaments of concentrated water vapour transport in the atmosphere that originate in the central Pacific Ocean. They produce copious rainfall when they lift as they flow over the mountainous coastal terrain of BC and the western United States (US) extending inland (Sharma and Déry, 2019). ARs transport warm, moist air during the late fall and early winter. This warm air locally raises the altitude of the freezing level resulting in more precipitation falling as rain instead of snow at higher elevations increasing snowmelt, where snow is present in the watershed (Guan et al., 2016). AR-related floods are typically larger than non-AR-related floods in coastal watersheds in BC making these floods a distinct population (Sharma and Déry, 2020b). The November 14, 2021 AR was a rain-on-snow event where the streamflow generated by rainfall was increased by melting snow, associated with a rapid rise in temperature (Gillett et al., 2022). While streamflow was generated by rain-on-snow, rainfall was the dominant factor in the flood magnitude.

Following the November 15, 2021 flood, an urgent need emerged to estimate the peak flow of the Coldwater River to inform long-term reconstruction and mitigation efforts. The flood event was recorded at the *Coldwater River at Brookmere* (08LG048) (upstream) and *Coldwater River at Merritt* (08LG010) (downstream) hydrometric stations, which are both maintained by the Water Survey of Canada (WSC). Initially, both stations recorded peak flows of approximately 400 m^3/s. This estimate was subsequently revised to 250 m^3/s at 08LG010 while the peak estimate was removed for 08LG048. However, considerable uncertainty persists in both measurements (i.e., 250 and 400 m^3/s) because they are based on stage-discharge rating curves developed prior to the event. Following the flood, the WSC observed considerable change to the riverbed at 08LG010, limiting the confidence in the stage discharge curve which had been stable for the previous decade (email from Luke Fennel at WSC, personal communication, March 17, 2022). In addition, water was flowing around the sites which was not measured. Given the uncertainty, both estimates of the event were deemed unreliable.

In support of ongoing programs and recovery from November 15, 2021 flood, BGC Engineering Inc. (BGC) was retained by several parties[1] to complete hydrotechnical hazard and risk assessments and flood hazard mapping in the Coldwater River and Nicola River watersheds. To support this effort, BGC has completed analyses of the November 15, 2021 flood (independent of ongoing WSC efforts) and a developed an updated flood frequency-magnitude relationship for the Coldwater River in Merritt. BGC also recognizes that many parties are supporting flood recovery and are relying on estimates of annual exceedance probabilities for peak flows. As such, BGC is providing Fraser Basin Council (FBC) with description of these technical analyses as a standalone report for the purpose of broader information sharing.

Intended readers of this document include but are not limited to the following: Emergency Management BC (EMBC), the Ministry of Forests, Lands, Natural Resource Operations and Rural Development (FLNRORD), the Ministry of Transportation and Infrastructure (MoTI), pipeline operators (Enbridge and Trans Mountain), First Nations and First Nations Emergency Services Society (FNESS), BC River Forecast Centre, City of Merritt, Indigenous Services Canada (ISC), First Nations governments, non-governmental organizations working on flood-related issues, and any Qualified Professionals working for them.

The objective of this work is to support alignment across organizations requiring an estimate of the frequency-magnitude relationship for the Coldwater River. The work is based on current data and methods, and it is not intended to represent “the” approach to examine Coldwater River flood hydrology. BGC anticipates the work will generate questions and comments and may be subject to future updates. BGC welcomes all feedback on this work through FBC.

[1] Fraser Basin Council, City of Merritt, BC, The Ministry of Transportation and Infrastructure, First Nations Emergency Support Services, Enbridge, Trans Mountain Pipeline Corporation, and BC River Forecast Centre.

2.0 NOVEMBER 14, 2021 AR EVENT

The November 14, 2021 AR in the Coldwater River watershed resulted in a peak flow that was primarily generated by rainfall and was increased by snowmelt, associated with a rapid rise in temperature (Gillett et al., 2022). A detailed account of the event is included in Gillett et al. (2022). The key points are summarized in the following sections for context.

2.1. Synoptic Setting

In meteorology, the synoptic scale corresponds to a horizontal scale on the order of 1000 km typical of large-scale atmospheric processes. The November 14, 2021 AR carried high water vapour from the tropics inland along the Fraser River valley (Gillett et al., 2022). The maximum IVT of the event was estimated to be 550 kg/m/s (Gillett et al., 2022). The AR resulted in two days of intense rainfall over the region. This AR is rated as a Category 3 event based on the Ralph scale over the study area (Table 2-1), which does not adequately reflect the extreme hydro-geomorphic response that was witnessed by this event. For comparison, the AR is rated a Category 4 at grid cells on the western edge of the event near Vancouver Island, but a Category 2 over the eastern, inland portion of the region (Gillett et al., 2022).

A novel AR rating system is currently being developed by Environment Canada and Climate Change (ECCC). This rating system expands the Ralph et al. (2019) system by including further hydro-meteorological variables and their respective predicted return periods which are then weighted and averaged. Furthermore, the individual categories will be linked to, and calibrated by known damages incurred such ARs. According to the evolving rating system, this event would be rated as an AR4 to AR5.

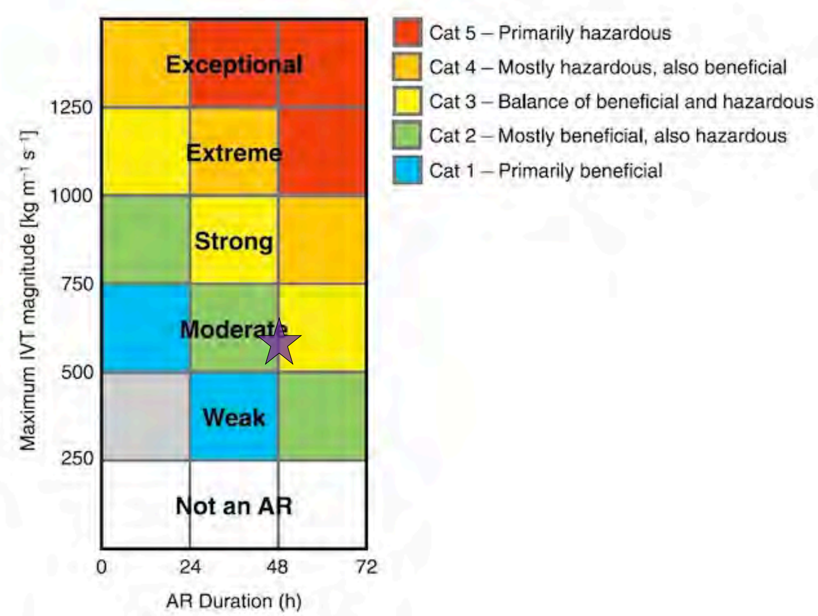

Figure 2-1. AR rating system (Ralph et al., 2019). The approximate rating for the November 14, 2021 AR is depicted by the purple star.

ARs over the region typically travel from the south and west, with most having a southwesterly trajectory. The November 14, 2021 AR was more westerly, steered by a high-pressure ridge to the south and a low-pressure trough to the north. The AR orientation was aligned with the orientation of the Fraser River valley, facilitating the inland penetration of the precipitation (Gillett et al., 2022). This alignment induced an orographic uplift from Vancouver, BC, to Merritt, BC, to Hope, BC, after which the rainfall was funneled down to more localized watersheds, like the Coldwater River.

2.2. Rainfall

The maximum two-day rainfall depth during the event ranged between 400 and 500 mm north of the Fraser River valley. The two-day rainfall depth exceeded 300 mm in the mountains around the Fraser River valley. The two-day rainfall depth was recorded to be 243 mm at the Coquihalla Summit climate station (Figure 2-2). The return period (% AEP[2]) of the two-day event was equivalent to approximately 50 years (based on ERA5[3] data) to 100 years (based on CaPA[4] data) over the study area defined by the black box in Figure 2-2 (Gillett et al., 2022). The distribution of TWO-day precipitation between 1950 and 2021 (based on ERA5 data) and 1980 to 2021 (based on CaPA data) were characterized using the GEV distribution (Figure 2-3).

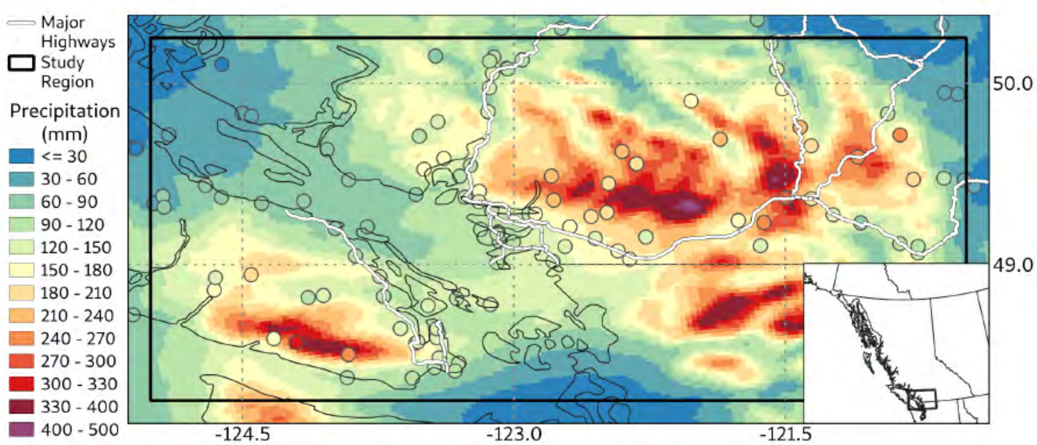

Figure 2-2. Two-day rainfall for November 14 and 15, 2021 based on the 2.5 km CaPA analysis data (colours) and from precipitation gauges (circles) (Gillett et al., 2022). The black box delineates the boundary of the study area considered in Gillett et al., (2022).

[2] Annual exceedance probability (AEP) is defined as the annual probability that a flood of given magnitude will be exceeded in any one year. The AEP is used alongside the return period. For example, the 100-year event (1% AEP).

[3] ERA reanalysis (Hersbach et al., 2020), and its extension back to 1950 (Bell et al., 2021) is a precipitation product of the European Centre for Medium Range Weather Forecasts (ECMWF) providing hourly estimates of a large number of atmospheric, land, and oceanic climate variables. This data product is suitable for event attribution given its record length.

[4] Canadian Precipitation Analysis (CaPA) combines available surface observations with numerical weather prediction (NWP) output in to produce estimates of precipitation on a 2.5-km grid at each synoptic hour (0000, 0600, 1200, and 1800 UTC) (Lespinas et al., 2015; Fortin et al., 2018; Gasset et al., 2021). This data product is suitable for characterising precipitation variations at a small scale.

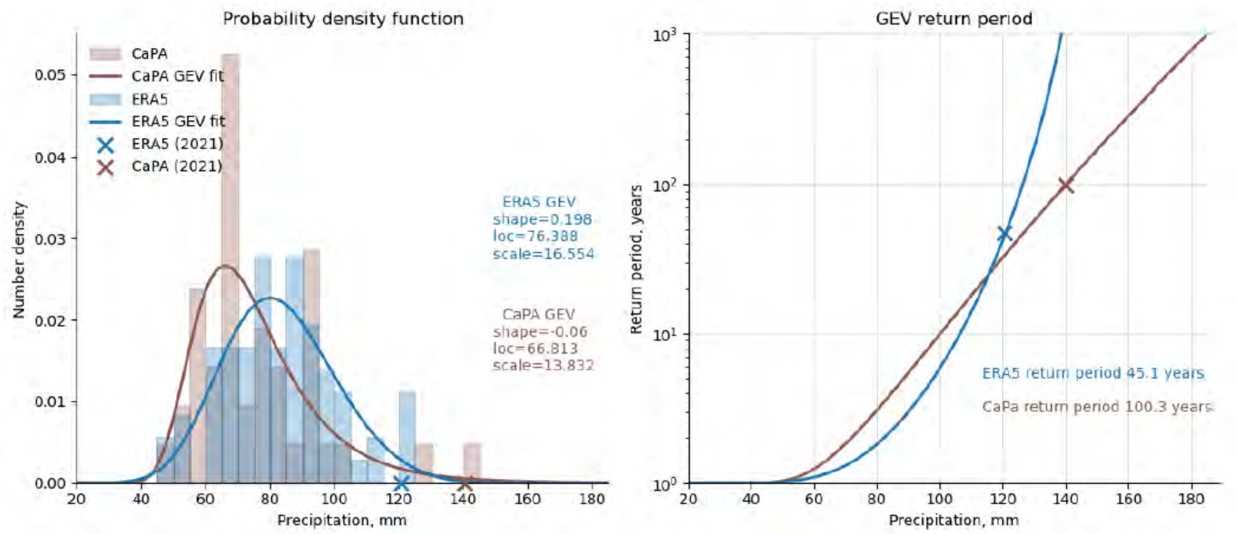

Figure 2-3. Probability density function for two-day precipitation based on ERA5 and CaPA data (left) and frequency-magnitude relationship for the two-day precipitation event (right) (Gillett et al., 2022). The crosses show the two-day precipitation for November 14 and 15, 2021 event over the study area defined by the black box in Figure 2-2.

The maximum two-day rainfall depth in the Coldwater River was observed in the upper watershed around the Coquihalla Summit with a value of 329 mm from November 14 to 16, 2021 based on the high resolution CaPA gridded dataset (Table 2-1, Figure 2-4). The return period (% AEP) of the event for that grid cell based CaPA data was estimated to be >100,000 years (0.001% AEP) (Figure 2-5). For comparison, the two-day rainfall depth averaged over the Coldwater River watershed was estimated to be 134 mm over the same time period with an associated return period of approximately 100 years (1% AEP) (Table 2-1, Figure 2-4). The return period (%AEP) for the averaged two-day rainfall depth over the Coldwater River watershed (100 years) aligns with the 50 to 100 years range reported by Gillett et al., (2022) in the region.

Table 2-1. Two-day rainfall depth for the Coldwater River watershed from November 12 to November 17, 2021.

Date	Averaged over the Watershed[1]		Maximum in Watershed (Latitude: 49.755, Longitude: -121.051)	
	Two-day Rainfall (mm)	Approximate Return Period[2] (years)	Two-day Rainfall (mm)	Approximate Return Period (years)
November 12 to 14	14	< 2	60	< 10
November 13 to 15	74	< 10	181	500 to 1,000
November 14 to 16	134	100	329	> 100,000
November 15 to 17	83	< 10	198	1,000 to 2,000

Notes:

1. CaPA data averaged from the Coquihalla Summit to the City of Merritt.
2. Approximate return period based on the point frequencies from the BC Extreme Flood Project. The point frequencies chosen is located in the upper watershed (Latitude: 49.755, Longitude: -121.051). This location is considered representative because the rainfall was concentrated in the upper watershed.

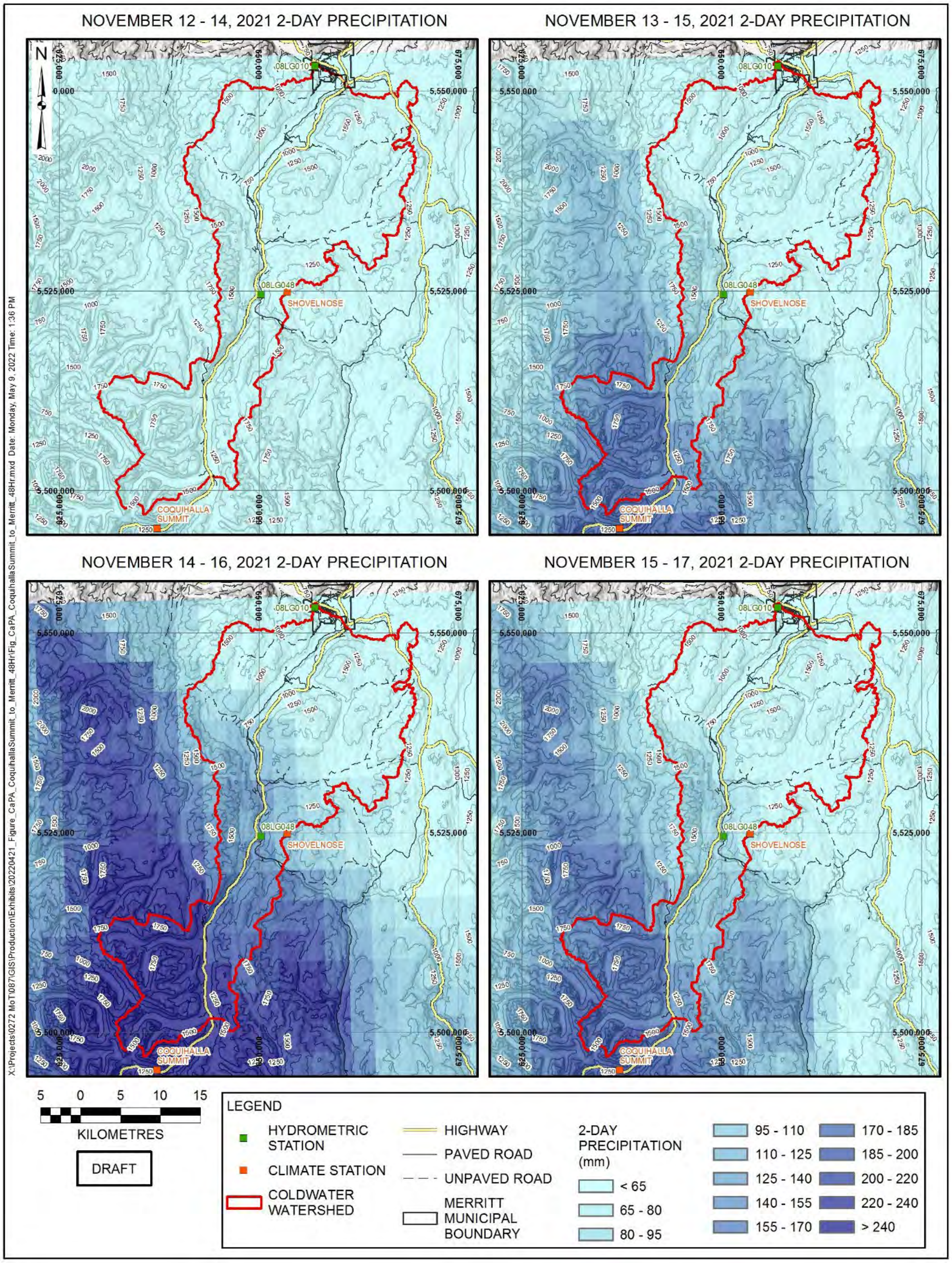

Figure 2-4. Spatial distribution of the two-day precipitation in the Coldwater River watershed from November 12 to 17, 2021 based on the 2.5 km CaPA data.

The return period (% AEP) of the two-day rainfall depth in the Coldwater River watershed was estimated based on point precipitation frequencies from the BC Extreme Flood Project (i.e., BC MetPortal) (Figure 2-5). The two-day frequency-magnitude relationship used to define the point precipitation frequencies was developed using the Schaefer-Wallis-Taylor climate region method based on L-Moments regional analysis (Schaefer et al., 2018). The period of record spans 1851 to 2019. Daily point precipitation data for the mid-latitude cyclone[5] storm type were acquired from observation stations of various sources from across BC. For additional information on the frequency-magnitude relationship used to define point precipitation frequencies, refer to DTN and MGS Engineering (2020).

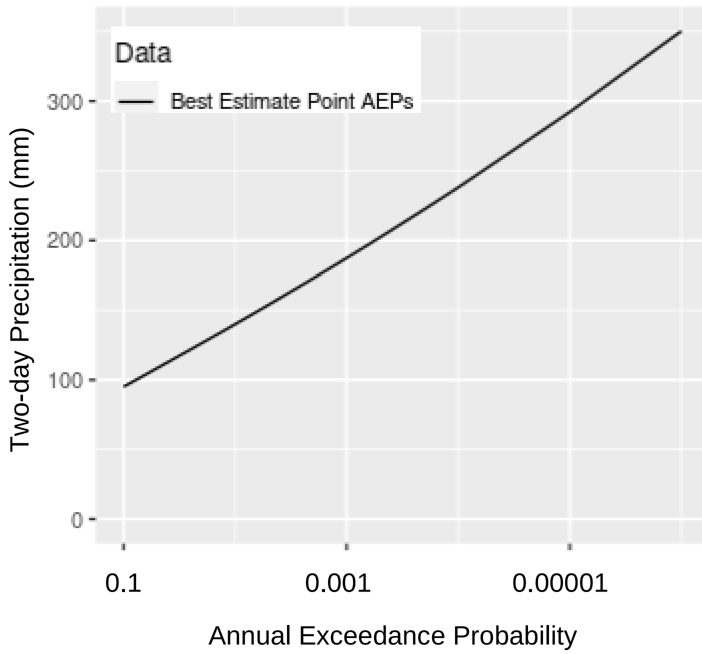

Figure 2-5. Frequency-magnitude relationship for the two-day precipitation event in the upper watershed of the Coldwater River (Latitude: 49.755, Longitude: -121.051) directly from the BC Met Portal.

2.3. Streamflow

The maximum peak flow in the Coldwater River was recorded on November 15, 2021 and was caused by the two-day rainfall and snowmelt (Gillett et al., 2022). Wind common during rainstorms likely promoted additional melt by advecting a high volume of relatively warm, unsaturated air over the snowpack. The following climate observations were made at the Automated Snow Weather Station (ASWS) 1C29P (Shovelnose Mountain), located to the east of Highway 5 at an elevation of 1460 m in the mid-watershed of the Coldwater River. The streamflow data are based on the *Coldwater River in Merritt* (08LG010) hydrometric station.

[5] Mid-latitude cyclones are storms that format middle and high latitudes outside of the tropics and include ARs.

- Precipitation occurred during the evening of November 13, paused, and resumed early in the morning of November 14. Precipitation fell continuously until November 16 (Figure 2-6a).
- The November 13 precipitation falling as snow contributed to an 11 mm increase in snow SWE just before the onset of melt (Figure 2-6b).
- The AR brought considerably warmer air to the region. The air temperature increased 8°C from a low of - 2.6°C on the evening of November 13 to a high of 5.6°C on November 14. Air temperature remained above 0°C until late afternoon on November 15 (Figure 2-6c). The snowpack started to melt 10 hours after arrival of the storm when temperatures at the station exceeded 0°C on November 14. Snowmelt continued until November 15. Some melt is present on November 16 as temperatures dip below zero which seems unlikely.
- Streamflow in the Coldwater River began to rise shortly after the onset of the melt and peaked in the evening of November 15, coinciding with the end of both snowmelt and rainfall (Figure 2-6d).

Snowmelt depth was 21 mm and rainfall depth was 83 mm for a total of 104 mm over two days from November 14 to November 16 (Gillett et al., 2022). These results show that the hydrological response to the AR event in the Coldwater River watershed was caused by rain-on-snow conditions where streamflow was generated by precipitation in the form of rainfall augmented by snowmelt associated with a rapid increased in air temperature over the region (Gillett et al., 2022). The total runoff contribution of rain was approximately four times higher than that of snow.

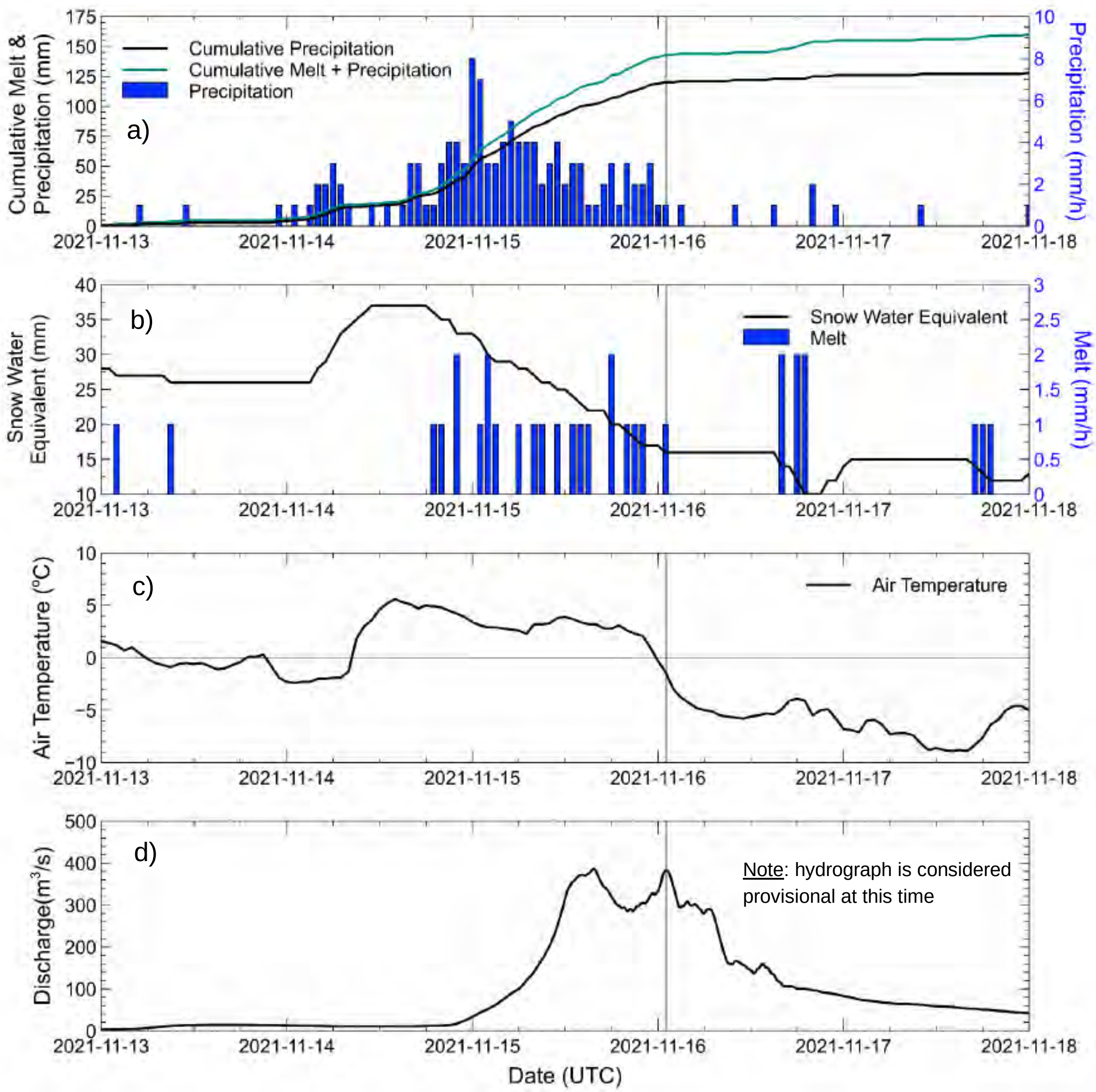

Figure 2-6. Hydro-meteorological conditions for the Coldwater River watershed with a) hourly precipitation, cumulative precipitation, and cumulative melt plus precipitation, b) hourly SWE and melt, and c) hourly air temperature and d) streamflow (Gillett et al., 2022). Precipitation, SWE, air temperature, and melt data are from ASWS 1C29P (Shovelnose Mountain; 1460 m elevation), and streamflow data are from the *Coldwater River at Merritt* (08LG010) hydrometric station. All data are plotted for the period November 13, 2021, to November 18, 2021 (Gillett et al., 2022).

2.4. Antecedent Conditions

Antecedent soil moisture conditions can have an important impact on the hydrological response of a watershed to water inputs by controlling available water storage (Cao et al., 2020). The fall preceding the November 14, 2021 AR was among the wettest on record suggesting limited soil storage capacity prevailed prior to the event. The cumulative precipitation averaged over southwestern BC is shown in Figure 2-7 (left). Individual precipitation events correspond to periods where the cumulative precipitation rises sharply. The cumulative precipitation over November 14 and 15, 2021 period was among the highest compared to historical events (Gillett et al., 2022).

Soil moisture is a complementary indicator of antecedent conditions because fall and winter precipitation can occur as snow or rain. The antecedent precipitation index[6] (API) can be used as a proxy for soil moisture in the absence of direct measurements or modelled estimates. The 30-day API for each year is shown in Figure 2-7 (right). The 2021 API (red line in Figure 2-7) shows wet conditions among the highest observed historically throughout October and the start of November over the region (Gillett et al., 2022). These wet conditions suggest that local watersheds had limited soil storage capacity. The purple line shows 1990 for reference to the Skagit River/Sumas River floods (Hubbard, 1994). Both the 1990 and 2021 flood events resulted from heavy rainfall in November.

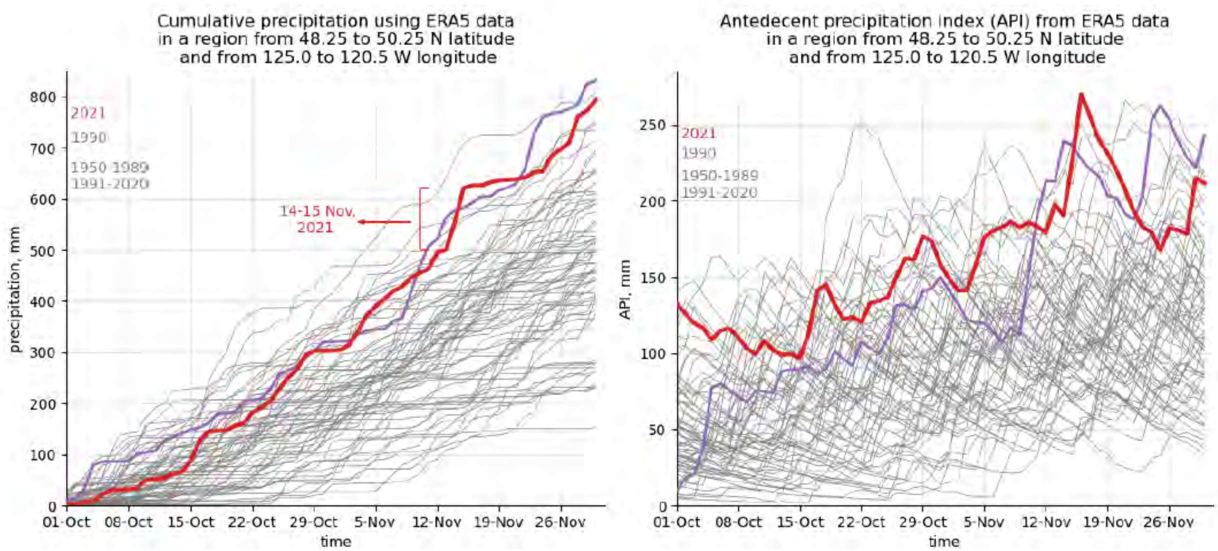

Figure 2-7. Cumulative total precipitation (left) and the 30-day antecedent precipitation index (API) (right) averaged over southern BC from October 1, 1950, based on the ERA5 reanalysis data. The 2021 event is shown in red and 1990 is shown in purple for reference.

Records available from snow pillow sites in both the SNOw TELemetry (SNOTEL) network in the United States (Natural Resources Conservation Service, 2022) and the Automated Snow Weather Station (ASWS) network in British Columbia (Ministry of Environment and Climate Change Strategy, 2009) show that the SWE was higher than normal but not extreme. The weather conditions were primed for snow to contribute to this event. The SWE ranged between the 70th and 90th percentile of historical daily observations for the three-day period centered on November 13 (Figure 2-8) (Gillett et al., 2022).

6 The API is a weighted running mean of daily precipitation where recent events are weighted more heavily over the course of 30 days (Heggen, 2001).

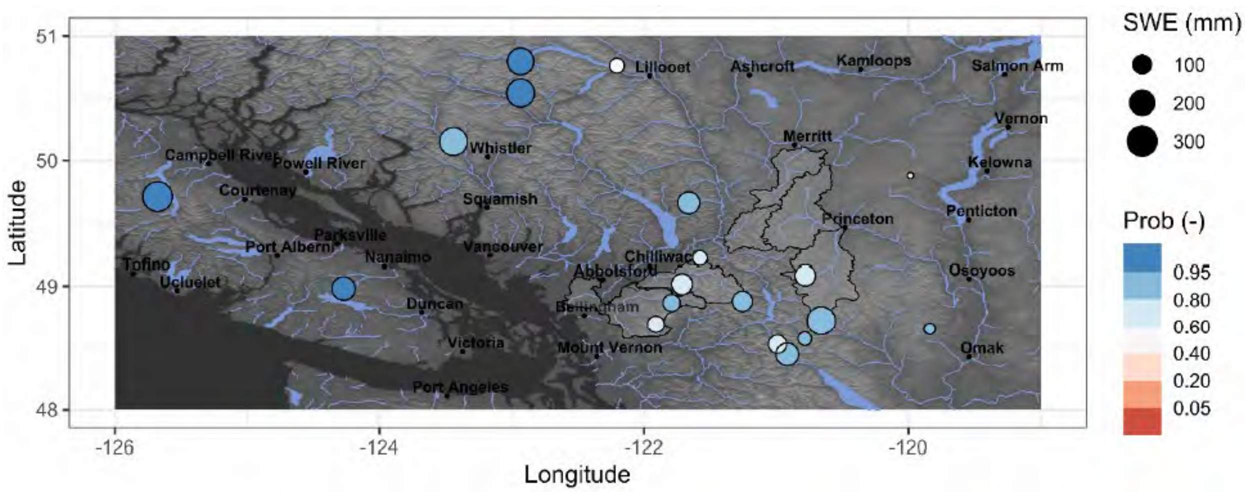

Figure 2-8. Antecedent SWE as of November 13, 2021, as an annual probability of non-exceedance for snow pillow locations with records ≥ 20 years (Gillett et al., 2022).

The average snow water equivalent (SWE) on November 13, 2021 in the upper Coldwater River watershed (upstream of Brookmere) was 125 mm, ranging from 11 mm to 260 mm based on the SNOWDAS data[7] (Figure 2-9). The SWE increased 2% on November 14, 2021 and decreased throughout the day on November 15, 2021 coinciding with the sustained above zero temperature to a minimum average of 100 mm (-20%) on November 16, 2021.

7 The SNOWDAS dataset contains snowpack properties like depth and snow water equivalent from the NOAA National Weather Service's National Operational Hydrologic Remote Sensing Center (NOHRSC) SNOw Data Assimilation System (SNODAS). The temporal coverage spans September 28, 2003 to present at a 1-day temporal resolution.

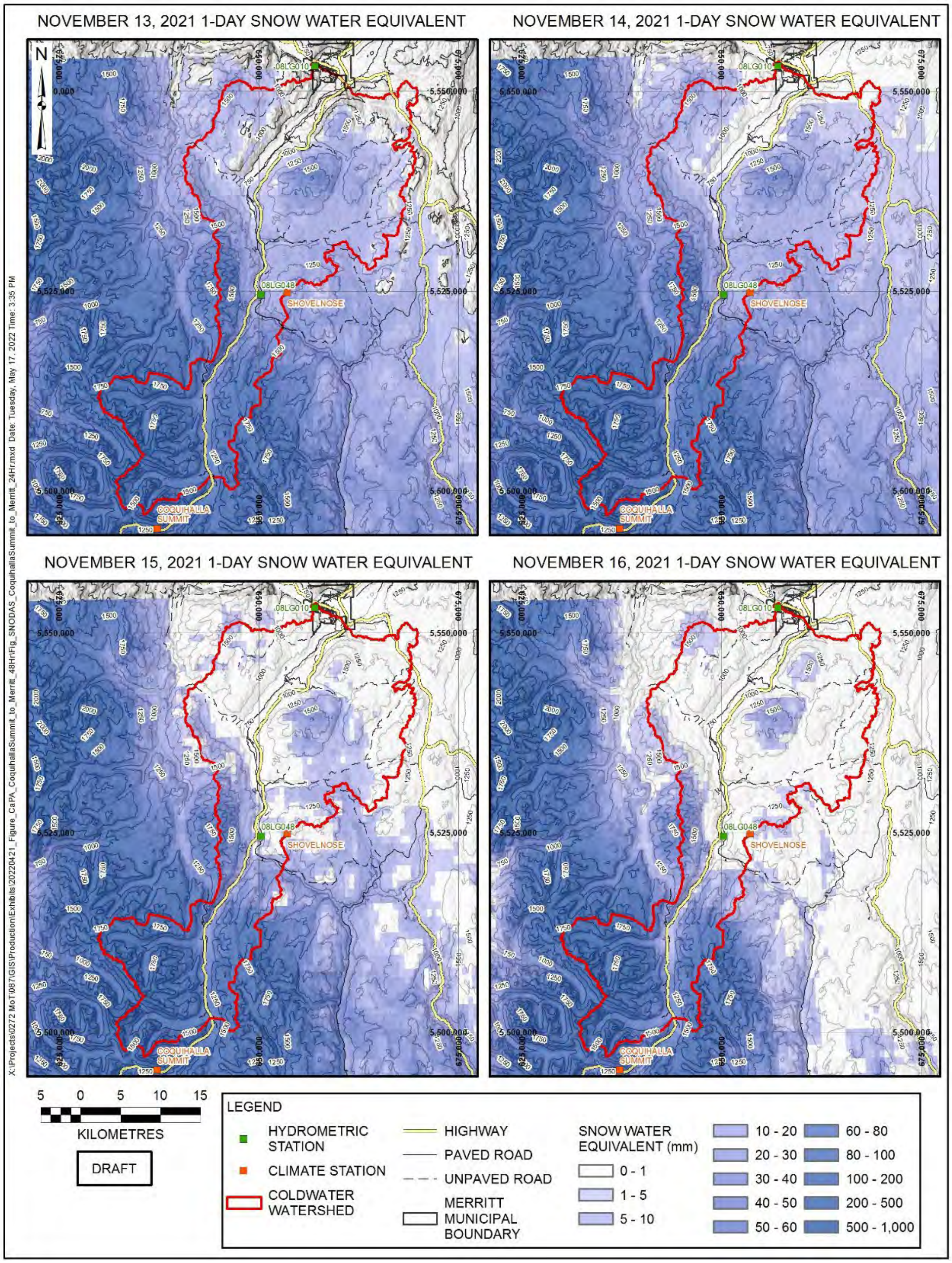

Figure 2-9. Spatial distribution of one-day SWE in the Coldwater River watershed from November 13 to 16, 2021 based on the 1.0 km SNODAS data.

3.0 COLDWATER RIVER WATERSHED

3.1. Climate

Climate is a driver of watershed hydrology by controlling the water inputs (rainfall and snow) through temperature by the Clausius-Clapeyron relation which implies that specific humidity increases approximately exponentially with temperature assuming unlimited water and energy for evaporation (Wark, 1966, 1988). The Coldwater River watershed lies in the Northern Cascade Ranges Ecoregion characterized by a mountainous area lying in the rain shadow created by the southern Coast Mountains and the northern Cascade Mountains (Figure 3-1). Moist Pacific air is often present in the western portion through low mountain passes and valleys like the lower Fraser River and the Coquihalla River (Demarchi, 2011). Dry interior air can also enter from the lower Fraser River valley. This region is characterized by both coastal forests and dry interior being transitional between the two types of climates (Demarchi, 2011).

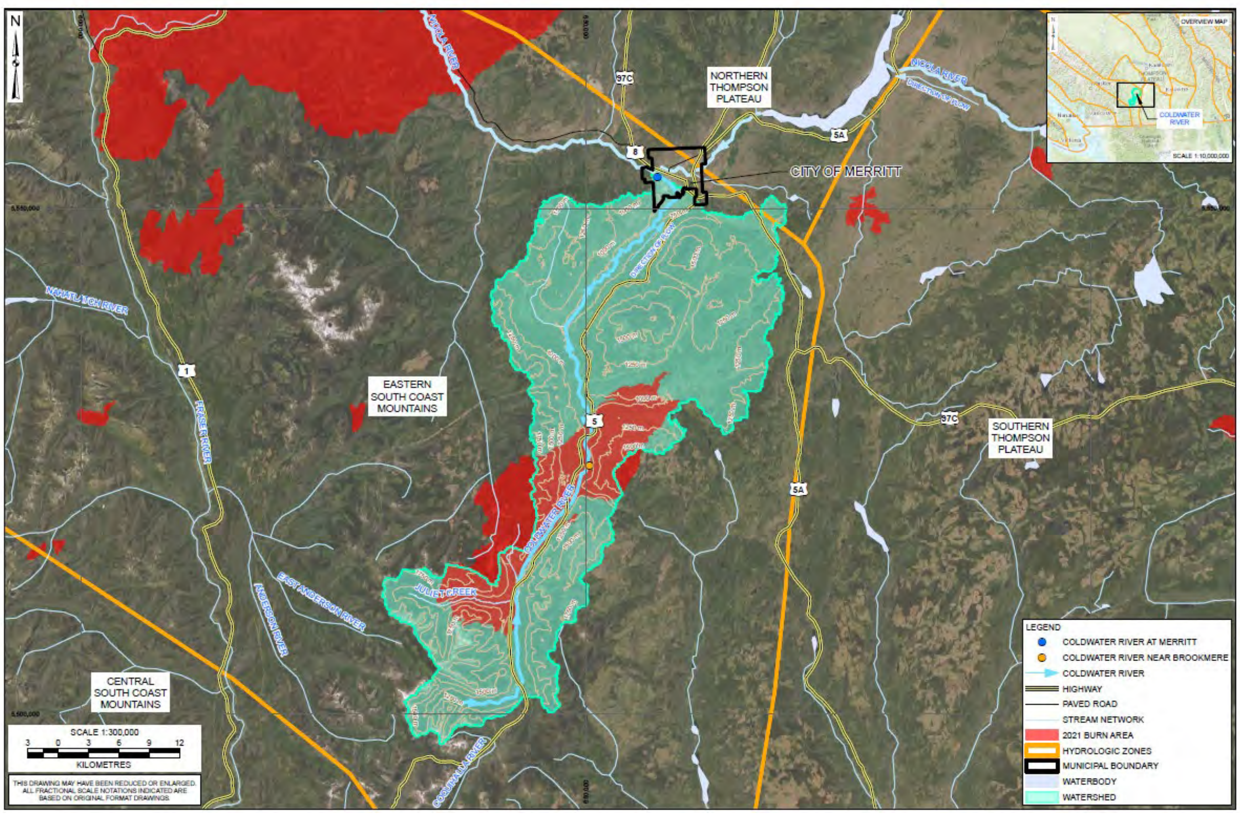

Figure 3-1. Location map showing the Coldwater River watershed.

Averaged over the Coldwater River watershed, the historical mean annual temperature (MAT) is approximately 3.0ºC. The precipitation increases starting in September with a maximum in the winter months and decreases at the onset of spring with a minimum in the summer months Wang et al. (2016). Such descriptive statistics of temperature do not consider the extreme temperatures that were recorded in the region at the end of June 2021. For example, temperatures in Lytton, BC increased to 49.6ºC breaking the national maximum heat record. Temperature also rose to extreme levels in nearby towns including Ashcroft (48.1ºC), Kamloops (47.3ºC), and Lillooet (46.8ºC). Extreme weather is more likely with climate change as the atmosphere and oceans warm allowing the atmosphere to become super saturated with water vapour.

3.2. Hydrologic Regime

The hydrologic regime is the relationship between water inputs and streamflow outputs over time in a watershed. The present-day hydrologic regime in the Coldwater River watershed is nival-pluvial[8] with the annual peak flood typically occurring from snowmelt in the spring (day of year 90 to 180). In some years, however, ARs in the fall (day of year 250 to 335) and winter months (day of year 335 to 90) generate large floods, the magnitude of which exceeds that of the snowmelt flood in the spring. The *Coldwater River at Brookmere* hydrometric station (08LG048) has been recording streamflow since 1965. Annual hydrographs for this hydrometric station up to 2020 are presented in Figure 3-2.

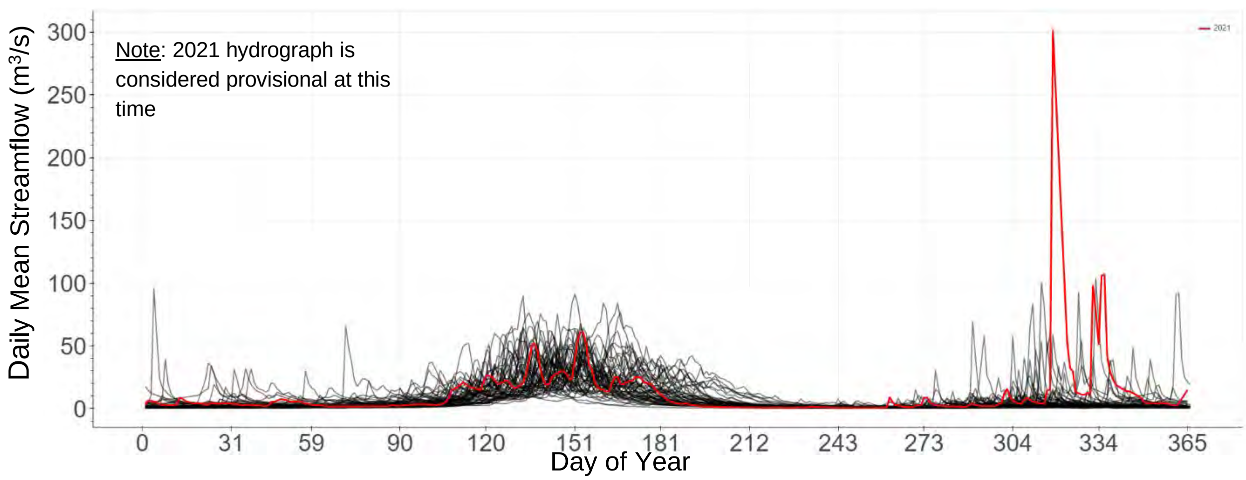

Figure 3-2. Historical daily mean hydrographs superimposed for from 1965 to 2021 at the *Coldwater River at Brookmere* (08LG048) hydrometric station. The provisional time series for 2021 is included in red for reference.

3.3. Atmospheric Rivers

ARs are important sources of water to Coastal Mountain watersheds, like the Coldwater River. The variability and trends of ARs have been characterized for the lower latitudes (47.0º to 53.5ºN) in BC (from approximately northern Washington to Prince George) (Sharma & Déry, 2019). The annual AR frequency is 29 on average over this range in latitude from 1948 to 2016. A lower AR frequency is present from the 1960s until mid-1970s and corresponds to the negative phase of the Pacific Decadal Oscillation (Meehl et al., 2009). The frequency is highest in the fall (September, October, November) and lowest during the spring (March, April, May). A statistically

8 Mixed hydrological regime characterized by two peaks: in spring, linked to snowmelt, and in fall, linked to rainfall.

significant ($p<0.05$) trend is present over the 1979 to 2016 period, with an increase of 1.2 events per decade (Sharma & Déry, 2019).

ARs contributed up to 90% of annual maximum precipitation in coastal regions of Central BC during the 1979 to 2017 period (Sharma & Déry, 2020a). Results of a seasonal analysis show the highest contribution of ARs to annual maximum precipitation occurs in the fall with approximately a 75% contribution in the Coast Mountains (Sharma & Déry, 2020a). The contribution of ARs to precipitation was calculated based on the fraction of precipitation attributed to ARs to total annual (and seasonal) precipitation. The contribution of ARs to annual maximum precipitation does not show widespread changes over time across BC from 1979 to 2012 (Sharma & Déry, 2020a). However, the frequency of ARs across BC and southeastern Alaska increased between 1979 and 2016 (p-value <0.05) (Sharma & Dery 2019). Climate models predict changes to phenomena that cause extreme precipitation events, such as ARs. These changes could influence the future frequency and location of floods in Canada (Bonsal et al., 2019).

Not all AR events result in AR-related peak flows. While there may be anywhere between 0 and 29 ARs per year in southwestern BC (from 1967 to 2017), these events do not generate a hydrological response[9] every time. Precipitation is driven by net moisture convergence rather than by the Integrated Vapour Transport[10] (IVT) itself, thus there is not a perfect correlation between IVT and precipitation for AR events in the region (Mo et al., 2021). In addition, the control of watershed characteristics and antecedent conditions (Cao et al., 2020), and the magnitude and position of the AR event, relative to watershed orientation (Gillett et al., 2022) can also control the hydrological response magnitude.

3.4. Snowmelt

The Coldwater River watershed is characterized by a complex topography where precipitation takes the form of rain and snow. The historical mean annual precipitation (MAP) across the watershed is 1,268 mm, of which approximately 678 mm (53%) is snowfall over the 1971 to 2000 period (precipitation as snow [PAS]) based on data from Wang et al. (2016). The elevation range in the watershed spans 900 m to 2,000 m. For comparison, 25% of the mean annual precipitation is snowfall over the same period at the weather station in Merritt, BC (Station ID= 247, elevation = 609 m) highlighting the control of topography on the snow proportion. The Coldwater River watershed responds to snow accumulation over the winter (day of year 335 to 90) by melting in the spring (day of year 90 to 180) every year. The magnitude of the snowmelt-related peak flow is a function of the rate at which snow melts, which is dependant in part on weather. For example, hot temperatures melt snow fast, warm temperatures melt snow slowly, and below zero temperatures maintain the snowpack. In addition, falling rain on snow makes the snow melt faster

9 A hydrological response is defined as a measurable increase in streamflow in a watershed above the baseflow level in response to water input before receding to back baseflow conditions.

10 Moisture transport in the atmosphere is characterized by the vertically integrated horizontal water vapour transport at specific levels (e.g., 1000 hPa to 300 hPa). Levels in the atmosphere (i.e., altitude) are expressed by atmospheric pressure for meteorological purposes.

and adds water. Wind common during storms can promote additional melt by advecting a high volume of relatively warm, unsaturated air over the snowpack. The snowmelt-related peak flows in the Coldwater River are a function of the snowpack, temperature (and wind), and rainfall.

3.5. Landcover

Landcover is an important factor influencing the hydrological response of a watershed to water inputs in the form of rain and/or snow. The watershed at the *Coldwater River at Brookmere* hydrometric station (08LG048) was more than 95% forested prior to the August 2021 wildfires. Approximately 30% of the watershed was burned during the 2021 wildfires in the region. The soils in the watershed are characterized by a combination of silt loam (70%) and sand clay loam (30%). Sand clay loam soils have low infiltration rates when thoroughly wetted. Sand clay loams have moderately fine to fine structure and can impede vertical water movement (Ross et al., 2018).

The effects of wildfire on a watershed's hydrological response are complex. The loss of vegetation canopy can increase the snowmelt and rainfall reaching the ground surface, loss of forest floor litter can decrease water storage, loss of root structures can decrease ground stability (Winkler et al., 2010). Studies have shown wildfires can exacerbate peak flows due to a decrease in soil moisture storage and soil infiltration rates resulting from hydrophobic soils (e.g., Ebel et al., 2012). The magnitude of post-fire floods and geomorphic change can be affected by the timing, magnitude, duration, and sequence of rainstorms (Brogan et al., 2017). Given this complexity, the role of the August 2021 wildfires on the magnitude of the November 2021 event was beyond the scope of this study.

4.0 DATA

4.1. Estimating the Magnitude of the November 15, 2021 Flood

4.1.1. Terrain

Detailed topographic data of the floodplain from a high-resolution lidar datasets were acquired both before and after the November 15 2021 event. The pre-flood lidar was obtained by BGC from GeoBC. The pre-flood lidar was acquired on April 25, 2018. The post-flood lidar was obtained by BGC from McElhaney. The post-flood lidar was acquired November 26, 2021. BGC contracted Ecoscape Environmental Consultants Ltd (Ecoscape) both before and after the event to conduct bathymetric surveys. The pre-flood survey was conducted between September 9 to 16, 2020. The bathymetric survey covers the full extents of the Nicola and Coldwater Rivers within the city limits of Merritt and extends from 250 m east (upstream) of the city limits along the Nicola River. The post-flood survey included only the Coldwater River and was conducted between March 7 and 8, 2022. Details on terrain preparation for the preflood model can be found in the 2021 report BGC provided to the FBC (BGC, June 4, 2021) and the post-flood model used the same methodology for its terrain preparation.

4.1.2. High-water Marks (HWMs)

High-water marks (HWMs) were surveyed by Ecoscape between March 7 and 8, 2022 and HWM photos collected by FLNRORD on February 8, 2022, by BGC on February 17, 2022 were used to supplement these results. The HWMs collected included rafted debris on fence lines, markings on buildings, and overbank large woody debris deposits (see Figure 4-1 for an example). The HWMs collected by Ecoscape were formally surveyed and hence have minimal error associated with their geographic coordinates. The highwater mark photos collected by FLNRORD and BGC staff had an uncertainty associated with the geographic coordinates of typically +/- 4 m from the accuracy of the GPS of the devices used to take the photos (phones and tablets). Post-flood ortho imagery and lidar collected on November 26, 2021 were used to verify that the coordinates of the photos approximately matched those of the image shown. The elevation of rafted debris above the ground surface was determined using a tape measure when it was present in photos and using the diamonds in chain link fences as a scale when a tape measure was not included in photos. For the latter case, an assumption was made that the diamonds had a typical mesh length of 2'' or approximately 5 cm. Videos taken by FLRNORD and members of the public during the flood event were also examined to identify the extents of the November 15, 2021 flood within Merritt.

Figure 4-1. Example of a HWM in Merritt, BC. Rafted debris along the fence is clearly visible. Photo: BGC, February 17, 2022.

4.2. Frequency-Magnitude Relationship

4.2.1. Atmospheric Rivers

Historical AR events have been catalogued between 1948 and 2017 by the Scripps Institute of Oceanography (SIO-R1-AR). The AR catalogue is available at http://cw3e.ucsd.edu/Publications/SIO-R1-Catalog/. This AR catalogue provides the frequency, duration, and landfalling location of ARs along the North American West Coast from 20^{o} to 60^{o}N (Gershunov et al., 2017). This dataset has been used by a number of researchers to characterize changes to AR characteristics over time (Sharma & Déry, 2019; 2020a,b). This dataset was used to relate historical AR events to hydrological responses, if any.

4.2.2. Historical Streamflow

Annual maximum daily mean (Q_{max}) and daily instantaneous (Q_{imax}) peak flows are recorded at the *Coldwater River at Brookmere* (08LG048) and the *Coldwater River at Merritt* (08LG010) hydrometric stations. The analysis was completed using the data at the 08LG048 hydrometric station given the greater number of instantaneous estimates with no data gaps in the record and consistent automatic continuous recording methods (Table 4-1). The early century records (1913 to 1921) collected at the 08LG010 were not considered in the analysis given the 40-year gap. Manual, and seasonal data collection resumed in 1961. The magnitude of the early century records falls within the range of variability of the later peak flow data suggesting that their inclusion would have limited influence on the frequency-magnitude relationship.

Table 4-1. Hydrometric station information for the *Coldwater River at Brookmere* (08LG048).

Station Information	Coldwater River at Brookmere
Station ID	08LG048
Latitude (°)	49.8542
Longitude (°)	-120.9085
Watershed Area (km^2)	316
Real-time recording	Yes
Record Period	1965 to 2021
Record Length (years)	56
Number of published instantaneous peak flows	53[1]
Approximate elevation (m)	1000
Hydrologic regime	Natural

Note:
1. Records do not all have both the daily mean and daily instantaneous values.

4.3. Projected Daily Mean Streamflow

Streamflow projections are not available in the Coldwater River. However, daily mean streamflow at the *Coquihalla River above Alexander* (08MF068) hydrometric station are modelled from 1945 to 2100 by the Pacific Climate Impact Consortium (PCIC) under naturalized streamflow conditions. The daily mean streamflow was simulated using runoff and baseflow generated with an upgraded version of the Variable Infiltration Capacity (VIC-GL) model that is coupled to a glacier model (Schnorbus, in prep) and routed with RVIC (Lohmann et al., 1998, 1996; Hamman et al., 2016). The projected daily mean streamflow at the *Coquihalla River above Alexander*

(08MF068) hydrometric station was used to infer the impacts of climate change on daily mean streamflow in the Coldwater River watershed.

The VIC-GL model was calibrated at 46 sites over the Fraser River watershed. The *Coquihalla River above Alexander* (08MF068) was not included in this calibration due to the small watershed area (720 km^2) relative to the other watersheds (minimum 1,000 km^2). The calibration performance was evaluated by PCIC using performance metrics including the Kling-Gupta efficiency (KGE; Gupta et al., 2009), the Nash-Sutcliffe efficiency for log-transformed streamflow (LNSE; Nash & Sutcliffe, 1970) and the bell membership function (BMF; Zhao & Bose, 2002). The possible value ranges for the various metrics are -∞ to 1 for KGE (1 is best), -∞ to 1 for LNSE (1 is best) and 0 to 1 for BMF (1 is best). The model performance is generally high over the calibration period with a relative bias between zero and 19% (Table 4-2).

Table 4-2. Calibration metrics and evaluation periods.

Calibration Metrics	Streamflow	Evapotranspiration	Snow Cover (SCA)	Glacier Mass Balance (B)
Statistics	KGE, LNSE, NSE	BMF	KGE	BMF
Result	KGE 0.61 to 0.99 LNSE -0.56 to 0.99 NSE 0.51 to 0.99	0.37 to0.71	0.69 to 0.95	0.04 to 1.0
Calibration Period	1991 to 2000	1991 to 2000	2000 to 2005	1985 to 1999

The VIC-GL model was used to project daily mean streamflow driven by the six General Circulation Models (GCMs) from the CMIP5 models under the Representative Concentration Pathway (RCP) 8.5, statistically downscaled with the Bias Correction/Constructed Analogues with Quantile mapping reordering (BCCAQ) method using PNWNAmet-driven[11] streamflow as the target (PCIC, 2020) (Table 4-3). The RCP 8.5 emission scenario assumes an unconstrained increase of greenhouse gases in the atmosphere. The high emissions pathway presents a realistic scenario that frames the upper bounds at present. Projected daily mean streamflow at *Spius Creek near Canford* (08LG008) and *Nicola River near Spences Bridge* (08LG006) hydrometric station were also compared to assess consistency in the projections over the region.

[11] The PNWNAmet is a long-term, temporally consistent, gridded daily meteorological dataset for northwestern North America (Werner et al., 2019).

Table 4-3. The six GMC models used to drive PCIC's VIC-GL model.

GCMs
ACCWAA1.0_rcp85_r1i1p1
CanESM2_rcp85_ r1i1p1
CCSM4_ rcp85_ r1i1p1
CNRM.CM5_ rcp85_ r1i1p1
HadGEM2.ES_ rcp85_ r1i1p1
MPI.ESM.LR_ rcp85_ r1i1p1

4.4. Watershed Characteristics

Climate projections are not available in the Coldwater River. The projections in daily mean streamflow in the *Coquihalla River above Alexander Creek* (08MF068) were used to infer the impacts of climate change in the Coldwater River. The Coquihalla River was considered representative of the Coldwater River given its proximity and similar mixed hydrologic regime for the purpose of characterising future trends in AR- and snowmelt-related peak flows. The Coquihalla River is a tributary of the Fraser River with its watershed located in the Cascade Mountains, like the Coldwater River watershed. The similarity between both watersheds was assessed qualitatively using a suite of characteristics selected based on the potential to influence the magnitude of flood events. This comparison of watershed characteristics is not intended to be exhaustive. Several data sources were used to compile the watershed characteristics which are described in the following sections.

4.4.1. Watershed Statistics

The Shuttle Radar Topography Mission (STRM) dataset (Farr et al. 2007) was used to extract the watershed elevation statistics. The watershed elevation statistics were averaged over the watershed area. This dataset was used to calculate the watershed area (just for watersheds over 1000 km^2), relief, length, and slope. The centroid statistics were also extracted from this dataset.

4.4.2. Climate Variables

The Climate North America (ClimateNA) dataset was used to estimate the climate variables for each watershed polygon (Wang et al., 2016). The climate variables were averaged over the watershed area and were based on the average for the period 1961 to 1990.

4.4.3. Landcover

The North American Land Change Monitoring System (NALCMS) land cover products include the 2005 land cover map of North America. This dataset includes 19 land cover classes derived from 250 m Moderate Resolution Spectroradiometer (MODIS) image composites (Latifovic et al., 2012). This dataset was used to calculate the percent forest, percent wetland and lake, and the urban portion of the watershed.

4.4.4. Curve Number

The curve number (CN) is an empirical parameter used for predicting runoff from rainfall. BGC integrated the land cover (NALCMS) and the hydrologic soils group (HYSOGs250m) datasets to infer the average CN over each watershed. The NALCMS dataset is described in Section 4.4.3. The HYSOGs250m dataset represents typical soil runoff potential at a 250 m spatial resolution (Ross et al., 2018). Hydrologic soils groups are defined based on soil texture, depth to bedrock or depth to groundwater. There are four basic groups: A, B, C, D. Four additional groups are included where the depth to bedrock is less than 60 cm: AD, BD, CD, and DD. The area covered by each hydrologic soils group is summed for a total area over the watershed for each hydrologic soils group.

The CN was assigned following guidance from the USGS (1986). The CN values for soils where the depth to bedrock or depth to groundwater is expected to be less than 0.6 m from the surface (i.e., D soils) were assumed to be the same as the case where it is not expected to be close to the ground surface. The CN value assignment for the combinations of land cover and hydrologic soils groups identified in the watersheds is presented in Table 4-4. The CN values were averaged over the watershed area using a weighted mean. The weight reflects the percentage of the area covered by a given CN value.

Table 4-4. CN values based on the integration between the land cover and soils datasets.

Land Cover (NALCMS 2005)	Cover Type (USGS, 1986)	Soils			
		HSG-A	HSG-B	HSG-C	HSG-D
Temperate or sub-polar needleleaf forest	Woods - Good	30	55	70	77
Temperate or sub-polar broadleaf deciduous forest	Woods - Good	30	55	70	77
Mixed forest	Woods - Good	30	55	70	77
Temperate or sub-polar shrubland	Brush - brush-weed-grass mixture with brush the major element - Fair	35	56	70	77
Temperate or sub-polar grassland	Pasture, grassland, or range—continuous for grazing - Good	39	61	74	80
Sub-polar or polar grassland-lichen-moss	Pasture, grassland, or range—continuous for grazing - Good	39	61	74	80
Sub-polar or polar barren-lichen-moss	Desert shrub - major plants include saltbrush. Greasewood, creosotebush, blackbrish, bursage, palo verde, mesquite, and cactus - good	49	68	79	84
Sub-polar taiga needleleaf forest	Woods - Good	30	55	70	77
Cropland	Row crops - straight row (SR)	63	74	81	85
Barren land	Desert shrub - major plants include saltbrush. Greasewood, creosotebush, blackbrish, bursage, palo verde, mesquite, and cactus - good	49	68	79	84
Urban and built-up	Urban districts - commercial and business	89	92	94	95
Snow and ice	NA	0	0	0	0
Wetland	NA	0	0	0	0
Water	NA	0	0	0	0

5.0 METHODS

5.1. Estimating the Magnitude of the November 15, 2021 Flood

As an independent effort, the magnitude of the November 15, 2021 flood for the Coldwater River at Merritt was estimated using a two-dimensional (2-D) hydraulic model developed for Fraser Basin Council on behalf of the Town of Merritt in 2021 (BGC, June 4, 2021). The model was built in HECRAS 6.2, a public domain hydraulic modeling program developed and supported by the United States Army Corps of Engineers (USACE) (Brunner & CEIWR-HEC, 2021). The methodology used by BGC is described in the following sections.

5.1.1. Calibrating Manning's Roughness Values

Manning's roughness values (n)[12] were calibrated by comparing the modelled flood extents to those of the May 16, 2018 flood as observed in Copernicus Sentinel-1 satellite imagery. This flood event corresponded to a 2- to 5-year event for the Coldwater River (08LG010 – *Coldwater River at Merritt* hydrometric station) and a 50-year event for the Nicola River (08LG065 – *Nicola River at the outlet of Nicola Lake* hydrometric station). A Manning's n of 0.025 for the main channel of the Coldwater and Nicola Rivers achieved a good match between the modelled and observed flood extents as shown in Figure 5-1.

The Manning's n values used for the present work are shown in Figure 5-2 and Table 5-1. Further discussion on model calibration is provided in BGC (June 4, 2021).

[12] Manning's n is a coefficient representing the friction applied to flow by the channel it is passing through.

Figure 5-1. Model results for inundation extent (blue line) plotted against the observed flooding captured on May 16, 2018. Photo source: Modified Copernicus Sentinel data [May 16, 2018]/Sentinel Hub.

Table 5-1. Associating land class with Manning's n.

Land Class	Manning's n	Color
1. Forest	0.1	
2. Grassland	0.035	
3. Urban and Built-up	0.05	
4. Main Channel	0.025	

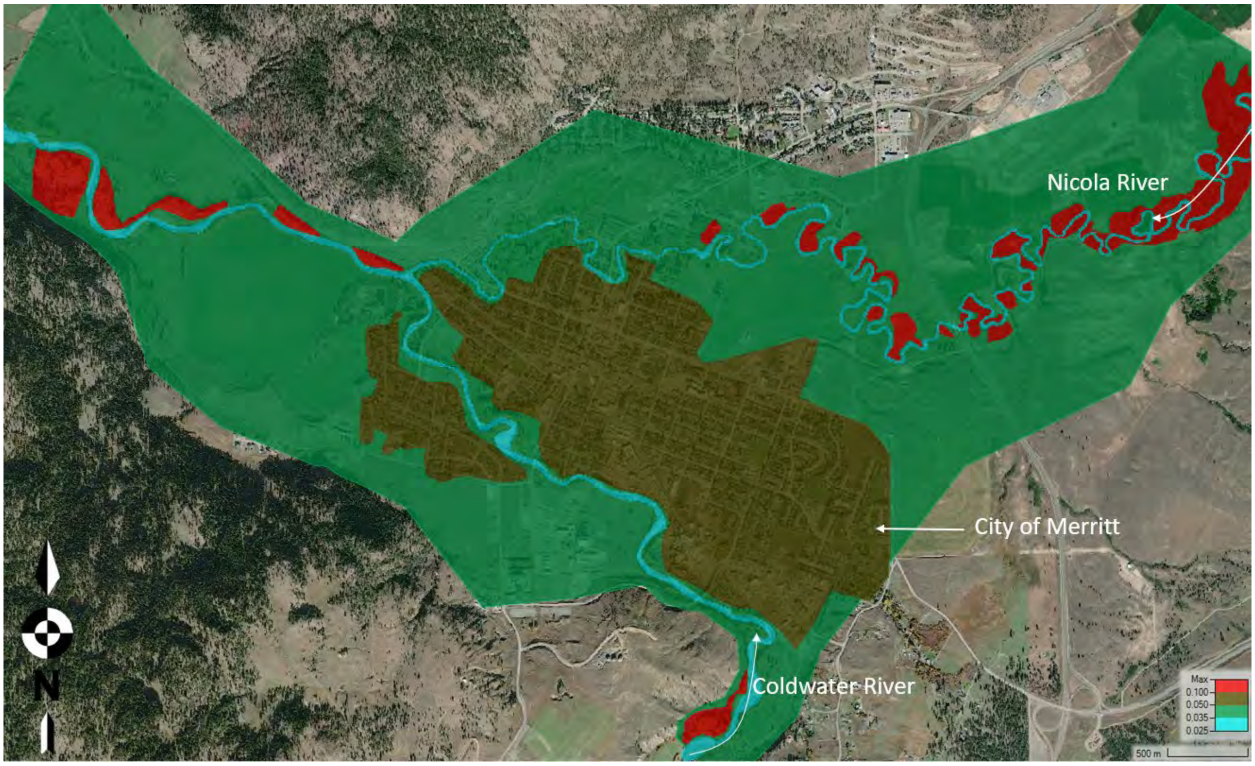

Figure 5-2. Manning's n roughness layer defined for the model.

5.1.2. Estimating Flood Magnitude

Four different discharge scenarios for the Coldwater River were run to compare against the HWMs: 400, 300, 250, and 200 m^3/s. Each scenario was run for an 8-hour event, ramping up to the peak flow in 2 hours and with the model reaching steady state after 6 hours. This duration roughly matches the duration of peak flows measured at the *Coldwater River at Merritt* (08LG010) hydrometric station during the event. There was typically 0.01 m or less change in water surface elevation (WSE) between 1 hour after the peak discharge was reached and the end of the run in the areas where the HWM were collected. This suggests that running the model to steady state rather than approximating a hydrograph did not meaningfully impact the results. The depth of water, inundation extents, and WSE results were compared to those surveyed and observed in the photos and videos of the event (see Drawing 01).

5.1.3. Comparing Pre- and Post-flood Terrain in Estimating Flood Magnitude

The flood magnitude was initially estimated using the pre-flood terrain. The pre-flood terrain was available based on recent floodplain mapping work completed by BGC for FBC (BGC, June 4, 2021). The post-flood terrain was characterized on March 7 and 8, 2021 by Ecoscape. The same four discharge scenarios for the Coldwater River were run to compare against the HWMs: 400, 300, 250, and 200 m^3/s using a similar methodology as the pre-flood terrain (Section 5.1.2). An additional 500 m^3/s run was also performed using the post-flood terrain.

5.2. Frequency-Magnitude Relationship

The standard practice to estimate the frequency-magnitude relationship is based on the annual maxima series (AMS) to which a statistical distribution (e.g., Generalized Extreme Value) is fit. This approach is adequate for watersheds where peak flows are driven by a single process like snowmelt. However, it can be inappropriate for watersheds where peak flows are caused by more than one process, like snowmelt and ARs, that may form a separate data population thus violating the rules of data homogeneity in statistical analysis (Waylen & Woo, 1982; 1983).In the Coldwater River watershed, ARs have been related to 7 of the largest 10 floods on record suggesting that ARs exert an important control on the statistical distribution of annual maximum flood events (Figure 5-3). Snowmelt-related floods occur more often with a magnitude that is typically less than AR-related peak flows in this watershed. On occasion, rain-on-snow events occur in the spring but these events do not dominate the historical record.

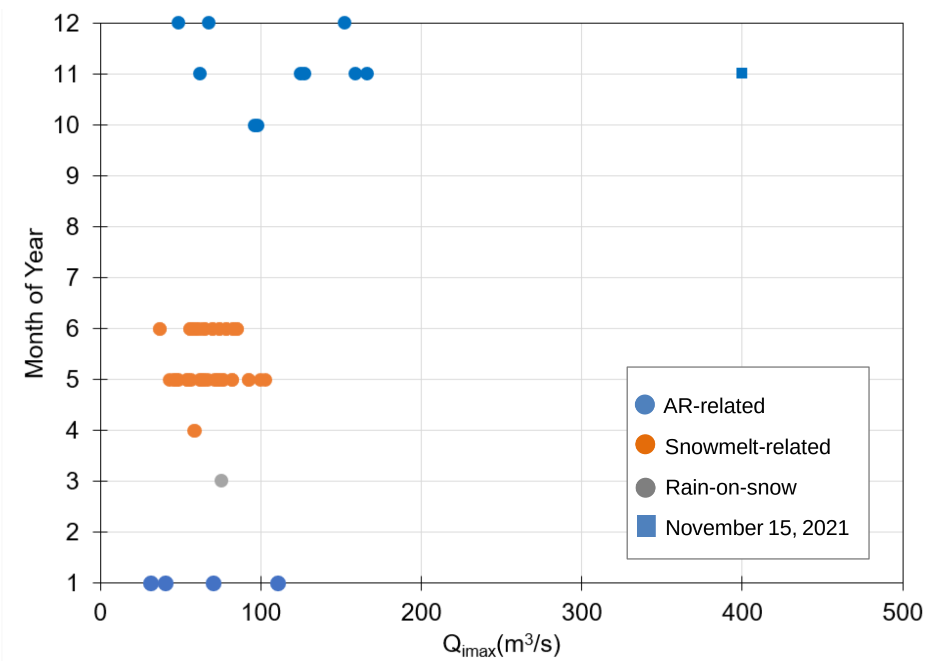

Figure 5-3. Timing of the historical annual maximum instantaneous peak flow estimates recorded at the *Coldwater River at Brookmere* (08LG048) hydrometric station over the 1965 to 2020 period.

Peak flows driven by snowmelt and ARs have different distributions as defined by their shape and magnitude of quantiles in the Coldwater River watershed (Figure 5-4). For example, snowmelt-related floods tend to have the largest peak flow for lower return period events (i.e., approximately 2-year [50% AEP] to 10-year [10% AEP]). However, AR-related floods tend to have the largest peak flow for higher return period events (i.e., 20-year [5% AEP] and above).

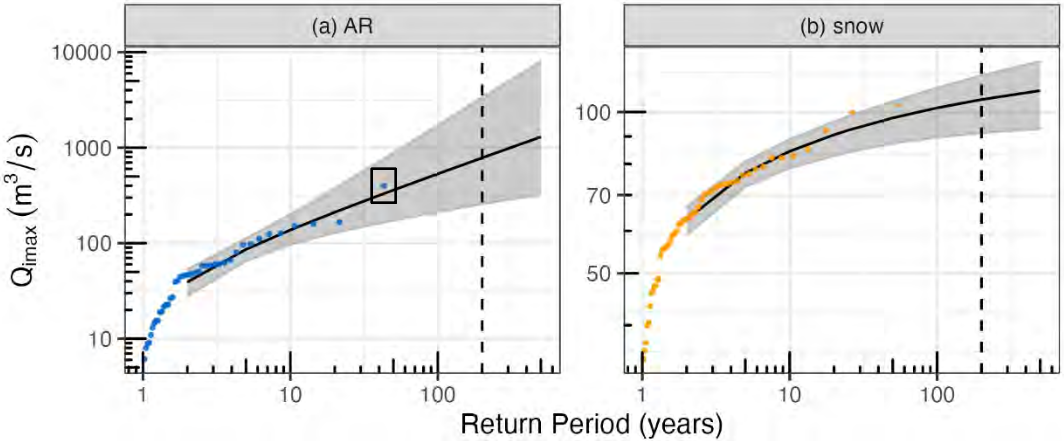

Figure 5-4. Frequency-magnitude relationships for AR-related (a) and Snowmelt-related (b) peak flows. The 90% confidence intervals are calculated using the bootstrap statistical method with 1000 iterations. Both axes are on a log-10 scale. A GEV distribution is assumed to illustrate the differences between both datasets. The November 15, 2021 event is highlighted by the black box in (a).

Another statistical approach was warranted given the mixed hydrological regime in the Coldwater River watershed. BGC engaged Dr. Vincenzo Coia from the Department of Statistics at The University of British Columbia (UBC) to provide technical direction on a statistical approach to a frequency-magnitude relationship in the Coldwater River considering a mixed hydrologic regime where both types of flood events are captured. With his support, a statistical model for the annual maxima was built combining models for both snowmelt- and AR-related floods (Waylen and Woo, 1982; Bobotas & Koutras, 2019).

A related practice is to estimate the frequency-magnitude relationship based on peaks over threshold (POT). The distribution fit to these data represents any “large” event, which occurs at a random frequency, and could be pooled to obtain the distribution of the annual maximum flood. While this method may indeed result in a well-fit model, preliminary results (based on AR-related peaks) suggest poorer model performance, and so it was not pursued as part of this analysis.

The frequency-magnitude relationship was built for the following return periods (% AEP): 20-year (5% AEP), 50-year (2% AEP), 100-year (1% AEP), 200-year (0.5 % AEP), and 500-year (0.2 % AEP).

5.2.1. Differentiating between AR and Snowmelt-related Peak Flows

BGC compiled a dataset of historical peak flows related to ARs and snowmelt. Snowmelt-related peak flows were extracted for every freshet over the record period from April to June. To associate an AR with a peak flow, all ARs within the Coldwater River watershed were identified from September to March from 47.5° to 50° N using the SIO-R1 Catalog (Gershunov et al., 2017). These AR events were cross-referenced with the daily mean streamflow recorded at the *Coldwater River at Brookmere* (08LG048) hydrometric station. An AR event was associated with a daily mean peak flow if the hydrological response occurred on or up to 6 days after the AR event. The daily mean peak flow is considered AR-related if the IVT field exceeds the 250 kg/m/s threshold value within at least one of those 7 days (Sharma & Déry, 2020b). Both AR-related and snowmelt-related peaks appear to be independent, including temporally.

Rain-on-snow events are present in the AMS in the spring. However, the role of ARs on snowmelt in the spring contributing to rain-on-snow events was not considered explicitly in the statistical model because only a few of those events are present in the dataset, the peak flow magnitude is in between snowmelt-related and AR-related peak flows, and the AR frequency seems to be the lowest in the spring, at least historically (Sharma & Déry, 2019). Consequently, a statistical model for the annual maxima was built combining models for both snowmelt- and AR-related floods only.

5.2.2. Dataset Extension

A total of 56 years of annual maxima data are available. Out of these, 53 Q_{imax} records are available of which 12 occurred from October through to January related to AR events and the remaining 41 Q_{imax} records occurred following snowmelt in the spring. The Q_{imax} records were extended from an annual maxima series to a double maxima series (DMS), where one snowmelt-related peak (corresponding to April, May, and June) and one AR-related peak (if present, corresponding to September through March) were included for each year on record.

The DMS was constructed using the available Q_{max} data. The Q_{imax} were inferred from the Q_{max} by fitting a linear regression between both estimates available in the historical record. A flood type-specific regression was built for snowmelt- and AR-related peak flows separately.

Both Q_{imax} and Q_{max} records were not available for all annual maxima data points to build the regression. For example, a total of 10 pairs were available for the AR-related peaks (not 12) while 38 pairs were available for the snowmelt-related peak flows (not 53). The slope of the regression was calculated using the least squares estimate and the coefficient of determination (R^2) was calculated to assess the overall fit of the regression.

5.2.3. Historical Trend Characteristics

The historical trend was characterized for both snowmelt- and AR-related peak flows to guide the need for a non-stationary approach. The trends were characterized using the Sen's[13] slope and the Mann-Kendall[14] test. The alpha threshold level was selected to be 0.001 for statistical significance to make sure the trend is real.

5.2.4. Statistical Model Development

The frequency-magnitude relationship was established by combining models for AR-related and snowmelt-related peak flows. The frequency analysis was based on the maximum value for each of the snowmelt- and AR-related peak flows by splitting the year (January to December) in two

[13] The Sen's Slope is a non-parametric estimate of the slope of the line practical when the data elements don't fit a straight line.

[14] The non-parametric Mann-Kendall test is widely used to detect consistently increasing or decreasing trends through time.

forming the Dual Maximum Series (DMS) – one peak flow in the spring in response to snowmelt and one peak in the fall/winter in response to an AR event, if any.

A suite of probability distributions was compared given the uncertainty in how well the tail behaviour can be defined due to the limited large flood events in the record characteristic of heavy tailed distributions[15]. The specific distributions were selected by considering goodness-of-fit metrics and hypothesis testing including the Akaike Information Criterion[16] (AIC), the Bayesian Information Criterion[17] (BIC), and the Anderson-Darling Criterion[18] (ADC) for a suite of distributions including Normal, Log Normal, Gumbel (EV1), Freshet (EV2), GEV, Pearson Type III, and Log Pearson Type III. The GEV and Log Pearson Type III were added regardless for comparison based on the standard of practice in Canada (Zhang et al., 2020) and the US (England et al., 2019). The Gumbel distribution was also considered explicitly given its use in the prediction of floods generated by mixed processes (Waylen & Woo, 1982, 1983).

The maximum likelihood estimate (MLE) method of inference (i.e., “fit method”) is theoretically the most efficient approach to determine distribution parameters. It requires a relatively large sample size (i.e., > 40 records) to achieve convergence of the distribution parameter estimates. This method was used to estimate the parameters of the GEV and Log Normal distributions for the snowmelt-related floods; however, the maximum goodness-of-fit estimates (MGE) method of inference was used instead to fit the Pearson distributions (Pearson Type III, Log Pearson Type III) for the AR-related floods due to convergence issues with the MLE. Separate simulations indicated that both MGE and MLE yielded comparable estimates of the 200-year (0.5% AEP) flood. Alternative inference methods such as the method of moments or linear moments were considered given their better small sample properties compared to MLE; however, they were not used because they rely on the sample mean which may not be appropriate for heavy tailed cases.

The annual maximum flow (AMS) distribution can be obtained by noting that the peak flow in any given year is the maximum of the snowmelt-related peak flow and the AR-related peak flow. Such a distribution can be obtained in terms of its probability of non-exceedance (1 - AEP) of a given peak flow value, which can be obtained by multiplying the respective non-exceedance probabilities of the snowmelt-related and AR-related peak flows (Waylen & Woo, 1982). The computation involved with this type of model combination was done through the distplyr R package (Coia et al., 2022).

15 Heavy tailed distributions are made up of mostly small values with outliers of very high values. Thus, heavy tailed distributions will go to zero slower than other distributions. The tail behaviour can be difficult to model given the limited number of events of high value.

16 The AIC is a measure to assess the relative fit of models to data. This measure is based on the log-likelihood with a penalizing term for the number of variables.

17 The BIC is similar to the AIC but the BIC has a larger penalty term for the number of variables.

18 The ADC is a statistical test that gives more weight to the tails of distributions.

5.2.5. Model Performance

A “leave one out” cross-validation approach based on the quantile score was used to assess the performance of the different choices of distributions and subsequently inform the best choice of models. This type of cross-validation was used to assess how accurate the statistical model performs in practice. The influence of each year was assessed individually by first fitting models without that year’s data, and then calculating the quantile score using that year’s data. The overall score was obtained by averaging each year’s score. The overall score was calculated for each return period (% AEP). The model with the lowest quantile score is considered the best for that specific return period (% AEP).

5.2.6. Sensitivity Analysis

A sensitivity analysis is a study of how different values of an independent variable influence a dependent variable. A sensitivity analysis was conducted given the uncertainty in the magnitude of the November 15, 2021 flood (independent variable) recorded at the *Coldwater River at Brookmere* (08LG048) and the *Coldwater River at Merritt* (08LG010) hydrometric stations. The sensitivity of the frequency-magnitude relationship (dependent variable) was assessed using a flood magnitude of 300 m^3/s and 500 m^3/s for the November 15, 2021 flood. The wide range in peak flows considered in the sensitivity analysis (300 to 500 m^3/s) reflects the influence of peak flow magnitude on water surface elevation in the Coldwater River at Merritt given the flat topography.

5.2.7. Pro-rating to Merritt

The flood frequency analysis was completed for the *Coldwater River at Brookmere* (08LG048) hydrometric station. The Q_{imax} measurements were transferred downstream by prorating the estimates proportionally by watershed area using Equation 5- 1:

$$\frac{Q_U}{Q_G} = \left(\frac{A_u}{A_G}\right)^n \qquad \text{[Eq. 5-1]}$$

where Q_U is the Q_{imax} (m^3/s) at Merritt, Q_G is the Q_{imax} (m^3/s) at Brookmere, A_u is the watershed area (km^2) at Merritt (917 km^2), and A_G is the watershed area at Brookmere (316 km^2), and *n* is a site-specific exponent related to peak flow data at both locations.

Typically, a value for *n* is chosen based on the watershed area size (Watt, 1989). For the Coldwater River, an average exponent value of approximately 0.06, ranging from 0 to 0.27, was calculated based on 11 paired observations of Q_{imax} at both hydrometric stations between 2005 and 2020. Of these observations, two are AR-related, eight are snowmelt-related, and one is likely a rain-on-snow event based on timing. Given the limited number of data points, the influence of the flood-type (AR-related vs. snowmelt-related) on this exponent could not be assessed statistically. However, it is likely that the relationship is seasonal with a different relationship in the spring compared to the fall.

This low average n value suggests that little flow accumulates in the Coldwater River between Brookmere and Merritt, despite the difference in watershed areas (600 km^2) and over 20 small tributaries. As a result, flood magnitude between Brookmere and Merritt were assumed to be approximately the same. This conclusion is consistent with the precipitation pattern observed during the November 15, 2021 flood, with most of the precipitation occurring in upper to mid reaches of the watershed with limited accumulation between Brookmere and Merritt (Figure 2-4).

5.3. Accounting for Climate Change

5.3.1. Accuracy of the VIC-GL Model

The capability of a hydrological model to simulate snowmelt peaks varies from its ability to simulate rainfall, especially AR-related. The accuracy of the VIC-GL model in estimating the magnitude of the historic annual maximum daily mean streamflow for both snowmelt- and AR-related peak flows was assessed by comparing modelled and recorded annual maximum daily mean data at the *Coquihalla River above Alexander* (08MF068) hydrometric station over the 1965 to 2020 time period by means of a correlation analysis. In addition, the largest historical flood events recorded (e.g., 1990, 1995, 2003, 2006, and 2007) were compared with the model results to assess the VIC-GL model accuracy on different flood types.

5.3.2. Future Trend Characteristics

The future trends in peak flows were characterized by extracting three separate time series from PCIC's projected daily mean streamflow at the *Coquihalla River above Alexander Creek* (08MG068) hydrometric station for each of the six GMC runs under RCP 8.5:

1. the AMS;
2. the annual maximum rainfall-related (AR and non-AR) peak flows; and
3. the annual maximum snowmelt-related peak flows.

The rainfall-related (AR and non-AR) peak flows were extracted for the September to March period. The September to March peak flows were not differentiated between AR-related and those related with other types of rainfall systems. The snowmelt-related peaks were extracted for the April to August period.

Curves were fit to the projected maximum flows for the three separate time series (e.g., AMS, rainfall-related [AR and non-AR], and snowmelt-related) using a LOESS regression, representing the geometric mean across time of the pooled data from the six GCMs. LOESS[19] regression was selected to capture the subtleties of the trends. The scales were removed from each curve by dividing out the current (2022) value of the curve, capturing how many times greater each future year's geometric mean is compared to the geometric mean in 2022 – the "dimensionless scaling factors". These scaling factors are assumed to hold for the *Coldwater River at Brookmere* (08LG048) watershed.

[19] Loess regression is a nonparametric technique that uses local weighted regression to fit a smooth curve.

5.3.3. Assessing Validity of Scaling Assumption

The magnitude shift due to climate change is not likely to be the same for different quantiles (e.g., 2-year [50% AEP] and the 200-year [0.5% AEP] event). The reliability of the scaling assumption was verified using PCIC's projected streamflow data by observing the residuals (as defined as a ratio of simulated peak flows to the LOESS geometric mean) of the simulated maxima about the fitted geometric mean curves. If the distribution of the residuals appears to be constant over time, the scaling assumption was deemed reasonable, suggesting that the dimensionless scaling factors capture the key changes in the peak flow distribution based on the six GCMs.

5.3.4. Climate-adjusted Case

The dimensionless scaling factors were subsequently used to re-scale the peak flow distributions (AMS, snowmelt-related, and rainfall-related [AR and non-AR]) to the *Coldwater River at Brookmere* (08LG048) watershed, so that future peak flow distributions compare to the current peak flow distribution by the same multiple that future geometric means compare to the current geometric mean in PCIC's projected daily mean streamflow.

Two methods were compared for obtaining the future peak flow distributions:

4. the dimensionless scaling factors were applied to the AMS distribution, for which the best estimate is the DMS-based (stationary) distribution, and
5. the dimensionless scaling factors were applied to the snowmelt-related and AR-related peak flow distributions, which were subsequently combined via maximization for each future year (as in the stationary DMS-based approach).

In either case, a distribution for the annual maximum is obtained for each future year, from which a single climate-adjusted FM relationship can be obtained to inform infrastructure development. Three methods for obtaining a climate-adjusted FM relationship are discussed in the results.

5.3.5. Characterizing Variability

A bootstrap statistical approach was taken to characterize the variability in the six GCMs. Instead of using each GCM to obtain six separate model projections, the GCM data were pooled, from which many bootstrap resamples (more than just six) were drawn. This variability is taken together with the uncertainty in the distribution fitting procedure to obtain overall confidence intervals for the climate-adjusted frequency-magnitude relationship.

5.4. Watershed Similarities between the Coldwater River and the Coquihalla River

A suite of 18 characteristics including watershed, climate, and physiography were extracted over the Coldwater River and Coquihalla River watersheds based on the potential to influence the magnitude of flood events (Table 5-2). A qualitative comparison between both watersheds was used to infer the appropriateness of the scaling factor transfer from the Coquihalla River above Alexander Creek watershed to the Coldwater River at Merritt.

Table 5-2. List of selected watershed characteristics.

Type	No.	Acronym	Characteristic	Units	Dataset	Reference
Watershed	1	Centroid_Lat	Latitude at the centroid location in the watershed polygon	degrees	STRM	Farr et al. (2007)
	2	Centroid_Long	Longitude at the centroid location in the watershed polygon	degrees		
	3	Centroid_Elev	Elevation at the centroid location in the watershed polygon	m		
	4	Area	Area of the watershed polygon	km2		
	5	Relief	Maximum minus minimum watershed elevation	m		
	6	Length	Area divided by perimeter	km		
	7	Slope	Watershed length divided by relief times 100	%		
Climate	8	MAP	Mean annual precipitation	mm	Climate NA	Wang et al., (2016)
	9	MAT	Mean annual temperature	oC		
	10	PAS	Precipitation as snow	mm		
	11	PPT_wt	Winter precipitation (Dec, Jan, Feb)	mm		
	12	PPT_sp	Spring precipitation (Mar, Apr, May)	mm		
	13	PPT_sm	Summer precipitation (Jun, Jul, Aug)	mm		
	14	PPT_fl	Fall precipitation (Sep, Oct, Nov)	mm		
Physiographic	15	Forest	Forest cover in the watershed	%	NALCMS	Latifovic et al. (2012)
	16	Water_Wetland	Wetland and open water cover in the watershed	%		
	17	Urban	Urban cover in the watershed	%		
	18	CN	Inferred based on integrating land cover and soils cover	unitless	NALCMS and HYSOGs250m	Latifovic et al. (2012) and Ross et al., (2018)

6.0 RESULTS

6.1. Estimating the Magnitude of the November 15, 2021 Flood

As shown in Table 6-1, for the model using preflood terrain the 400 m^3/s model run is the best match to the observed HWMs as characterized by the lowest error from modelling. Similarly, based on videos taken during the flooding (Irnie, 2021), inundation of Houston Street occurred up to at least Granite Avenue, a region that was only inundated in the 400 m^3/s run. This result suggests that the peak flow in the Coldwater River during the November 15, 2021 flood was approximately 400 m^3/s, consistent with the original estimate at the 08LG048/08LG010 hydrometric stations. Modelling with the post-flood terrain, the 300 m^3/s run results in lowest error, though all runs using the post flood terrain. Notably the error for this run is higher than those achieved for the 300 and 400 m^3/s runs using the preflood terrain. A table with all the measured HWMs and modelled WSE at those locations is provided in Appendix A.

Table 6-1. Average difference between model results and observed HWMs for each scenario.

Terrain	Scenario Discharge (m^3/s)	Mean Difference in WSE (m)	Normalized Root Mean Squared Error
Preflood	400	0.02	0.13
Preflood	300	0.20	0.15
Preflood	250	0.31	0.18
Preflood	200	0.41	0.24
Post Flood	500	-0.15	0.21
Post Flood	400	-0.08	0.19
Post Flood	300	-0.01	0.18
Post Flood	250	0.23	0.22
Post Flood	200	0.29	0.22

6.2. Frequency-Magnitude Relationship

6.2.1. Linear Regression between Q_{imax} and Q_{max}

The linear regressions between paired observation (Q_{imax} and Q_{max}) for AR-related-, and snowmelt-related peak flows are shown in Figure 6-1. The average ratio between Q_{imax} and Q_{max} (I/D ratio) is larger for AR-related peak flows (1.49) compared to snowmelt peaks (1.13) in the Coldwater River watershed.

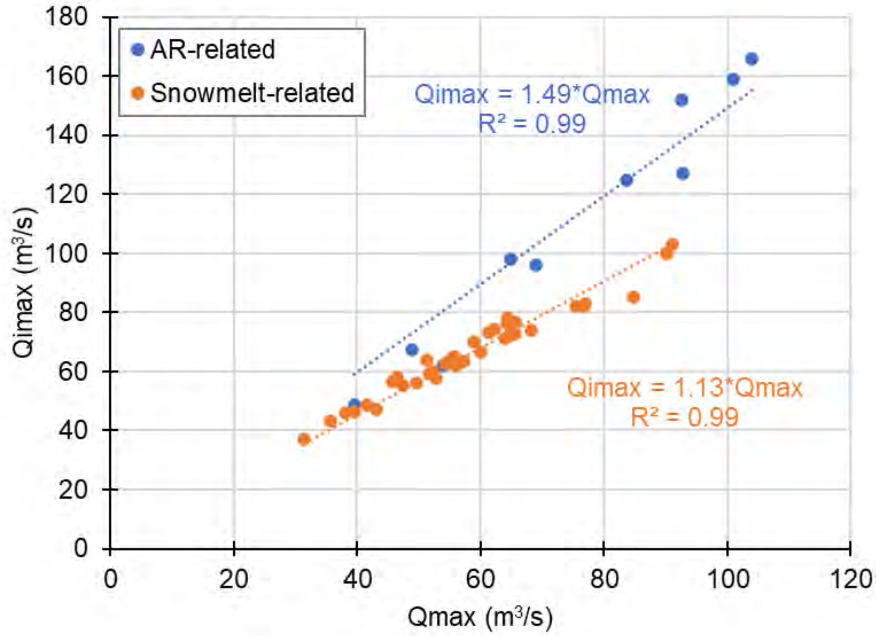

Figure 6-1. Regression between paired observation (Q_{imax} and Q_{max}) for AR-related peak flows (blue), and snowmelt-related peak flows (orange).

6.2.2. Historical Trend Characteristics

The magnitude of AR-related annual maximum peak flows has not changed between 1967 and 2021 in the Coldwater River watershed. The Sen's slope is slightly positive 0.45 with and 0.34 without the November 15, 2021 flood. The trend is not significant with (p-value = 0.26) or without (p-value=0.49) the November 15, 2021 flood (Figure 6-2a). The record peak flow is the November 15, 2021 flood with an estimated value of 400 m^3/s (Section 6.1). The next largest peak flow was recorded in 1995 with a value of 166 m^3/s in response to an AR event at the end of November. The AR-related peak flows range from 6 to 400 m^3/s, with a median value of 47 m^3/s. The AR-related peak flows are skewed to the right and characterized by a heavy right tail with the presence of a few large events (Figure 6-2b).

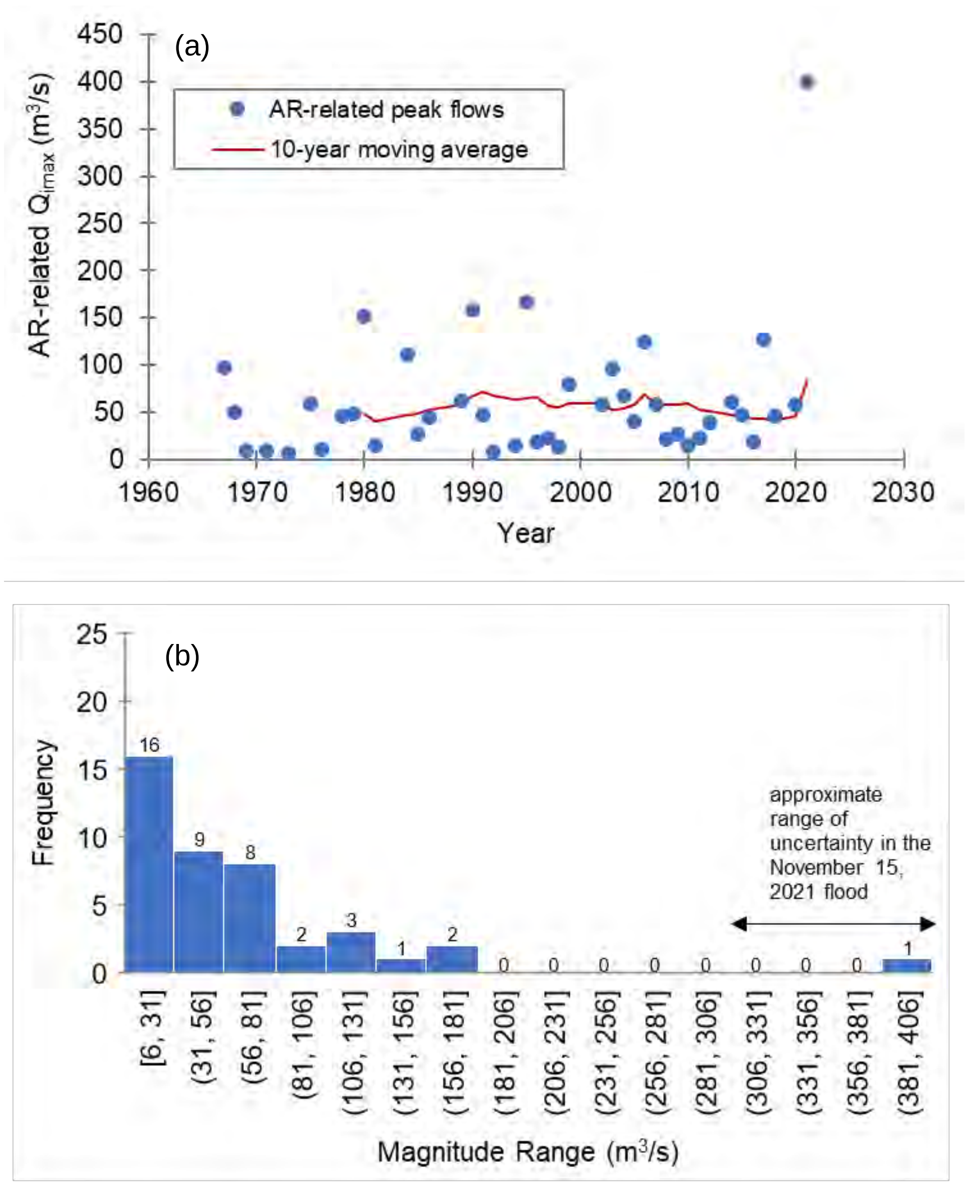

Figure 6-2. Temporal change in AR-related peak flows a) and corresponding histogram b) at the *Coldwater River at Brookmere* (08LG048) hydrometric station over the 1967 to 2021 period.

The magnitude of snowmelt-related annual maximum peak flows does not have a statistically significant upwards or downwards trend over the 1967 to 2021 period (p-value = 0.84) (Figure 6-3a). The largest snowmelt-related peak flow was recorded in 1972 with a value of 103 m^3/s recorded at the end of May. The snowmelt-related peak flows range from 35 to 103 m^3/s, with a median value of 63 m^3/s. The snowmelt-related peak flows are slightly skewed to the right and characterized by a short right tail with the presence of several large events (Figure 6-3b).

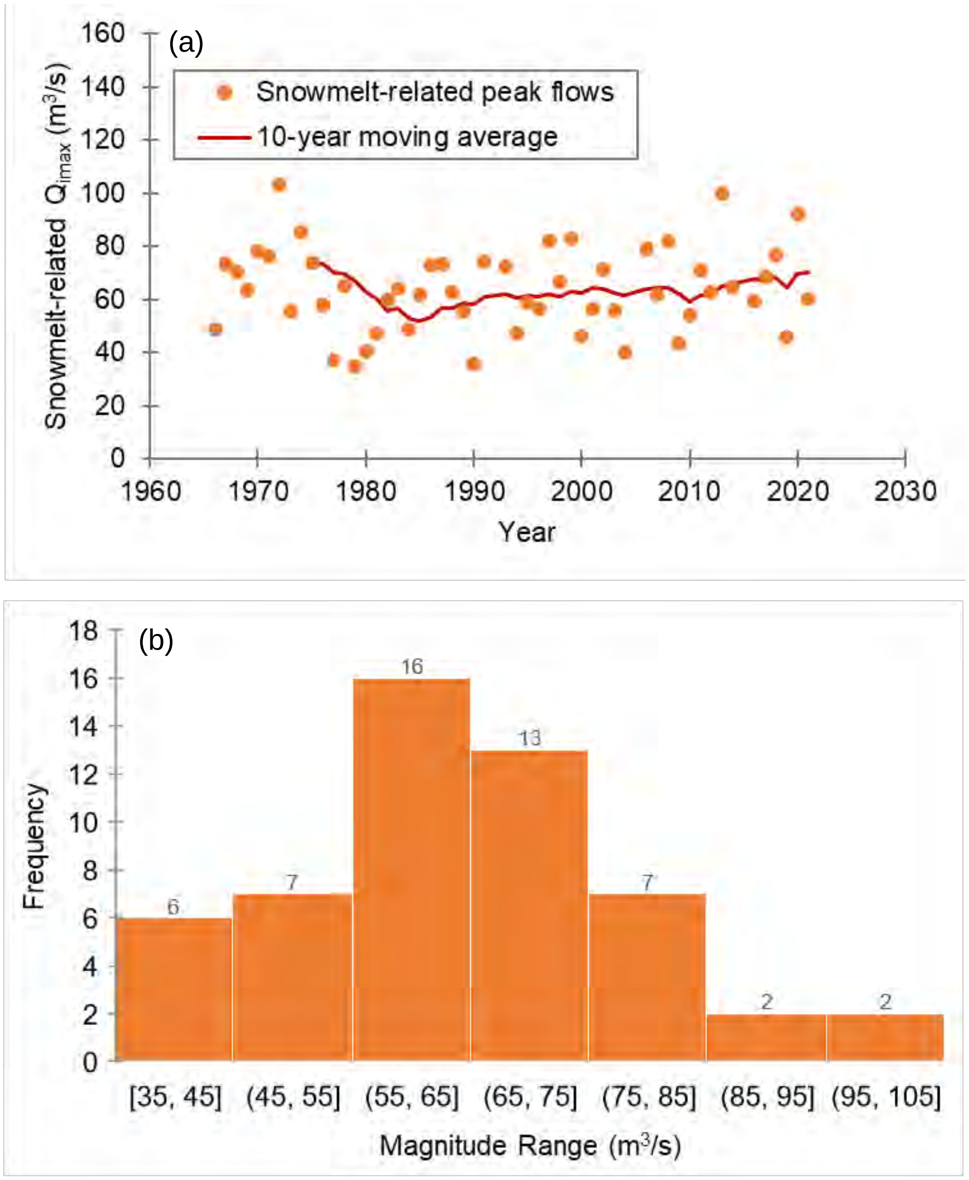

Figure 6-3. Temporal change in snowmelt-related peak flows a) and corresponding histogram b) for the *Coldwater River at Brookmere* (08LG048) hydrometric station over the 1966 to 2021 time period.

6.2.3. Statistical Model Development

A suite of distributions was compared for the analysis of AR- and snowmelt-related peak flows including the Normal, Log Normal, Gumbel (EV1), Freshet (EV2), GEV, Pearson Type III, and Log Pearson Type III using the AIC, BIC, and ADC. Results for the selected distributions are summarized in Table 6-2 for AR-related peak flows. In addition to the Log Normal distribution for the AR-related peak flows, the GEV, the Log Pearson Type III, and the Pearson Type III were carried forward for comparison. The Pearson Type III was added as a candidate because it captured the tail behaviour well in the case where the November 15, 2021 flood was overestimated.

Table 6-2. Distribution selection for AR-related peak flows.

Statistical Tool	Distribution Selection	Score / Reasoning
AIC	Log Normal	428.5
BIC	Log Normal	432.0
ADC	Log Normal	0.13
AIC	Pearson Type III	426.4
ADC	Pearson Type III	0.10
---	GEV	Standard for Canada
---	Log Pearson Type III	Standard for the US

Results for the selected distributions are summarized in Table 6-3 for snowmelt-related peak flows. In addition to the Normal distribution for the snowmelt-related peak flows, the GEV, the Gumbel (EV1), and the Log Pearson Type III were carried forward for comparison.

Table 6-3. Distribution selection for snowmelt-related peak flows.

Statistical Tool	Distribution Selection	Score / Reasoning
AIC	Normal	444.6
BIC	Normal	448.5
ADC	Normal	0.05
---	GEV	Standard for Canada
---	Log Pearson Type III	Standard for the US
---	Gumbel (EV1)	use in the prediction of floods generated by mixed processes (Waylen and Woo 1982).

6.2.4. Model Performance

The frequency-magnitude relationships show that the influence of the snowmelt-related peak flow distribution is not strong, as shown by the similarity in the frequency-magnitude relationship for any given AR-related peak flow distribution (Figure 6-4). However, the influence of the AR-related peak flow distribution is prominent as shown by the differences in the frequency-magnitude relationship for any given snowmelt-related peak flow distribution.

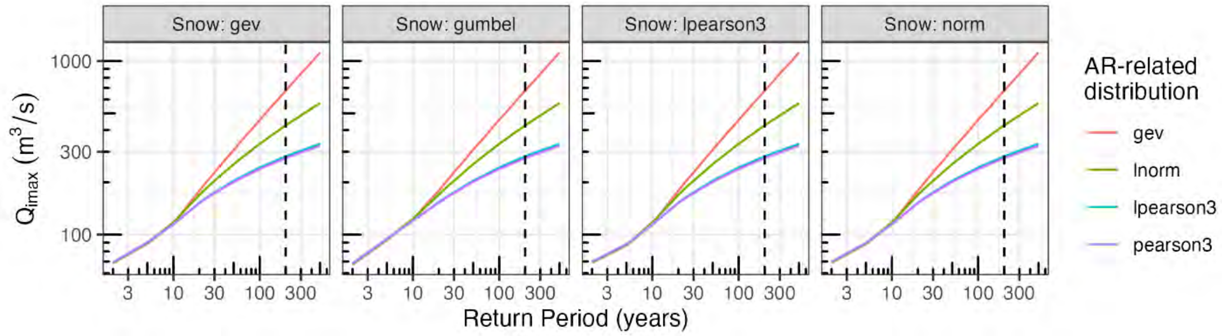

Figure 6-4. Frequency-magnitude relationship for the annual maximum Q_{imax} using different snowmelt distributions (across different panels) and different AR distributions (in different colours). Axes are on a log-10 scale. Models include the November 15, 2021 flood. The dashed line shows the 200-year (0.5% AEP) event.

The four distributions for snowmelt-related peak flows (i.e., Normal, GEV, Log Pearson Type III, and Gumbel) show nearly identical quantile scores for the 200-year flood event (0.5% AEP) (Figure 6-5). Given this similarity, the GEV distribution was chosen for snowmelt-related peak flows because of its flexibility when extrapolating to longer return periods (lower % AEPs). No additional snowmelt-related peak flow distributions were used when forming a final DMS-based model.

The four distributions for AR-related peak flows (i.e., Log Normal, Pearson Type III, Log Pearson Type III, and GEV) result in a range of quantile scores for the 200-year (0.5% AEP) flood event (Figure 6-5). The AR-related peak flow distribution resulting in the lowest (best) quantile score is the Pearson Type III (1.0), compared to the GEV, having the highest quantile score (3.0). To account for a range of tail behaviours, a mixture of three distributions was used for the AR-related peak flow distribution when building a final model: the GEV, Log Normal, and Pearson Type III. Note that an identical model is obtained when taking a mixture at the final model level, as opposed to the AR-related peak flow level – that is, a mixture of the DMS-based distributions resulting from each of the three choices of AR-related peak flow distributions.

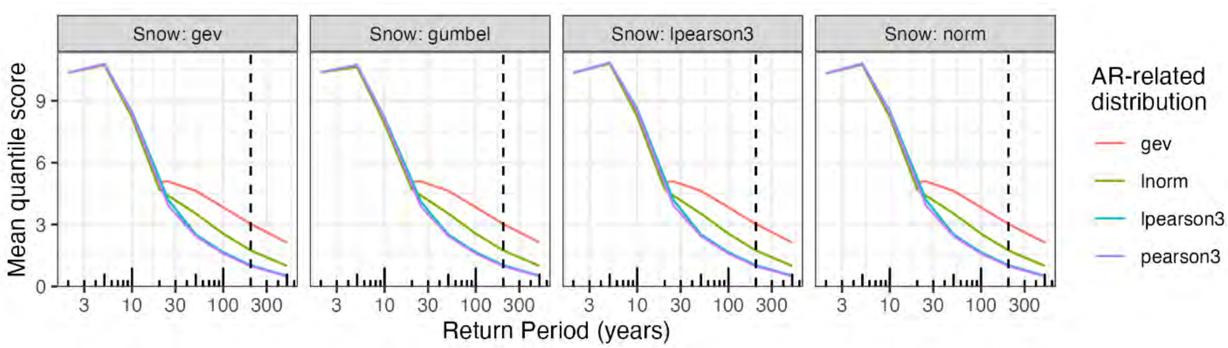

Figure 6-5. Mean quantile scores comparing each DMS model combination, plotted for each return period (% AEP) on a log-10 scale. The snowmelt-related peak distributions span different panels, and AR-related peak distributions span different colours. Models include the November 15, 2021 flood. The dashed line shows the 200-year (0.5% AEP) event. Smaller scores indicate a better model, though comparisons are only meaningful within each return period (% AEP).

The quantile score for the proposed DMS-based model is consistently lower (better) than the standard practice AMS-based model across all return periods (% AEP), a feature that remains true even when a DMS-based model is built using only one of the three AR-related peak flow distributions instead of their mixture (Figure 6-6). The quantile score for the 200-year flood (0.5% AEP) for the DMS-based model is 1.9, lying in the middle of its three constituent models, compared to a quantile score of 4.6 for the AMS-based model. The best estimate for the frequency-magnitude relationship is thus defined by the DMS-based approach.

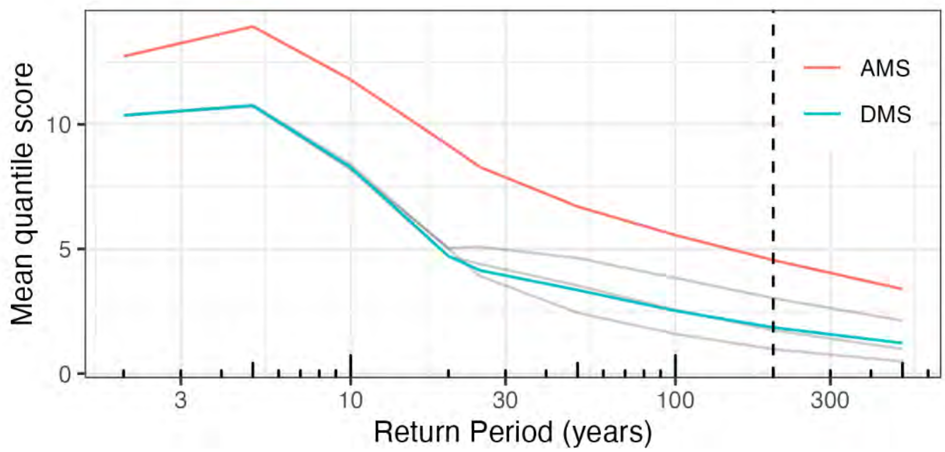

Figure 6-6. Mean quantile scores comparing the standard AMS-based model to the DMS-based model for each return period (% AEP), which is on a log-10 scale. The dashed line corresponds to the 200-year return period (0.5% AEP). Smaller scores indicate a better model, though comparisons are only meaningful within each return period (% AEP). Models include the November 15, 2021 flood. The faded gray curves represent the scores for the DMS-based models built using each of the three models composing the AR-related peak flow distribution.

6.2.5. Stationary Case

The frequency-magnitude relationship based on the standard (AMS-based) approach and the combined (DMS-based) approach is depicted in Figure 6-7. An inflection point emerges around the 10-year (10% AEP) event in the DMS-based model where peak flows become AR-related (Figure 6-7b) and the frequency-magnitude relationship becomes steeper; a feature that is not present in the frequency-magnitude relationship based on the standard approach (Figure 6-7a, Figure 6-8). The implication of this inflection point is that the largest flood event (400 m^3/s) has a shorter return period (higher % AEP) in the DMS-based model compared to the AMS-based model – a result that can be visualized by carrying the largest data point over to the right until it reaches the model curve.

The 90% confidence interval is wider on the frequency-magnitude relationship for the DMS-based model for the higher return period (% AEP) events compared to the standard (AMS-based) model. In part, this is due to the larger magnitude estimates in the DMS-based model. After accounting for this phenomenon by calculating the coefficient of variation (CV), the standard (AMS-based) model (0.42 CV) is still slightly narrower than the DMS-based model (0.53 CV) by about 21%. However, the DMS-based model still performs better (i.e., lower quantile score) overall

(Figure 6-6) due to its improved accuracy (i.e., more flexible shape) over the standard (AMS-based) model.

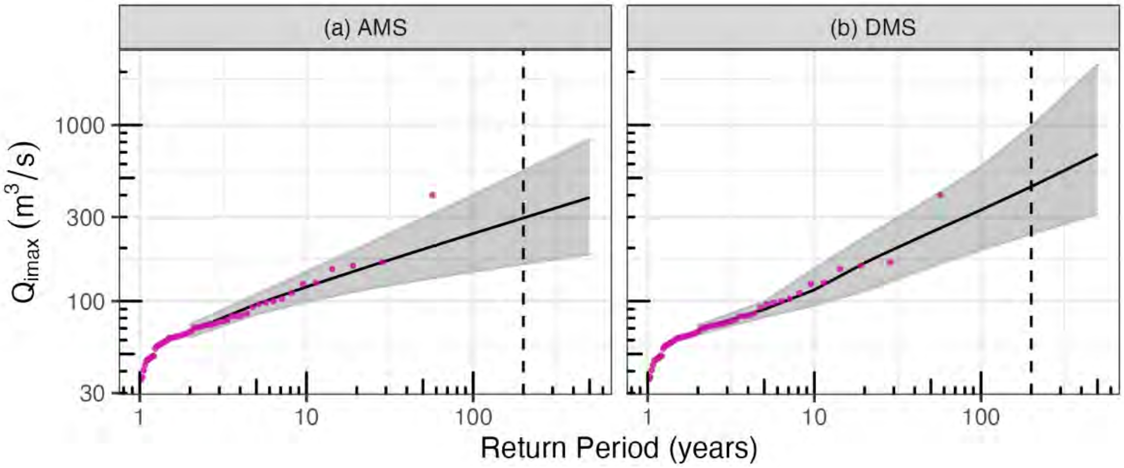

Figure 6-7. Frequency-magnitude relationship based on (a) the standard approach (AMS), and (b) the combined approach (ensemble of DMS models), with 90% bootstrap confidence bands. Both axes are on a log-10 scale. The dashed line corresponds to the 200-year event (0.5% AEP). The points represent the empirical return periods using the AMS data.

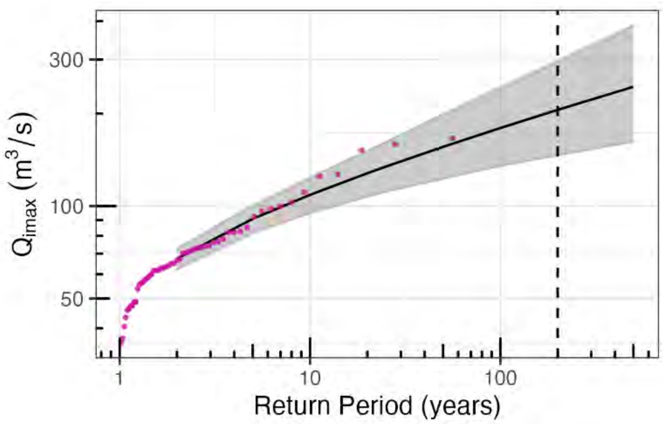

Figure 6-8. Frequency-magnitude relationship excluding the November 15, 2021 flood from the dataset, using the standard approach (AMS). Plotting parameters are otherwise identical to Figure 6-7.

The frequency-magnitude relationship over a range of return periods (% AEPs) is listed in Table 6-4. The 200-year (0.5% AEP) event in the Coldwater River in Merritt is estimated to be 445 m^3/s ranging from 240 to 980 m^3/s using the DMS-based model. This estimate is based on the assumption that the November 15, 2021 flood was 400 m^3/s. For comparison, the 200-year (0.5% AEP) event in the Coldwater River in Merritt is estimated to be 295 m^3/s ranging from 160 to 545 m^3/s using the standard (AMS-based) model including the November 15, 2021 flood. The 200-year (0.5% AEP) event using the DMS-based model lies within the confidence interval of the standard (AMS-based) model. The 200-year (0.5% AEP) event using the DMS-based model without the November 15, 2021 flood is 325 m^3/s.

Table 6-4. Frequency-magnitude relationship over a range of return periods (%AEPs), with and without the November 15, 2021 flood, in the Coldwater River at Merritt, BC. The 90% confidence intervals are based on 1,000 bootstrap iterations.

Return Period (%AEP)	Standard Approach[1] with November 15, 2021 (m^3/s)			Standard Approach[1] without November 15, 2021 (m^3/s)			Combined Approach[2] with November 15, 2021 (m^3/s)			Combined Approach[2] without November 15, 2021 (m^3/s)		
	Estimate	Lower CI	Upper CI	Estimate	Lower CI	Upper CI	Estimate	Lower CI	Upper CI	Estimate	Lower CI	Upper CI
2 (50% AEP)	70	65	75	65	60	75	70	65	75	70	65	75
5 (20% AEP)	95	85	110	90	80	100	90	80	100	90	80	95
10 (10% AEP)	120	100	145	110	95	125	115	95	155	105	90	130
20 (5% AEP)	150	115	200	130	105	150	165	115	230	145	105	185
50 (2% AEP)	195	130	295	155	125	200	245	155	380	205	135	285
100 (1% AEP)	240	150	400	180	135	245	330	195	580	260	170	390
200 (0.5 % AEP)	295	160	545	205	145	295	445	240	980	325	210	560
500 (0.2 % AEP)	385	185	830	245	160	385	680	315	2190	450	265	1060

Notes:

1. The updated (post-event) analysis based on a standard approach to frequency analysis (AMS) assumes the GEV distribution and the maximum likelihood estimate (MLE) method of inference for parameter estimation.
2. The updated (post-event) analysis is based on a combined approach (ensemble of DMS models [GEV, Log Normal, and Pearson Type III]). The MLE was used to estimate the parameters of the GEV and Log Normal distributions. The maximum goodness-of-fit estimates (MGE) method of inference was used instead to fit the Pearson Type III distribution due to convergence issues with the MLE.

6.2.6. Sensitivity Analysis

Results of a sensitivity analysis show that as the estimate of the November 15, 2021 flood increases, so does the estimate of the flood associated with each return period (% AEP) event (Table 6-5). However, when compared to the 90% confidence intervals, all three estimates fall within the range of uncertainty. For example, the 90% confidence interval for the 200-year (0.5% AEP) event ranges from 340 to 615 m^3/s assuming 300 m^3/s for the November 15, 2021 flood. While the 200-year (0.5% AEP) increases up to 475 m^3/s assuming 500 m^3/s for the November 15, 2021 flood, the estimate remains within the uncertainty bounds. These results suggest that the uncertainty in the tail behaviour of the model itself is greater than the influence of the November 15, 2021 flood magnitude (assuming it is between 300 and 500 m^3/s). This is not surprising given the limited number of large flood events of that magnitude in the historic record.

Table 6-5. Frequency-magnitude relationship assuming a range of magnitudes for the November 15, 2021 event. The 90% confidence intervals are based on 1,000 bootstrap iterations.

November 15, 2021 Peak Flow Estimate (m^3/s)	20-year (5% AEP) Peak Flow (m^3/s)			50-year (2% AEP) Peak Flow (m^3/s)			200-year (0.5% AEP) Peak Flow (m^3/s)		
	estimate	Lower CI	Upper CI	estimate	Lower CI	Upper CI	estimate	Lower CI	Upper CI
300	160	115	220	235	155	360	415	240	850
400	165	115	230	245	155	380	445	240	980
500	170	115	240	255	155	405	475	240	1070
Range	10	0	20	20	0	45	60	0	220

Performance statistics of the DMS-based approach as defined by the quantile score are comparable in all cases (e.g., 300 m^3/s, 400 m^3/s, and 500 m^3/s) with an overall slight improvement (reduction in quantile score) for the 300 m^3/s case. This result suggests that the magnitude of the November 15, 2021 flood does not influence the choice of statistical model used to build the frequency-magnitude relationship. For comparison, the 200-year (0.5% AEP) estimate without consideration of the November 15, 2021 flood is 325 m^3/s, which is a large difference compared to the estimate with the consideration of the November 15, 2021 flood which is 445 m^3/s.

6.3. Accounting for Climate Change

6.3.1. Assessing Accuracy of the VIC-GL Model

The capability of the VIC-GL model at the *Coquihalla River above Alexander Creek* (08MF068) hydrometric station to simulate the magnitude of snowmelt peaks varies from its ability to simulate the magnitude of AR-related peaks (Figure 6-9). While both flood types are captured by the VIC-GL model, its ability to simulate the magnitude of snowmelt-related peak flows is much better compared to AR-related peak flows. Results of a correlation analysis shows that there is a positive relationship between annual maximum daily mean peak flows recorded and simulated

(PNWMAmet-driven peak flows) (Figure 6-10). However, the VIC-GL model underestimates the magnitude of both snowmelt- and AR-related peak flows. The magnitude of AR-related peak flows is underestimated by over 4 times compared to that of snowmelt-related peak flows.

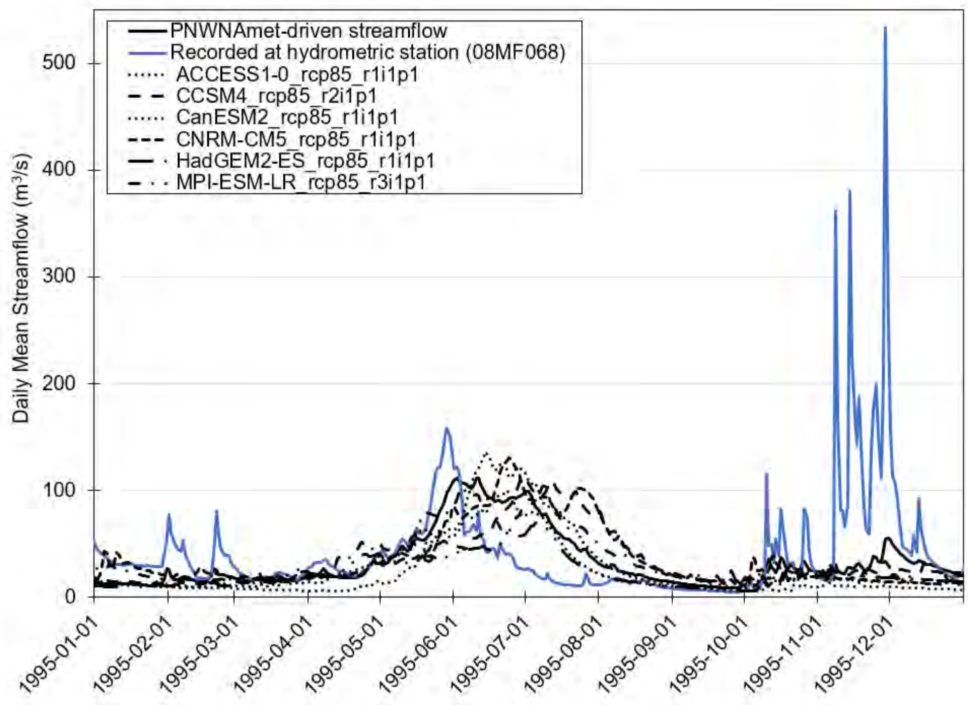

Figure 6-9. Simulated (six GCM runs of the VIC-GL model) and recorded daily mean streamflow for 1995 at the *Coquihalla River above Alexander Creek* (08MF068).

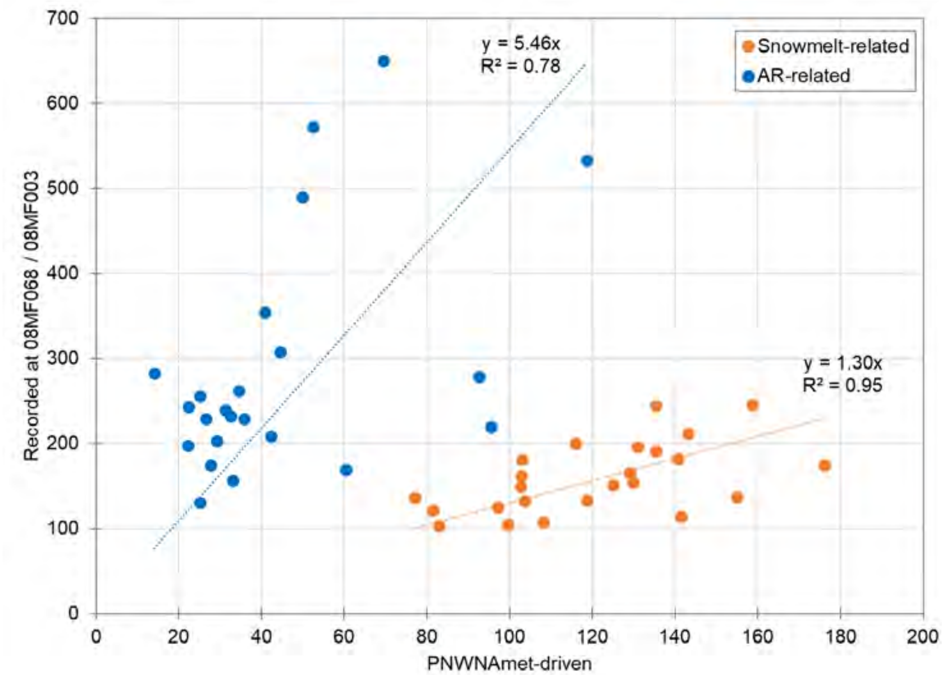

Figure 6-10. Correlation between annual maximum daily mean peak flows (m^3/s) recorded (08MF068 and 08MF003) and simulated (PNWNAmet-driven peak flows) for AR-related and snowmelt-related peak flows over the 1958 to 2012 period.

A total of 50% of the peak flows in the historical AMS are AR-related over the 1958 to 2020 period at the *Coquihalla River above Alexander Creek* (08MF068). The presence of AR-related peak flows is not adequately captured in the simulated historical AMS as driven by the six GMC-run VIC-GL models (Figure 6-11). The absence of AR-related peak flows in the simulated historical AMS shows that it is not representative of the flood types that have occurred historically in this watershed.

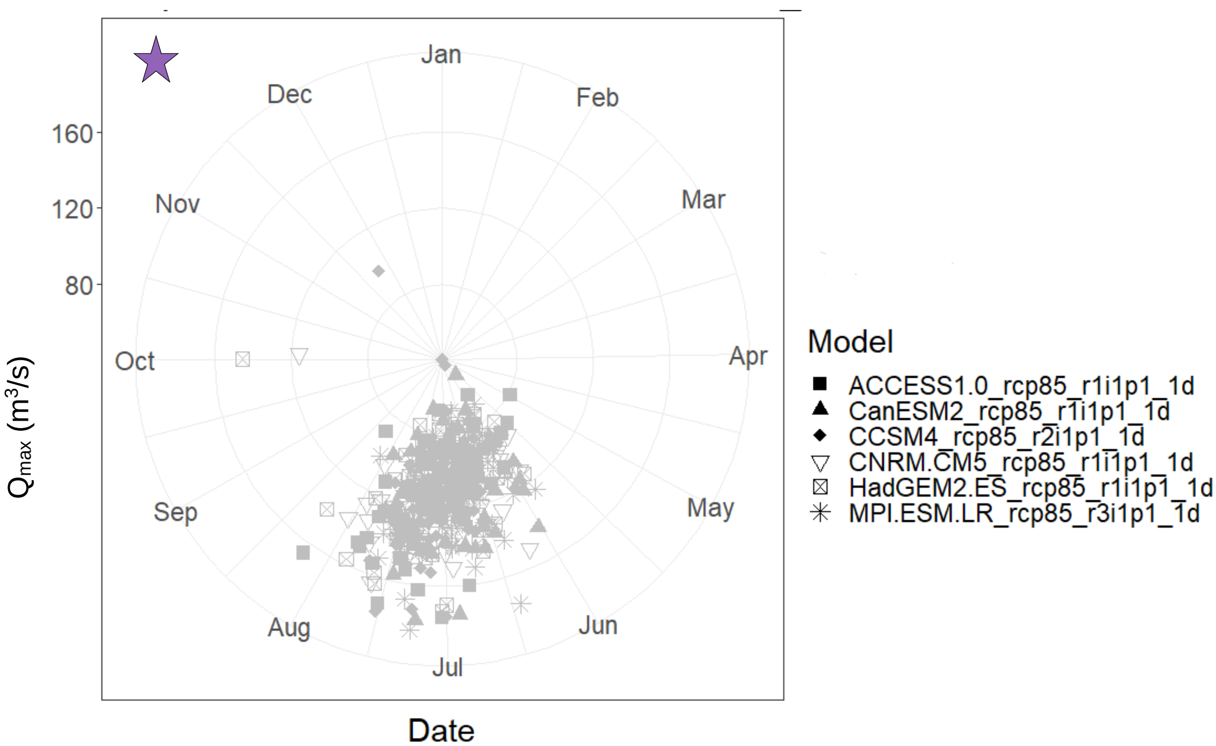

Figure 6-11. Simulated annual maximum peak flow timing based on the six GCM-run VIC-GL model over the 1946 to 2012 period at the *Coquihalla River above Alexander Creek* (08MF068) hydrometric station depicted in a polar plot. The November 15, 2021 event is shown by the purple star with a magnitude of over 1,000 m^3/s (off the chart).

6.3.2. Future Trends in Daily Mean Streamflow

The future trend in the AMS for daily mean peak flow at the *Coquihalla River above Alexander* (08MF068) hydrometric station is projected by PCIC to decrease over time until approximately 2060, when the watershed becomes rainfall-dominant and peak flows increase sporadically until 2100 (Figure 6-12a). The trend is not statistically significant (p-value >0.05) for any one GCM scenario over this time. The PCIC projections, however, do not appropriately capture the distribution of the AMS as recorded by the WSC (Figure 6-12b), and underestimate the proportion of maxima that are already rainfall-related over the historical period.

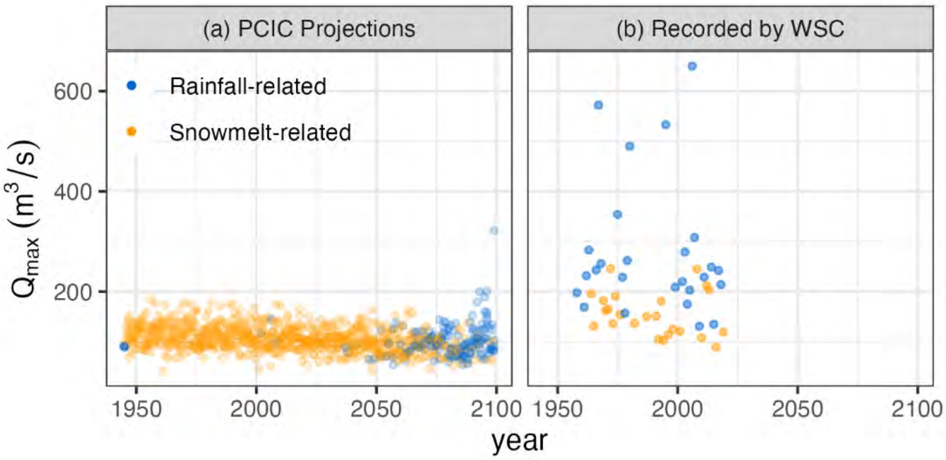

Figure 6-12. Time series for the AMS (a) as projected by the six PCIC GCMs (shown pooled), and (b) as recorded by the WSC for the Coquihalla River above Alexander (08MF068) hydrometric station.

A clearer picture arises when investigating the projected trends in the DMS, obtained by assuming the maximum peak flow that occurs in the fall/winter (September to March) period is rainfall-related (AR and non-AR), and the maximum peak flow that occurs over the spring period (April to August) is snowmelt-related (Figure 6-13). The rainfall-related (AR and non-AR) peak flows are projected to increase over time, and are the main culprit behind the lack of alignment in the AMS distributions (Figure 6-13b). The snowmelt-related peak flows, on the other hand, are projected to decrease over time (Figure 6-13c). The rainfall-related (AR and non-AR) and snowmelt-related trends are statistically significant[20] (both p-values $< 10^{-16}$) based on a Kendall correlation test for each process.

The magnitude and direction of the trends in both rainfall-related (AR and non-AR) and snowmelt-related peak flows align well with those projected by PCIC at the *Spius Creek near Canford* (08LG008) and the *Nicola River near Spences Bridge* (08LG006) hydrometric stations.

[20] Even after accounting for a higher chance of error arising due to testing multiple hypotheses (by inflating the p-values through a Bonferroni correction), the largest p-value is 0.038.

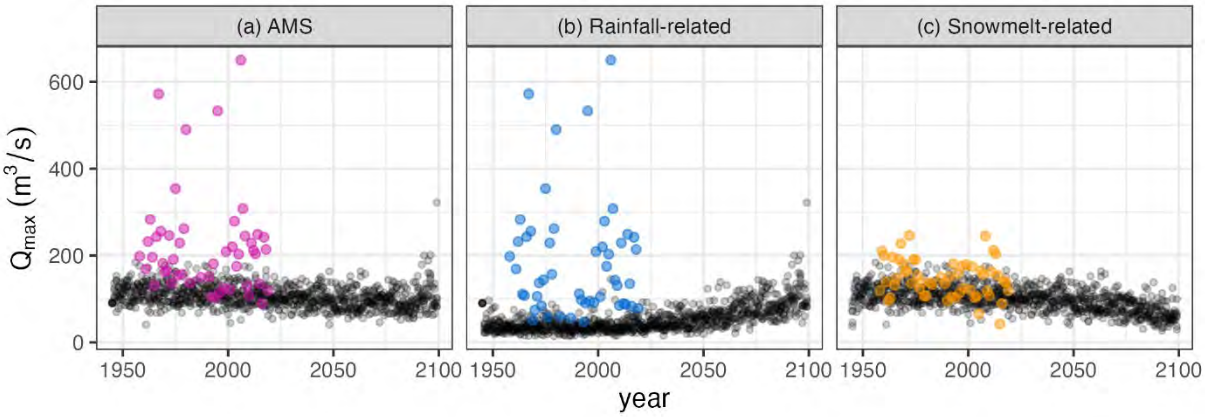

Figure 6-13. Time series for (a) the AMS, (b) annual maximum daily mean for rainfall-related (AR and non-AR) peak flows in the fall/winter (September to March), and (c) annual maximum daily mean for snowmelt-related peak flows in the spring/summer (April to August) for the *Coquihalla River above Alexander* (08MF068) hydrometric station as modelled by PCIC using six GCMs (black circles). The corresponding daily mean measurements recorded at the hydrometric station are shown by the coloured circles.

6.3.3. Assessing Validity of Scaling Assumption

The residuals for the AMS and snowmelt-related peak flows show a flaring out of the nine decile lines (Figure 6-14a,b). The flaring out is significant assuming a 0.05 threshold for the 0.1-quantile (p- value = 0.001) and 0.9-quantile (p-value = 0.02) decile slopes for the AMS as well as the last (p- value = 0.02) slope for snowmelt-related peak flow. The 0.1-quantile slope is not statistically significant for the snowmelt-related peak flows (p-value = 0.08). This significant flaring indicates that the scaling assumption for these processes may not be appropriate.

The residuals appear to be stationary over time for the rainfall-related (AR- and non-AR) peak flows suggesting that the distribution is not changing due to climate change aside from this scaling factor (Figure 6-14c). The flaring out is not statistically significant for the 0.1-quantile (p-value = 0.91) and the 0.9-quantile (p-value = 0.28) slopes providing evidence in favour of the scaling assumption for this flood-type. Because the rainfall-related (AR and non-AR) distribution becomes increasingly dominant in the future, the potentially poor assumption in the AMS and snowmelt-related cases is considered negligible for higher return period (% AEP) events.

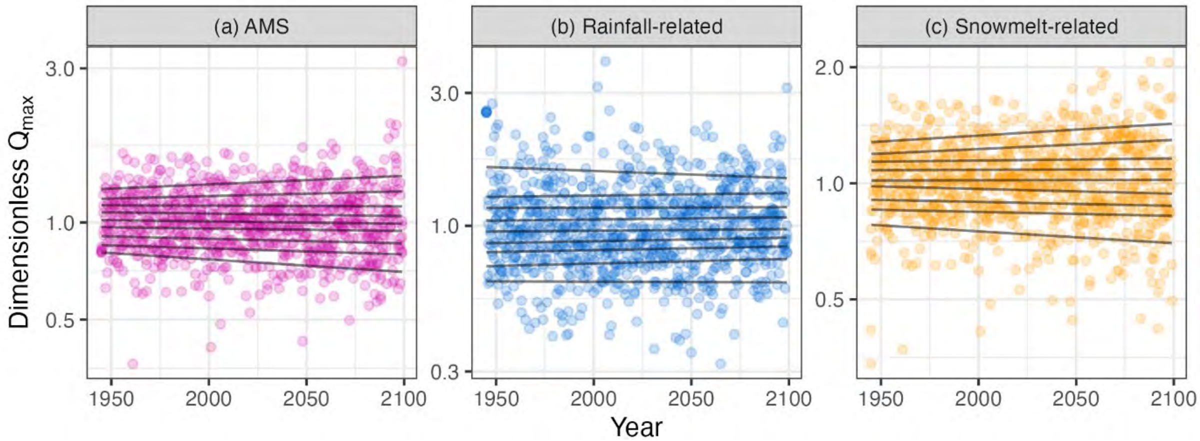

Figure 6-14. Residuals for (a) the AMS, (b) annual maximum daily mean for rainfall-related (AR and non-AR) peak flows in the fall/winter (September to March), and (c) annual maximum daily mean for snowmelt-related peak flows in the spring/summer (April to August) for the *Coquihalla River above Alexander (08MF068)* hydrometric station as modelled by PCIC. The lines represent the linear trend in the 0.1, 0.2, …, 0.9 quantiles across time.

6.3.4. Climate-adjusted Case

Return period (% AEP) projections based on dimensionless scaling factors from the AMS see minor change over time (Figure 6-15a) compared to the return period (% AEP) projections based on dimensionless scaling factors from the DMS, which sees an immediate and rapid positive increase (Figure 6-15b).

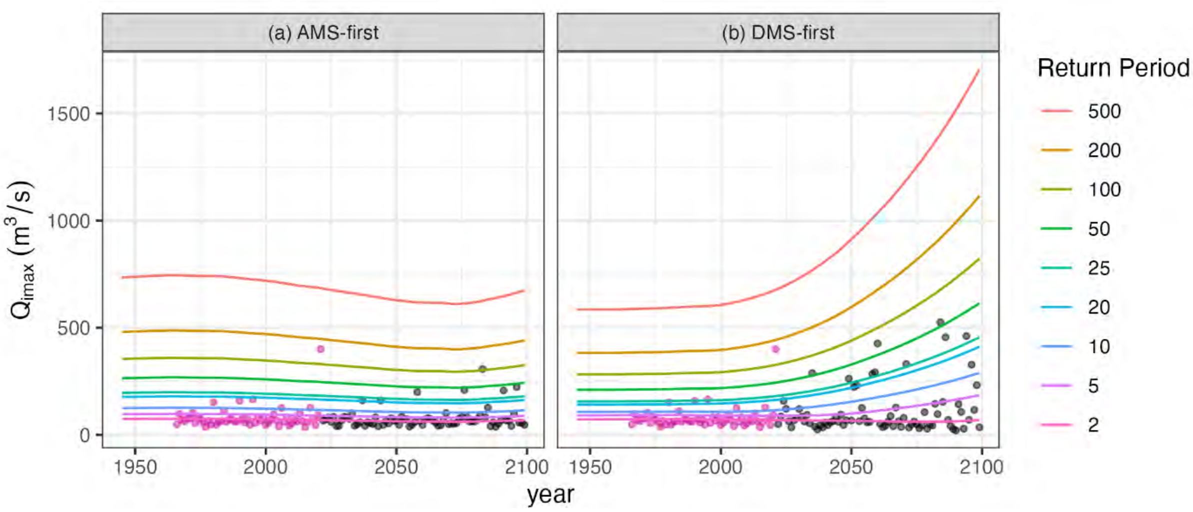

Figure 6-15. Return period (% AEP) projections in the *Coldwater River at Brookmere* (08LG048) assuming the (a) AMS trend directly, or (b) individual DMS trends first before combining via maximization. Historical recorded data are in purple; simulated data from the PCIC model are in black.

The frequency-magnitude relationship can be defined as the peak flow that is exceeded once every 2 (50% AEP), 5 (20% AEP), 10 (10% AEP), 20 (5% AEP), 50 (2% AEP), 100 (1% AEP), 200 (0.5% AEP), and 500 years (0.2% AEP) on average assuming stationarity. In a non-stationary context, the frequency-magnitude relationship requires explicit definition because the exceedance probability associated with a flood magnitude changes with each consecutive year. The climate-adjusted frequency-magnitude relationship must combine the frequency-magnitude relationship for each future year of interest. The climate-adjusted frequency-magnitude relationship can be defined in several ways with specific probability implications in a changing climate (Table 6-6).

Table 6-6. The climate-adjusted 200-year (0.5% AEP) event definitions, estimate, and implications in a changing climate.

No.	200-year (0.5% AEP) event	Definition	Statistical Modelling Approach			Implications
			AMS direct trend translation	DMS-first trend translation	Ensemble of both	
1	Maximum peak flow	The maximum 200-year (0.5% AEP) peak flow in the next 75 years.	445	1075	835	This definition results in the highest design flood because it implies that the only time this annual exceedance probability is realistic is near the end of the 75 years given the projected increasing trend in AR-related peak flows.
2	Matching the number of exceedances	Peak flow associated with 0.375 number of exceedance s over the next 75 years	415	730	605	This definition results in a value, such that the arithmetic mean AEP is 0.5%. (Note that this is different from the average 200-year (0.5% AEP) events).
3	Matching the probability of exceedance	The peak flow associated with a 31% chance of being exceeded at least once in 75 years (=1-0.995^{75}).	415	730	605	This definition also results in a value that is similar to the “number of exceedances” definition, because it matches the geometric mean of AEPs to 0.5% (as opposed to the arithmetic mean).

The “Maximum peak flow” definition of the 200-year (0.5% AEP) event results in the largest magnitude in the next 75 years given the increasing trend in AR related peak flows. The other two definitions result in the same overall 200-year (0.5% AEP) event (up to the whole number). These definitions require choosing a flood magnitude whose 75 future AEPs have an average that matches a pre-specified overall AEP (such as 0.5%). The "matching number of exceedances” definition uses the arithmetic mean (which scales to give the expected total number of exceedances), whereas the “exceedance probability matching” definition uses the geometric mean (which scales to give the probability of seeing at least one exceedance). The 75 AEPs associated with each overall AEP considered (from 0.2% to 50%) have almost identical arithmetic and geometric means, explaining the near identical results from both definitions.

The second definition (matching the number of exceedances) was used to obtain the climate-adjusted frequency-magnitude relationship because it (along with the third definition matching the probability of exceedance) is a translation of the stationary definition of the 200-year (0.5% AEP) peak flow, whereas the maximum value may be too high given the uncertainty in peak flow projections by the end of the century. The DMS-first method of translating the trend was selected as the statistical modelling approach to capture the role of ARs on peak flows in the future, despite this model yielding the largest estimates (Table 6-7, Figure 6-16). The ensemble model and the method based directly on the AMS are ultimately deemed inappropriate, due to their assumption that the watershed will become rainfall-dominant much later in the future than what the historical data suggests (that is, because the PCIC projections underestimate the distribution of rainfall-related [AR and non-AR] peak flows [Figure 6-9, Figure 6-13]).

Table 6-7. Climate-adjusted frequency-magnitude relationship over a range of return periods (%AEPs), with and without the November 15, 2021 flood, in the Coldwater River at Merritt, BC. The 90% confidence intervals are based on 100 bootstrap iterations[21].

Return Period (%AEP)	Climate-adjusted Combined Approach with November 15, 2021 (m^3/s)			Climate-adjusted Combined Approach without November 15, 2021 (m^3/s)			% Increase from the stationary case
	estimate	Lower CI	Upper CI	estimate	Lower CI	Upper CI	
2 (50% AEP)	65	60	75	65	60	70	0
5 (20% AEP)	115	90	145	105	90	125	30
10 (10% AEP)	180	130	235	165	125	200	55
20 (5% AEP)	265	170	370	230	160	285	60
50 (2% AEP)	400	245	620	335	220	440	65
100 (1% AEP)	540	320	930	430	280	615	65
200 (0.5 % AEP)	730	400	1600	545	345	890	65
500 (0.2 % AEP)	1110	540	3525	745	450	1535	65

21 A total of 100 bootstrap iterations was completed instead of 1,000 as was done for the stationary case given the extensive amount of time required to calculate (e.g., 20 hours for the 100 iterations for the climate-adjusted case).

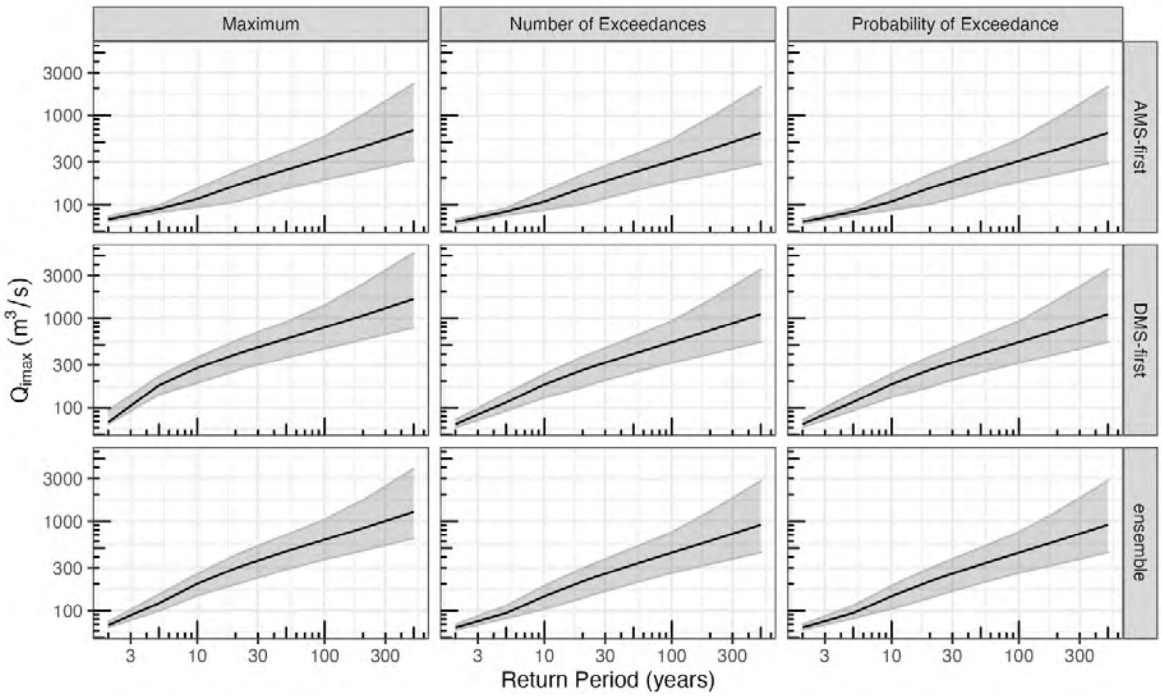

Figure 6-16. Climate-adjusted frequency-magnitude relationships, with the November 15, 2021 flood, in the Coldwater River at Merritt, BC. The 90% confidence intervals are based on 100 bootstrap iterations. The three definitions of the FM relationship span the columns; the three models span the rows.

6.4. Watershed Comparison between Coldwater River and Coquihalla River

A comparison of watershed characteristics between the Coldwater River and the Coquihalla was conducted to assess the reliability of the scaling assumption used to transfer peak flow projections from one watershed to the other. The Coldwater River at Brookmere, Coldwater River at Merritt, and the Coquihalla River above Alexander Creek watersheds share similar hydrologic, climate, and physiographic characteristics (Table 6-8). Key differences include the annual monthly precipitation which is approximately 25 to 30% higher in the Coquihalla River watershed compared to the Coldwater River at Brookmere, which is a function of its wider range in elevation (i.e., relief) increasing the influence of orographic effects. All three watersheds share similar physiographic characteristics with the Coldwater River at Merritt watershed having a slightly higher CN value compared to the others.

Table 6-8. Comparison of watershed characteristics in the Coldwater River at Brookmere, Coldwater River at Merritt, and the Coquihalla River above Alexander Creek.

Type	No.	Acronym	Characteristic	Units	Coldwater River at Brookmere	Coldwater River at Merritt	Coquihalla River above Alexander Creek
Watershed	1	Centroid_Lat	Latitude at the centroid location in the watershed polygon	degrees	49.7299	49.8966	49.4427
	2	Centroid_Long	Longitude at the centroid location in the watershed polygon	degrees	-121.0372	-120.9000	-121.1933
	3	Centroid_Elev	Elevation at the centroid location in the watershed polygon	m	1186	871	897
	4	Area	Area of the watershed polygon	km^2	316	917	720
	5	Relief	Maximum minus minimum watershed elevation	m	1,079	1,394	1,790
	6	Length	Area divided by perimeter	km	2.1	3.6	2.9
	7	Slope	Watershed length divided by relief times 100	%	50	38	62
Climate	8	MAP	Mean annual precipitation	mm	1,268	778	1,681
	9	MAT	Mean annual temperature	^oC	3.0	3.6	4.2
	10	PAS	Precipitation as snow	mm	678	388	695
	11	PPT_wt	Winter precipitation (Dec, Jan, Feb)	mm	497	300	665
	12	PPT_sp	Spring precipitation (Mar, Apr, May)	mm	263	154	321

Type	No.	Acronym	Characteristic	Units	Coldwater River at Brookmere	Coldwater River at Merritt	Coquihalla River above Alexander Creek
	13	PPT_sm	Summer precipitation (Jun, Jul, Aug)	mm	161	114	211
	14	PPT_fl	Fall precipitation (Sep, Oct, Nov)	mm	347	208	484
Physiographic	15	Forest[1]	Forest cover in the watershed	%	99	86	95
	16	Water_Wetland	Wetland and open water cover in the watershed	%	0.2	0.2	0.1
	17	Urban	Urban cover in the watershed	%	0	0.6	0.1
	18	CN_arcii	Inferred based on integrating land cover and soils cover	unitless	63	70	63

Note:

1. Estimate does not account for the proportion of the watershed that was burned in 2021.

7.0 DISCUSSION

7.1. Estimating the Magnitude of the November 15, 2021 Flood

Using a 2-D hydraulic model of the Coldwater River and observed HWMs, BGC's best estimate of the November 15, 2021 flood is 400 m^3/s using pre-flood terrain (this estimate matches the initial peak readings of both hydrometric stations on the Coldwater River) and 300 m^3/s using post-flood terrain. The error associated with the 400m^3/s run using pre-flood terrain is significantly lower (28% lower) than the error from the 300 m^3/s run using the post-flood terrain. This difference can possibly be attributed to sediment deposition during the falling limb of the floods hydrograph that would not have been present during the flood's peak.

In addition to terrain, the result is also sensitive to the selected Manning's n value used in the hydraulic model. An average difference of 0.2 m exists in WSEs measured for the 400 and 300 m^3/s model runs using pre-flood terrain. However, a 50% increase to the Manning's n values (a base value of 0.025 was used for the main channel) used for the 300 m^3/s model run produces an equivalent change in average WSE. The modelled Manning's n values used for the present work were calibrated using the May 16, 2018 flood event, where the main overbank flooding occurred along the Nicola River and downstream of the confluence of the Nicola and Coldwater rivers. Hence, the selected calibrated Manning's n values may not be as representative of the Coldwater River itself, which was largely confined to the main channel during the 2018 flood event.

Given the bed material of the channel, which includes gravel and cobbles, it is unlikely that an n value below 0.025 is representative. Likewise, while slightly higher n values for the channel and other land classes are possible[22], a 50% increase in the Manning's n to reconcile the WSE with the HWMs for a peak flow of 300 m^3/s seems unreasonable given the landcover and channel characteristics.

There is a continuum of Manning's n and discharge values that would produce the observed WSE, and pre and post flood terrain produce different results but based on the information currently available, 400 m^3/s is BGC's best estimate of the peak flow for the November 15, 2021, flood.

7.2. Frequency-Magnitude Relationship

7.2.1. Inclusion of the November 15, 2021 Flood

The November 15, 2021 flood was a rain-on-snow event with AR-related rainfall as the dominant contributor to the flood magnitude. The occurrence of AR-related floods in this watershed is not surprising given that they make up 25% of peak flows in the AMS. However, the magnitude of the flood (400 m^3/s) exceeded the flood of record (165 m^3/s) by 240%, generating uncertainty about the statistical population to which this event belongs. The combined approach (ensemble of DMS models) to the frequency-magnitude relationship recognizes two statistical populations of peak

22 Keeping in mind that roughness values for 2D models are typically lower than one-dimensional (1D) models, as the 2D models explicitly account for channel planform roughness which 1D models do not.

flows: AR-related and snowmelt-related in the Coldwater River watershed. The November 15, 2021 flood was included as part of the AR-related peak flows.

Although an outlier, inclusion of the November 15, 2021 flood in the AR-related peak flow dataset seems reasonable because extreme events like heatwaves, wildfires, and storms can have cumulative effects on the hydrological response of a watershed. These extreme events (annual and seasonal) have occurred historically, but are increasing in both magnitude and frequency, and lasting longer. Climate change is also increasing the likelihood that extreme events coincide, or are followed by one another, resulting in unprecedented hydrological responses. The November 15, 2021 flood on the Coldwater River could be an example of a hydrological response when an extreme rainfall event (and direction) follows an extensive summer wildfire that impacted a 30% of the upper watershed (Figure 3-1).

It is also possible that the November 15, 2021 flood is a unique hydrological response not solely attributable to AR-related peak flows. Rather, this flood could be part of its own statistical population (n=1) as defined by other characteristics such as the meteorological conditions that led to the storm and the micro-meteorological conditions that evolved during the storm. If this were the case, it may not be appropriate to include the event as part of the analysis.

At the present time, it is unknown whether the November 15, 2021 event is a rare flood in a stationary context or whether it represents a shift in the frequency-magnitude relationship. The November 15, 2021 flood may be an expression of the positive trend in the rainfall-related (AR and non-AR) peak flows as shown in PCIC's six GMC-run VIC model simulations (based on CMIP5 models). It appears that the trend in rainfall-related (AR and non-AR) peak flows emerges in approximately 2010 (Figure 6-12). While the November 15, 2021 flood was included in the analysis with a value of 400 m^3/s, the magnitude implicitly accounts for this trend. As a result, it may not be appropriate to include the 400 m^3/s value in the stationary frequency analysis without accounting for the impacts of climate change on the magnitude of the event.

There is no "right" approach to be taken and is likely a topic that would generate conflicting points of view among a wide range practitioners. For example, Dr. Michael Church is of the opinion that the November 15, 2021 event should not be included in the analysis because it is assigned a return period (% AEP) that is dictated by the length of the record which may not be close to the actual return period. Dr. Tricia Stadnyk is of the opinion that the November 15, 2021 event should be included in the analysis because its magnitude is physically grounded.

7.2.2. Is the frequency-magnitude relationship "right"?

The frequency-magnitude relationship is probably more "right" for lower return period (% AEPs) compared to higher return period (% AEP) events recognizing the width of the confidence intervals (Figure 6-7). In the Coldwater River watershed, the lack of large flood events in the historical record of comparable magnitude to the November 15, 2021 flood challenge a statistical model to define the tail behaviour of the probability distribution, regardless of whether the "standard approach" or a "combined approach" is used. Over a long time, the addition of large events will improve the ability of the statistical model to characterize the tail behaviour, decreasing changes to the magnitude of larger return period (lower %AEP) events, assuming all other statistical conditions remain the same.

Unfortunately, statistical conditions are time variant. A dataset must meet specific statistical requirements to be valid for frequency analysis including homogeneity, randomness, independence, and stationarity. Violation of any of these requirements precludes the use of a frequency analysis in theory and increases the degree of uncertainty in practice, as discussed in further detail below.

- Homogeneity implies that all data comes from the same statistical population of event. This statistical requirement was met as best as possible in this analysis by accounting for AR-related and snowmelt-related peak flows separately. However, there is a possibility that the November 15, 2021 flood does not belong to the AR-related peak flow dataset introducing uncertainty to the frequency-magnitude relationship, especially the tail behaviour. The sensitivity of the frequency-magnitude relationship to extreme events has been demonstrated here-in by a comparison of the analysis with and without the November 15, 2021 flood.
- In a hydrological context, randomness implies that the fluctuations in peaks flows occur in response to natural causes. However, peak flows can also be influenced by major watershed disturbances such as land use change (e.g., conversion to agriculture), forestry (e.g., logging), insect infestations (e.g., mountain pine beetle), and wildfires. Therefore, if large magnitude events, like the November 15, 2021 flood occur only in response to specific combinations of consecutive extreme events like heatwaves, wildfires, and storms, then these peak flows may not be considered entirely random.
- Independence implies that successive peak flows are independent of one another. The dependence between annual maxima tends to be weak supporting the AMS and DMS approach to frequency analysis. The snowmelt- and AR-related peak flow datasets were not tested for serial correlation given their nonsignificant trend at this time.
- The stationarity criterion requires that the data series not change with respect to time. Examples that violate the stationarity criterion include trends and cycles. Trends may reflect a gradual change in climate influencing the data series over time. Another factor that can violate the stationarity criterion is the presence of cycles such as long-term climate fluctuations. For example, the frequency of ARs is greater in BC during the neutral phases of El Niño/Southern Oscillation, the 2013/2014 Pacific oceanic blob, and during the positive phases of the Pacific Decadal Oscillation, and Pacific North American Pattern (Sharma and Déry, 2019). However, the influence of the lower AR frequency from the 1960s until mid-1970s corresponding to the negative phase of the Pacific Decadal Oscillation (Meehl et al., 2009) is not obviously present in the annual maxima for AR-related peak flows, so it was not accounted for in the analysis.

Irrespective of the statistical complexities of the analysis, it is worth noting that frequency-magnitude relationships are rarely static, evolving over time as more information is gathered. The Coldwater River watershed is no exception, and it is highly likely that the frequency-magnitude relationships documented here-in will require adjustment over time as large flood events occur and the statistical conditions of the dataset change. For example, as the hydrological regime shifts from a nival-pluvial to a more rainfall-dominated regime. These adjustments may result in considerable future changes to the higher return period (%AEP) events given these are characterized by the greatest uncertainty.

7.2.3. Is the projected trend in rainfall-related (AR and non-AR) peak flows realistic?

Current research shows that an increase in surface air temperature increases the atmospheric water vapour capacity in line with the Clausius-Clapeyron relation. This relation implies that specific humidity increases approximately exponentially with temperature (Wark, 1966, 1988). As a result, extreme daily precipitation events are projected to intensify by about 7% for each degree of global warming assuming unlimited water and energy for evaporation (Huntington, 2005). Further, increases in the global surface air temperature will increase the availability of atmospheric moisture required for the development of ARs (Sharma and Déry, 2020b). For the period 1980 to 2016, the cold season ARs along the West Coast of the United States have warmed (vertically averaged from 1000 to 750 hPa) on the order of 0.7 to 1.7 °C during owing to the combined influence of regional and oceanic warming (Gonzales et al., 2019). This increase in atmospheric water vapour capacity allows the IVT to be higher, resulting in more frequent exceedances of its defining threshold of 250 kg/m/s.

Landfalling atmospheric rivers over the lower latitudes of BC in the cold season are projected to increase in both strength and frequency in the CMIP5 climate models. An increase in the frequency of ARs in BC and the West Coast of the United States is projected for the period 2070 to 2100 (Dettinger, 2011) and 2100 (Radić et al., 2015). The rising influence of ARs could result in a 4x increase in cold season extreme rainfall frequency and a decrease in the return period (% AEP) of the largest historical flow from a 200-year (0.5 % AEP) to 50-year (2% AEP) event in the Fraser River watershed (Curry et al, 2019).

PCIC's six GMC-run VIC-GL model simulations (based on CMIP5 models) poorly capture the magnitude of historical AR-related peak flows in the *Coquihalla River above Alexander Creek* (08MF068) hydrometric station introducing doubt in their ability to project the magnitude of future rainfall-related (AR and non-AR) peak flows (Figure 6-9). The discrepancy in magnitude between historical AR-related peak flows simulated and those recorded at the hydrometric station may be related to:

- The physical processes may not be adequately captured, like the rapid runoff response to high rainfall rates. Notably, the VIC model simulations do a much better job of simulating snowmelt hydrographs which typically occur over a period of weeks.
- The muted hydrological response may be a function of the resolution of the gridded meteorological dataset (PNWNAmet at 50 km^2 resolution) used to drive PCIC's hydrological model compared to the size of the Coquihalla River above Alexander Creek watershed (720 km^2). Approximately 14 to 15 grid cells cover the spatial extent of the watershed and the meteorological granularity may not be high enough to adequately capture the magnitude of the hydrological response to ARs.

- The model timesteps may be too coarse to capture rapid runoff in smaller watersheds.

While the PCIC simulations do not capture the magnitude of historical AR-related peak flows, the simulations emulate the historical trend at *Coquihalla River above Alexander Creek* (08MF068) hydrometric station (Figure 6-12). The simulations over the recorded period (1965 to 2021) show a stationary trend in line with the trend in the AR-related peak flows. This stationary trend is consistent with the stationary proportion of ARs related to extreme streamflow (annual and seasonal maximum) for most watersheds across BC over the 1979 to 2016 period (Sharma and Déry, 2020b). Climate models are best used to inform the magnitude and direction of change as opposed to absolute estimates of variables because they are designed to estimate how average conditions change over an area through the next century. The magnitude and direction of the projected trends in both rainfall-related (AR and non-AR) and snowmelt-related peak flows align well with those projected by PCIC at the *Spius Creek near Canford* (08LG008) and the *Nicola River near Spences Bridge* (08LG006) hydrometric stations.

Given this information, the projected trend (magnitude and direction) in rainfall-related (AR and non-AR) peak flows was deemed representative of the climate change signal in the Coquihalla River watershed based on the information available today. However, it should be recognized that predicting future changes in peak flows events due to climate change is an emerging science with ongoing research. It is more likely than not that the climate change trends identified in this report will change in the next decade, as our cumulative understanding (and direct observations) of climate change impacts improves. Because of this uncertainty, there is no clear path forward on how to account for climate change impacts in selecting a design flood for current infrastructure projects. What is clear is that the projected trend (magnitude and direction) of AR-related peak flows due to climate change should be revised in the future as scientific understanding of AR processes evolve and as human behaviour changes with respect to carbon emissions in the atmosphere.

7.2.4. Differences between the original (pre-event) and updated (post-event) frequency-magnitude relationships

The differences between the original (pre-event) and updated (post-event) frequency-magnitude relationship is due to the influence of the November 15, 2021 flood on the statistical distribution, the different methods being used for frequency analysis, and different methods for accounting for the impacts of climate change.

BGC's June 2021 (pre-event) estimate of the 200-year (0.5% AEP) flood was 155 m^3/s based on a standard approach to frequency analysis using the AMS and assuming a GEV distribution with parameters estimated using the l-moments method of inference (BGC, June 2021). An upwards adjustment of 20% was applied to account for climate change resulting in a climate-adjusted 200-year (0.5% AEP) of 185 m^3/s as per EGBC (2018) guidelines.

BGC's updated (post-event) estimate of the 200-year (0.5% AEP) flood is 445 m^3/s ranging from 240 to 980 m^3/s based on a combined approach (an ensemble of DMS models) recognizing the different influence of AR-related and snowmelt-related peak flows on the frequency-magnitude relationship. In the Coldwater River watershed, the largest flood events are AR-related thus the 200-year (0.5% AEP) is based on the AR-related peak flow distribution. To account for climate change, the peak flow distributions in the Coldwater River were scaled to account for the trends in rainfall-related (AR and non-AR) and snowmelt-related peak flows as projected by PCIC at the *Coquihalla River above Alexander Creek* (08MF068) hydrometric station. The climate-adjusted 200-year (0.5% AEP) flood event is estimated to be 730 m^3/s, a 65% increase compared to the stationary case.

For comparison, a frequency-magnitude relationship based on a standard approach to frequency analysis using the AMS and including the November 15, 2021 flood results in a 200-year (0.5% AEP) flood of 295 m^3/s ranging from 160 to 545 m^3/s assuming a GEV distribution and MLE method of inference for parameter estimation. BGC's updated (post-event) estimate of the 200-year (0.5% AEP) flood (445 m^3/s) based on the combined approach (an ensemble of DMS models) falls within the uncertainty range defined by the 90% confidence interval (160 to 545 m^3/s). Given the wide confidence interval of higher return period (lower % AEPs) flood events, BGC's updated (post-event) estimate of the 200-year (0.5% AEP) based on the combined model (ensemble of DMS models) seems reasonable because it falls within the range of statistical uncertainty.

For context, including the November 15, 2021 flood in the frequency-magnitude relationship using the standard approach (AMS) assuming a GEV distribution and MLE method of inference for parameter estimation results in a 50% increase in the 200-year (0.5% AEP) (295 m^3/s) compared to the same analysis without (205 m^3/s). This comparison highlights the influence of the November 15, 2021 flood on the statistical distribution. Updated (post-event) and original (pre-event) frequency-magnitude relationships (stationary and climate-adjusted) over a range of return periods (% AEPs) are listed in Table 7-1.

Table 7-1. Updated (post-event) and original (pre-event) frequency-magnitude relationship over a range of return periods (%AEPs) for the Coldwater River at Merritt, BC. The 90% confidence intervals are based on 1000 bootstrap iterations.

Return Period (%AEP)	Original (pre-event) Standard Approach (AMS) (BGC, June 2021)		Standard Approach[3] with November 15, 2021 (m^3/s)			Combined Approach[4] with November 15, 2021 (m^3/s)			Combined Approach with November 15, 2021, Climate-adjusted[5] (m^3/s)			Combined Approach without November 15, 2021 (m^3/s)		
	Estimate[1]	Climate-adjusted[2]	Estimate	Lower CI	Upper CI	Estimate	Lower CI	Upper CI	Estimate	Lower CI	Upper CI	Estimate	Lower CI	Upper CI
2 (50% AEP)	---	---	70	65	75	70	65	75	65[6]	60	75	70	65	75
5 (20% AEP)	---	---	95	85	110	90	80	100	115	90	145	90	80	95
10 (10% AEP)	---	---	120	100	145	115	95	155	180	130	235	105	90	130
20 (5% AEP)	125	---	150	115	200	165	115	230	265	170	370	145	105	185
50 (2% AEP)	135	---	195	130	295	245	155	380	400	245	620	205	135	285
100 (1% AEP)	---	---	240	150	400	330	195	580	540	320	930	260	170	390
200 (0.5 % AEP)	155	185	295	160	545	445	240	980	730	400	1600	325	210	560
500 (0.2 % AEP)	165	195	385	185	830	680	315	2190	1110	540	3525	450	265	1060

Notes:

1. The original (pre-event) analysis is based on a standard approach to frequency analysis (AMS) using the GEV distribution and L-moment method of inference for parameter estimation. These results do not consider the November 15, 2021 flood event.
2. An upwards adjustment of 20% was applied to account for climate change as per EGBC (2018) guidelines.
3. The updated (post-event) analysis based on a standard approach to frequency analysis (AMS) assumes the GEV distribution and the MLE method of inference for parameter estimation.
4. The updated (post-event) analysis is based on a combined approach (ensemble of DMS models [GEV, Log Normal, and Pearson Type III]). The MLE was used to estimate the parameters of the GEV and Log Normal distributions. The maximum goodness-of-fit estimates (MGE) method of inference was used instead to fit the Pearson Type III distribution due to convergence issues with the MLE.
5. The rainfall-related (AR and non-AR) and snowmelt-related peak flow distributions in the Coldwater River were scaled to account for the trends as projected by PCIC using the six GCM-run VIC-GL model at the *Coquihalla River above Alexander Creek* (08MF068) hydrometric station.
6. The climate-adjusted 2-year (50% AEP) is 65 m^3/s which is lower than the stationary 2-year (50% AEP). This reduction is because the AR-related peak flow distribution that is being scaled every year into the future has 24% of its smallest values as “zero” because AR-related peak flows do not occur every year.

7.2.5. What is the “design flood”?

The frequency-magnitude relationship was adjusted for projected climate change assuming RCP 8.5 over the next 75 years. The climate-adjusted frequency-magnitude relationship is projected to shift such that the value for a given annual exceedance probability calculated over the next 75 years would be greater (60-64% for AEPs 0.2-5%) given the increasing trend in rainfall-related (AR and non-AR) peak flows.

The climate-adjusted 200-year (0.5% AEP) flood is estimated to be 730 m^3/s (400 m^3/s to 1600 m^3/s) by 2066 – a 64% increase compared to the stationary case (i.e., 445 m^3/s). The 730 m^3/s is approximately equivalent to today’s 575-year (0.17% AEP) flood and will become the 85-year (1.2% AEP) flood in 75 years (2096). For comparison, the stationary 200-year (0.5% AEP) flood event (e.g., 445 m^3/s) is projected to become the 25-year (4% AEP) flood in 75 years based on the climate-adjusted frequency. This reduction in return period (increase in % AEP) shows how the assumption in future time horizon in the design life of buildings and mitigation works influences the magnitude of the climate-adjusted design flood in the Coldwater River watershed given the projected increase in rainfall-related (AR and non-AR) peaks flows.

The climate-adjusted 200-year (0.5% AEP) flood may be difficult or impractical to use as the design basis for engineered structures depending on site-specific conditions. It would be prudent to consider some level of flexibility in the design of engineered structures, for example, adding additional pile[23] capacity in bridge foundations can allow for future channel widening, and resilient designs that plan for “failure”. A resilient design could include an overflow spillway or field along a diked river channel in the event the existing capacity is exceeded, or could include a bridge design assume the bridge deck and its approaches will be overtopped.

As the frequency and magnitude of extreme events increase due to climate change, so do the impacts and associated costs. Natural Resources Canada (NRCan) offers guidance on balancing the cost and consequences of climate change impacts on infrastructure (Boyd & Markamdya, 2021). The Federation of Canadian Municipalities (FCM) and the Insurance Bureau of Canada (IBC) commissioned Green Analytics to estimate the level of investment in municipal infrastructure and local adaptation measures needed to reduce the impacts of climate change (FCM and IBC, 2020). Investing in climate adaptation, or disaster mitigation, has been shown to outweigh the costs by a ratio of 6 to 1, especially relevant to aging infrastructure vulnerable to extreme events. This ratio means that it costs less to invest in adaptation or disaster mitigation than to restore infrastructure damaged by climate change (FCM and IBC, 2020).

7.3. Implications for Water Surface Elevation

The influence of the peak flow estimates on the water surface elevation (WSE) in the *Coldwater River at Merritt* were assessed for the stationary case (445 m^3/s), and both climate-adjusted cases

[23] Bridge piles are structures used in foundations made of long poles (referred as piles) that are driven into the ground under the bridge supporting the load of the bridge deck.

(605 m^3/s for the ensemble model, and 730 m^3/s for the DMS-first model). On average, there is relatively little impact on WSE with an average change of 0.25 m within the channel between the lowest and highest case. This average change is comparable between both pre and post flood terrain. The relatively small change is the result of the flow being distributed across a broad floodplain (i.e., the City of Merritt). If these flows were contained to the main channel by diking, the water surface differences would be substantial. There would be a >1 m average increase with the addition of dikes to the post flood terrain at the locations shown in Figure 7-1.

The influence of the peak flow estimates on the WSE is highly variable spatially (Figure 7-2), with up to a 0.70 m difference in WSE at station 3740 located 50 m upstream of the Houston Street bridge. The effect on in channel velocities is similar with only an average 0.1 m/s change between the stationary and maximum climate change discharges but high local variability (Figure 7-3). Once again, these differences would be more pronounced if the flows were contained by diking (>0.5 m/s average increase with the addition of dikes to the post flood terrain).

Figure 7-1. Location dikes (pink lines) tested in post flood model

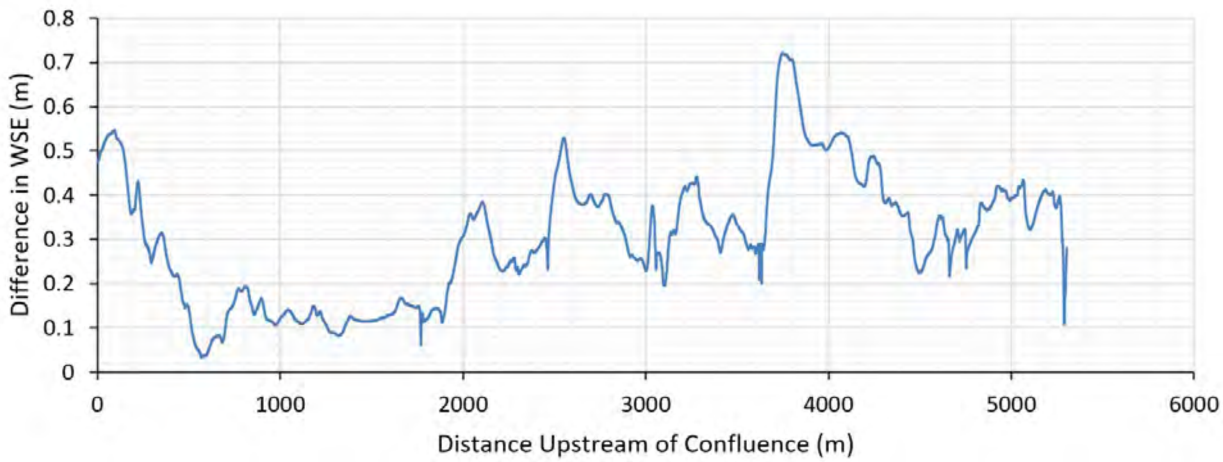

Figure 7-2. Change in the WSE in the Coldwater River going upstream from the confluence of the Nicola and Coldwater Rivers (Station 0 m) between 445 m^3/s and 730 m^3/s flow cases.

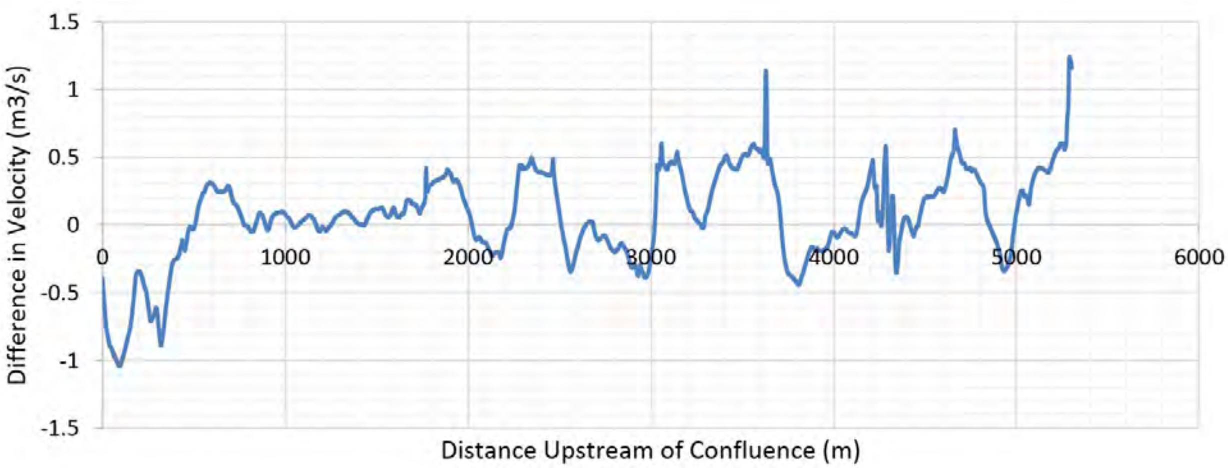

Figure 7-3. Change in the velocity in the Coldwater River going upstream from the confluence of the Nicola and Coldwater Rivers (Station 0) between 445 m^3/s and 730 m^3/s flow cases.

The variability in the changes of both WSE and velocities along the Coldwater River suggests that the impact of the climate-adjusted peak flow on WSE and velocity will have to be evaluated on a site-by-site basis within Merritt.

7.4. Intended Use of Frequency-Magnitude Relationship

Flood quantiles estimated to consider climate change are intended to support risk management decision making on a comparable time frame (75 years), including land use planning and the design of engineered risk control structures. Analyses, design, maps, policies, and regulations may incorporate assumptions about climate change (e.g., for estimates of Flood Construction Levels (FCL) or infrastructure design). The limitations and sources of uncertainty in this study that pertain to the frequency-magnitude relationship presented in this report are included in

Section 7.5. Reasons why derivative products informed by this updated frequency-magnitude relationship (e.g., hazard maps) might need to be updated are beyond the scope of the report.

7.5. Limitations, Assumptions, and Uncertainty

A list of limitations, assumptions, and sources of uncertainty in this study are listed below in order of appearance:

7.5.1. Estimating the Magnitude of the November 15, 2021 Flood

- As discussed in Section 7.1, uncertainty prevails in BGC's best estimate of the November 15, 2021 flood due to the hydraulic model's sensitivity to Manning's n.
- A source of uncertainty in the determination of the peak flows comes from limitations of the hydraulic modelling process and collection of HWMs used for model calibration.
    - Sediment transport and avulsion were not modelled as part of this work. As such the two terrains used in the model are only representative of snapshots in time of the river morphology which changed through the course of the flood. As shown in Figure 7-4 there were areas of both considerable aggradation and degradation (along with avulsions) that occurred within the channel between the 2020 and 2022 surveys conducted by Ecoscape.
    - As a result, WSEs at HWMs collected near areas of channel avulsion or rapid channel change may not be accurately represented by the model. Similarly, many of the HWMs were collected along fences, trees and other small features that were not incorporated into the model terrain but nonetheless likely had a local effect on water surface elevation during the flooding.
    - The measurements of these HWM themselves also have some degree of uncertainty as in some instances fence debris may only be partially intact (Figure 7-5), rafted debris may have moved in the intervening time between the flood and the collection of data or require judgment as to which portion to use (Figure 7-6). All these factors result in a certain amount of scatter in the data as shown in Figure 7-7. However, as over 100 HWMs were collected, the effects of errors at any individual point become less significant.

Figure 7-4. Quantifying the change in channel elevation between the 2020 and 2022 Ecoscape surveys

Figure 7-5. Survey photo 93: Rafted debris against a fence, portions of the debris have clearly fallen making it difficult to determine the HWM at this location. Photo: Ecoscape, March 8, 2022.

Figure 7-6. Survey photo 53: Rafted debris in trees, the height of debris varies by tree requiring judgement on which elevation to use. Photo: Ecoscape, March 8, 2022.

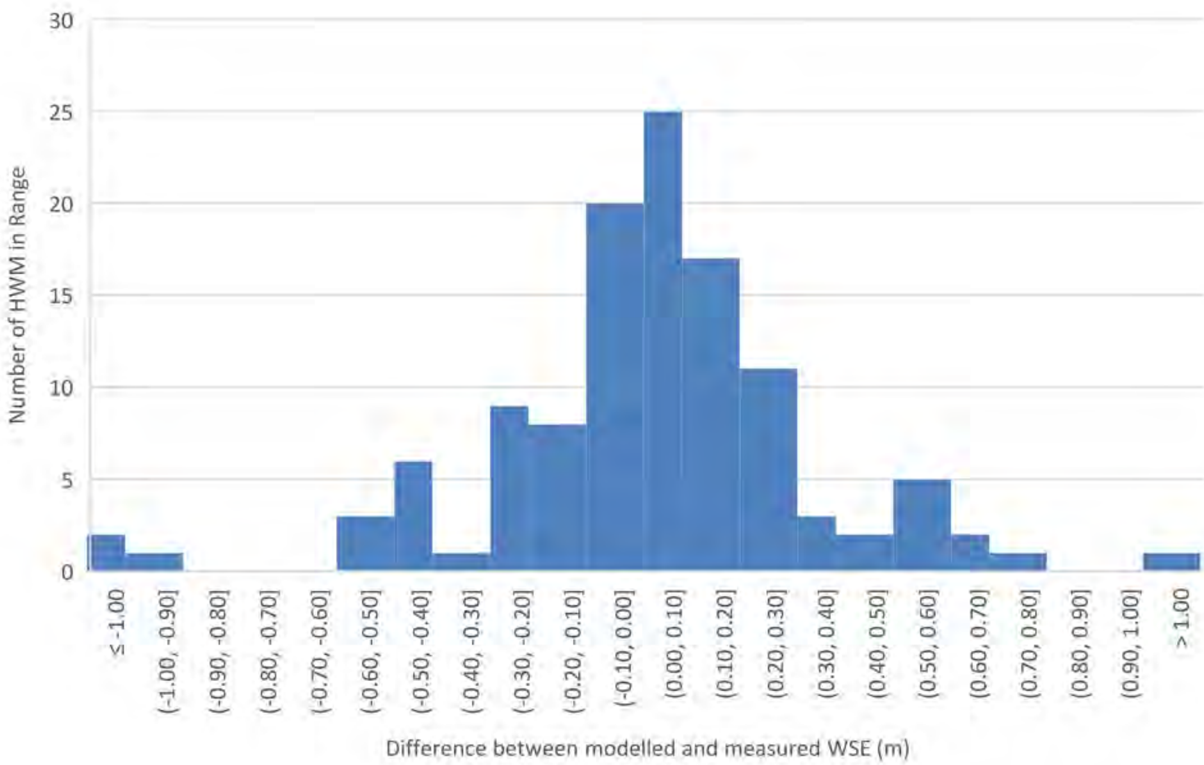

Figure 7-7. Distribution of errors between modelled WSE and surveyed HWMs for the 400 m^3/s run using the preflood terrain.

7.5.2. Updated (post-event) Frequency-Magnitude Relationship

- The role of ARs on snowmelt in the spring contributing to rain-on-snow events was not considered explicitly in the statistical model because there were only a few of those events in the dataset, the peak flow magnitude was in between snowmelt-related and AR-related peak flows, and the AR frequency seems to be the lowest in the spring, at least historically. Rain-on-snow events are becoming more common with climate change which may warrant their consideration in the future.
- The regression between Q_{max} and Q_{imax} was assumed linear across the range of peak flows for each flood type (AR-related and snowmelt-related peak flows). Given the limited number of AR-related peak flows (10), the trend could easily be some other distribution. Assuming linearity implies that the shape of the hydrograph is approximately the same where the relationship between the Q_{max} and the Q_{imax} doesn't change. In practice, antecedent moisture conditions and soil storage, geomorphology changes, and watershed disturbances can influence this relationship violating the linearity assumption.
- The record length for analysis of the snowmelt- (53) and AR-related (42) peak flows is technically not long enough to estimate the 200-year (0.5% AEP) flood because there is insufficient observation of higher quantile flows to assess the statistical distribution fit accurately. Recommendation for standard practice is the record length times two, which suggests that the 100-year (1% AEP) flood is the practical limit of the statistical model.
- The stationary frequency-magnitude relationship is based on the historical peak flows available at this time. However, large magnitude events control the frequency-magnitude relationship, especially if AR-related (Section 6.2.3). The Q_{imax} estimates may require a re-calculation following a large (greater than 50-year, 2% AEP) magnitude flood.
- It was assumed that projected trends in Q_{max} apply to Q_{imax}, which is a realistic assumption given these two quantities are highly correlated.
- The climate-adjusted frequency-magnitude relationship is based on the projection information available at this time. The assumptions made on changes to instantaneous peak flows due to climate change should be revised in the future as scientific understanding of AR and snowmelt processes evolve, as the controls of water change (i.e., diversions, dams, water intakes), and the watershed characteristics change. Human decisions and assumptions on behaviour today determines the rate of climate change in the future.
- Climate projections show there is limited linearity between peak flows of different magnitude (i.e., quantiles). For example, there is little change in the mean / median flow, but the extremes shift in the tail of the statistical distribution. The dimensionless scaling factors used to estimate the climate-adjusted frequency-magnitude relationship could result in a conservative estimate (i.e., underestimate the shift in the peak flow distribution) of larger flood events.
- Watershed disturbances such as land use change (e.g., conversion to agriculture), forestry (e.g., logging), insect infestations (e.g., mountain pine beetle), and wildfires may increase peak flows due to changes to hydrological processes. The projected increase in

the frequency of watershed disturbances imply that the peak flows will likely be higher and more variable in the future. Detailed analyses on the extent of disturbance in the Coldwater River watershed was beyond the scope of this work. Such watershed disturbances are also not incorporated into the PCIC hydrologic model for the Coquihalla River above Alexander Creek because it is computationally intensive, and the data are not always available. As a result, the historical and projected influence of disturbances to the Coldwater River watershed are unknown.

8.0 CONCLUSIONS AND RECOMMENDATIONS

8.1. Conclusions

- The instantaneous peak flow in the Coldwater River on November 15, 2021 flood was estimated to be approximately 400 m^3/s, in line with the first measurement recorded at the 08LG048/08LG010 hydrometric stations. This discharge corresponds to a return period of 160 years (0.63 % AEP) under a stationary climate assumption and 50 years (2% AEP) under a climate change assumption.
- The 200-year (0.5% AEP) event in the Coldwater River at Merritt in absence of climate change is estimated to be 445 m^3/s (ranging from 240 to 980 m^3/s for the 90% confidence intervals) based on the combined approach (ensemble of DMS models). This estimate is based on the assumption that the November 15, 2021 flood was 400 m^3/s.
- The climate-adjusted 200-year (0.5% AEP) flood event is estimated to be 730 m^3/s (ranging from 400 m^3/s to 1600 m^3/s for the 90% confidence intervals) – a 65% increase compared to the stationary case (i.e., 445 m^3/s). This large increase emphasizes that neglecting climate change in flood frequency analyses can no longer be justified. These findings show that climate change effects are profound and will influence the design of flood protection structures, Flood Construction Levels, and the design of infrastructure alongside or crossing watercourses.
  - This climate-adjusted 200-year (0.5% AEP) event will become the 200-year (0.5% AEP) flood in 2070, is approximately equivalent to today's 575-year flood (0.17% AEP), and will become the 85-year (1.2% AEP) flood in 75 years (2096).
- The frequency-magnitude relationship should be interpreted in context of the confidence intervals, which highlight increased uncertainty with increasing return period (decreasing % AEP) events.
- The frequency-magnitude relationship is based on current data and methods. BGC anticipates the work will generate questions and comments and may be subject to future updates.

8.2. Recommendations

- There is no guidance in the literature for transferring climate projections on peak flows from one watershed to another. A regional analysis to projected peak flow trend characterization is recommended to improve the climate-adjusted frequency-magnitude relationship, especially for AR-related peak flows.
- The stationary and climate-adjusted frequency-magnitude relationships are based on statistical models. Development of a hydrological model in the Coldwater River at Merritt watershed is recommended to assess the physical basis of the frequency-magnitude relationship, especially for higher return period (% AEP) events.
  - It is recommended that an ensemble of different hydrological models be used to characterize the hydrological processes in the watershed.

- It is recommended that the runoff be routed externally using a global routing product (e.g., Mizuroute) to standardize the hydrological model ensembles.

9.0 CLOSURE

We trust the above satisfies your requirements at this time. Should you have any questions or comments, please do not hesitate to contact us.

Yours sincerely,

BGC ENGINEERING INC.
per:

Melissa Hairabedian, M.Sc., P.Geo.
Hydrologist

Patrick Grover, Ph.D., P.Eng.
Hydrotechnical Engineer

Reviewed by:

Hamish Weatherly, M.Sc., P.Geo.
Principal Hydrologist

Matthias Jakob, Ph.D., P.Geo., P.L. Eng.
Principal Geoscientist

EGBC Permit To Practice: 1000944

KH/HW/rm/syt

REFERENCES

Bell, B., Hersbach, H., Simmons, A., Berrisford, P., Dahlgren, P., Horányi, A., et al. (2021). The ERA5 global reanalysis: Preliminary extension to 1950. *Quarterly Journal of the Royal Meteorological Society, 147* (741), 4186-4227. https://doi.org/10.1002/qj.4174

Boyd, R. and Markandya, A. (2021). Costs and Benefits of Climate Change Impacts and Adaptation; Chapter 6 in Canada in a Changing Climate: National Issues Report, (Eds.) F.J. Warren and N. Lulham; Government of Canada, Ottawa, Ontario.

Brogan, D.J., Nelson, P.A., & MacDonald, L.H. (2017). Reconstructing extreme post-wildfire floods: a comparison of convective and mesoscale events. *Earth Surface Processes and Landforms. 42*, 2505–2522. https://doi.org/10.1002/esp.4194

BGC Engineering Inc. (2021, June 4). *Merritt Detailed Flood Mapping Study, Nicola and Coldwater Rivers* [Report]. Prepared for Fraser Basin Council.

Bobotas, P. & Koutras, M.V. (2019). Distributions of the minimum and the maximum of a random number of random variables. *Statistics & Probability Letters, 146*, 57–64. https://doi.org/10.1016/j.spl.2018.10.023**.**

Bonsal, B.R., Peters, D.L., Seglenieks, F., Rivera, A., & Berg, A. (2019). Changes in freshwater availability across Canada; Chapter 6 in Canada's Changing Climate Report, (ed.) E. Bush and D.S. Lemmen; Government of Canada, Ottawa, Ontario, p. 261–342.

Brunner, G. W., & CEIWR-HEC. (2021). *HEC-RAS River Analysis System 2-D Modeling User's Manua*l. Retrieved from www.hec.usace.army.mil.

Cao, Q., Gershunov, G., Shulgina, T., Raph, F.M., Sun, N., & Lettenmaier, D.P. (2020). Floods due to Atmospheric Rivers along the U.S. West Coast: The Role of Antecedent Soil Moisture in a Warming Climate. *Journal of Meteorology, 21(8)*, 1827-1845. https://doi.org/10.1175/JHM-D-19-0242.1

Church, M., & Jakob, M. (2020). What is a Debris Flood? *Water Resources Research, 56*(8). https://doi.org/10.1029/2020WR027144

Coia, V., Joshi, A., Tan, S., & Zhu, Z. (2022). distplyr: Manipulation of Univariate Distributions. R package version 0.1.2.9000.

Curry, C.L., Islam, S.U., Zwiers, F.W., & Déry, S.J. (2019). Atmospheric rivers increase future flood risk in Western Canada's largest Pacific River. *Geophysical Research Letters, 46*, 1651–1661. https://doi.org/10.1029/2018GL080720

Demarchi, D.A. (2011). Ecoregions of British Columbia. Third Edition. Ministry of Environment. Victoria, British Columbia.

Dettinger, M.D., Ralph, F.M., Das, T., Neiman, P.J., & Cayan, D.R. (2011). Atmospheric rivers, floods and the water resources of California. *Water, 3*(2), 445–478. https://doi.org/10.3390/w3020445

DTN and MGS Engineering (2020). *British Columbia Extreme Flood Project, Regional Precipitation-Frequency Analysis for British Columbia – Technical Report (Bulletin 2020-2-RPFA)*. Report prepared by DTN, LLC and MGS Engineering Consultants, Inc. for the British Columbia Ministry of Forests, Lands, Natural Resources Operations, and Rural Development. May 2020.

DTN MetPortal—One-Stop Access to Online Precipitation-Frequency Tools and Data. Available online: https://www.dtn.com/weather/utilities-and-renewable-energy/metportal/ (accessed on 30 November 2021)

Ebel, B.A., Moody, J.A., & Martin, D.A. (2012). Hydrologic conditions controlling runoff generation immediately after wildfire. *Water Resources Research, 48*, W03529. https://doi.org/10.1029/2011WR011470

Engineers and Geoscientists of British Columbia (EGBC). (2018, July). Professional practice guidelines: Legislated flood assessments in a changing climate in BC. Retrieved from https://www.egbc.ca/getmedia/f5c2d7e9-26ad-4cb3-b528-940b3aaa9069/Legislated-Flood-Assessments-in-BC.pdf.aspx

England, J.F., Jr., Cohn, T.A., Faber, B.A., Stedinger, J.R., Thomas, W.O., Jr., Veilleux, A.G., Kiang, J.E., & Mason, R.R., Jr. (2018). *Guidelines for determining flood flow frequency—Bulletin 17C* (ver. 1.1, May 2019). U.S. Geological Survey Techniques and Methods, book 4, chap. B5, 148 p. https://doi.org/10.3133/tm4B5**.**

Farr, T.G., et al. (2007), The Shuttle Radar Topography Mission. Reviews of Geophysics, 45, RG2004, https://doi.org/10.1029/2005RG000183.

Fortin, V., Roy, G., Stadnyk, T., Koenig, K., Gasset, N., & Mahidjiba, A. (2018). Ten years of science based on the Canadian precipitation analysis: A CaPA system overview and literature review. *Atmosphere-Ocean, 56*(3), 178-196. https://doi.org/10.1080/07055900.2018.1474728

Gasset, N., Fortin, V., Dimitrijevic, M., Carrera, M., Bilodeau, B., Muncaster, R., et al. (2021). A 10 km North American precipitation and land-surface reanalysis based on the GEM atmospheric model. *Hydrology and Earth System Sciences, 25*(9), 4917-4945. https://doi.org/10.5194/hess-25-4917-2021

Gershunov, A., Shulgina, Ralph, F.M., Lavers, D.A., & Rutz, J.J. (2017). Assessing the climate-scale variability of atmospheric rivers affecting western North America. *Geophysics Research Letters, 44*. https://doi:.org/10.1002/2017GL074175.

Gillett, N., Cannon, A., Malinina, E., Schnorbus, M., Anslow, F., Sun, Q., Kirchmeier-Young, M., Zwiers, F., Seiler, C., Zhang, X., Flato, G., Wan, H., Li, G., & Castellan, A. (2022). Human influence on the 2021 British Columbia floods. Article available in preprint at SSRN but has not been peer-reviewed at this time https://papers.ssrn.com/sol3/papers.cfm?abstract_id=4025205

Gonzales, K.R., Swain, D.L., Nardi, K.M., Barnes, E.A., & Diffenbaugh, N.S. (2019). Recent warming of landfalling atmospheric rivers along the west coast of the United States. *Journal of Geophysical Research‐Atmospheres, 124*(13), 6810–6826. https://doi.org/10.1029/2018JD029860

Green Analytics Corporation (2020, February 20). *Investing in Canada's Future: The Cost of Climate Adaptation at the Local Level*. [Report]. Prepared for the Federation of Canadian Municipalities and the Insurance Bureau of Canada.

Guan, B., Waliser, D.E., Ralph, F.M., Fetzer, E.J., & Neiman, P.J. (2016). Hydrometeorological characteristics of rain-on-snow events associated with atmospheric rivers. *Geophysical Research Letters, 43*, 2964–2973, https://doi.org/10.1002/2016GL067978.

Gupta, H. V., Kling, H., Yilmaz, K. K., & Martinez, G. F. (2009). Decomposition of the mean squared error and NSE performance criteria: Implications for improving hydrological modelling. Journal of hydrology, 377(1-2), 80-91. https://doi.org/10.1016/j.jhydrol.2009.08.003.

Hamman, J., Nijssen, B., Brunke, M., Cassano, J., Craig, A., DuVivier, A., Hughes, M., Lettenmaier, D.P., Maslowski, W., Osinski, R., Roberts, A., & Zeng, X. (2016). Land Surface Climate in the Regional Arctic System Model. *Journal of Climate, 29*, 6543–6562. https://doi.org/10.1175/JCLI-D-15-0415.1

Heggen, R. (2001). Normalised Antecedent Precipitation Index. *Journal of Hydrologic Engineering (ASCE), 6*(5), 377–381.

Hersbach, H., Bell, B., Berrisford, P., Hirahara, S., Horányi, A., Muñoz-Sabater, J., et al. (2020). The ERA5 global reanalysis, *Quarterly Journal of the Royal Meteorological Society, 146*(730), 1999-2049. https://doi.org/10.1002/qj.3803

Hubbard, L.L. (1994). *Floods of November 1990 in Western Washington*. U.S. Geological Survey, Open-File Report 93-631. https://pubs.usgs.gov/of/1993/0631/report.pdf

Huntington, T.G. (2005). Evidence for intensification of the global water cycle: Review and synthesis. *Journal of Hydrology, 319*, 83–95. https://doi.org/10.1016/j.jhydrol.2005.07.003

Irnie, M. (2021). Merritt BC Flooded Evacuation Order 4:30pm November 15, 2021 [Video file]. Retrieved from https://youtu.be/gwUMPs6ULtI

Jakob, M., Davidson, S., Bullard, G., Busslinger, M., Collier-Pandya, B., Grover, P., & Lau, C-A. (2022). Debris-Flood Hazard Assessments in Steep Streams. *Water Resources Research, 58(*4). https://doi.org/10.1029/2021WR030907

Latifovic, R., Homer, C., Ressl, R., and Pouliot, D.A., Hossian, S., Colditz, R., Olthof, I., Chandra, G., Victoria, A. (2012). North American Land Change Monitoring System. Remote Sensing of Land Use and Land Cover: Principles and Applications. 303-324. 10.1201/b11964-24.

Lespinas, F., Fortin, V., Roy, G., Rasmussen, P., & Stadnyk, T. (2015). Performance evaluation of the Canadian precipitation analysis (CaPA). *Journal of Hydrometeorology, 16*(5), 2045-2064. https://doi.org/10.1175/JHM-D-14-0191.1

Lohmann, D., Nolte-Holube, R., & Raschke, E. (1996). A large-scale horizontal routing model to be coupled to land surface parametrization schemes. Tellus A 48, 708–721. https://doi.org/10.3402/tellusa.v48i5.12200(link is external).

Lohmann, D., Raschke, E., Nijssen, B., & Lettenmaier, D.P. (1998). Regional scale hydrology: I. Formulation of the VIC-2L model coupled to a routing model. *Hydrological Sciences Journal, 43*, 131–141. https://doi.org/10.1080/02626669809492107

Meehl, G.A., Hu, A., & Santer, B.D. (2009). The mid-1970s climate shift in the Pacific and the relative roles of forced versus inherent decadal variability. *Journal of Climate, 22*(3), 780–792. https://doi.org/10.1175/2008JCLI2552.1

Ministry of Environment and Climate Change Strategy. (2009). Automated Snow Weather Stations. Automated Snow Weather Stations - Province of British Columbia. https://www2.gov.bc.ca/gov/content/environment/air-land-water/water/water-science-data/water-data-tools/snow-survey-data/automated-snow-weather-stations (Accessed January 19, 2022).

Mo, R., So, R., Brugman, M.M., Mooney, C., Liu, A.Q., Jakob, M., et al. (2021). Column Relative Humidity and Primary Condensation Rate as Two Useful Supplements to Atmospheric River Analysis. *Water Resources Research, 57*(11), e2021WR029678. https://doi.org/10.1029/2021WR029678

Nash, E., and Sutcliffe, V. (1970). River flow forecasting through conceptual models Part 1 - A discussion of principles. Journal of Hydrology, 10 (1970), pp. 282-290.

Natural Resources Conservation Service. (2022). Automated Snow Monitoring. Monitoring Programs. https://www.nrcs.usda.gov/wps/portal/wcc/home/aboutUs/monitoringPrograms/automatedSnowMonitoring/ (Accessed January 19, 2022).

Pacific Climate Impacts Consortium (PCIC), University of Victoria. (2020, February). VIC-GL BCCAQ CMIP5 RVIC: Station Hydrologic Model Output. Downloaded from https://pacificclimate.org/data/station-hydrologic-model-output on February 15, 2022.

Radić, V., Cannon, A.J., Menounos, B., & Gi, N. (2015). Future changes in autumn atmospheric river events in British Columbia, Canada, as projected by CMIP5 global climate models. *Journal of Geophysical Research‐Atmospheres, 120*(18), 1651–1669. https://doi.org/10.1002/2015JD023279

Ralph, F.M., Rutz, J.J., Cordeira,J.M., Dettinger, M., Anderson, M., Reynolds,D., Schick, L.J., & Smallcomb, C. (2019). A scale to characterise the strength and impacts of atmospheric rivers. *American Meteorological Society, 100*(2), 269-289. https://doi.org/10.1175/BAMS-D-18-0023.1

Ross, C.W., Prihodko, L., Anchang, J., Kumar, S., Ji, W., & Haman, N.P. (2018). HYSOGs250m,global gridded hydrologic soilgroups for curve-number-based runoff modeling. *Scientific Data, 5*,150091. https://doi.org/10.1038/sdata.2018.91

Schnorbus, M.A. (in prep). Modelling glacier surface mass and energy balance with the VIC model. Dev.

Sharma, A.R. & Déry, S.J. (2019). Variability and trends of landfalling atmospheric rivers along the Pacific Coast of northwestern North America. *International Journal of Climatology, 40*, 544–558. https://doi.org/10.1002/joc.6227

Sharma, A.R. & Déry, S.J. (2020a). Contribution of atmospheric rivers to annual, seasonal, and extreme precipitation across British Columbia and southeastern Alaska. *Journal of Geophysical Research: Atmospheres, 123*. https://doi.org/10.1029/ 2019JD031823

Sharma, A.R., & Déry, S.J. (2020b). Linking atmospheric rivers to annual and extreme river runoff in British Columbia and southeastern Alaska. *Journal of Hydrometeorology, 21*(11), 2457-2472, https://doi.org/10.1175/JHM-D-19-0281.1.

United States Geological Survey (USGS). (1986). Urban hydrology for small watersheds. Technical report 55.

Wang, T., Hamann, A., Spittlehouse, D., & Carroll, C. (2016). Locally Downscaled and Spatially Customizable Climate Data for Historical and Future Periods for North America. *PLoS ONE 11*(6): e0156720. https://doi.org/10.1371/journal.pone.0156720

Wark, K. (1988) [1966]. *Generalized Thermodynamic Relationships. Thermodynamics (5th ed.)*. New York, NY: McGraw-Hill, Inc. ISBN 978-0-07-068286-3.

Watt, W.E. (Ed.). (1989). *Hydrology of floods in Canada: a guide to planning and design*. Ottawa, Canada: National Research Council Canada, Associate Committee on Hydrology.

Waylen, P. & Woo, M-K. (1982). *Prediction of annual floods generated by mixed processes. Water Resources Research, 18*(4), 1283-1286.

Waylen, P., & Woo, M-K. (1983). Annual floods in Southwestern British Columbia, Canada. *Journal of Hydrology, 62*, 95-105.

Werner, A.T., Schnorbus, M.A., Shrestha, R.R., Canon, A.J., Zwiers, F.W., Dayon, G., and Anslow, F. (2019). Data Descriptor: A long-term, temporally consistent, gridded daily meteorological dataset for northwestern North America. *Scientific Data, 6*, 180299. https://doi.org/10.1038/sdata.2018.299

Winkler, R.D., Moore, D., Redding, T. E., Spittlehouse, D.L., Smerdon, B.D., & Carlyle-Moses, D.W. (2010). The effects of forest disturbance on hydrologic processes and watershed response. In: *Compendium of Forest Hydrology and Geomorphology in British Columbia*. Pike, R.G., Redding, T.E., Moore, R.D., Winkler, R.D., and Bladon, K.D. (editors). B.C. Min. For. Range, Victoria, B.C., and FORREX. Land Manag. Handb. 66, pp. 179−212.

APPENDIX A
SUMMARY OF HWMs AND COMPARISON WITH HYDRAULIC MODELLING RESULTS

Table A-1 Summary of high-water marks (HWMs) and comparison with hydraulic modelling results using pre-flood terrain.

Survey Point	Photo_Name	Source	Easting	Northing	Elevation	Code	400 m^3/s Run		300 m^3/s Run		250 m^3/s Run		200 m^3/s Run	
							Modelled Elevation (m)	Offset (m)	Modelled Elevation (m)	Offset (m)	Modelled Elevation (m)	Offset (m)	Modelled Elevation (m)	Offset (m)
1042	Survey_Photo_51	Ecoscape	6.59E+05	5.55E+06	608.14	HW Evidence - Fence Debris	607.88	0.26	608.14	Dry	608.14	Dry	608.14	Dry
1066	Survey_Photo_52	Ecoscape	6.59E+05	5.55E+06	606.59	HW Evidence - Sediment Deposit	606.59	Dry	606.59	Dry	606.59	Dry	606.59	Dry
1092	Survey_Photo_53	Ecoscape	6.59E+05	5.55E+06	606.44	HW Evidence - Rafted Debris	606.06	0.39	605.84	0.61	605.72	0.72	605.58	0.87
1093	Survey_Photo_54	Ecoscape	6.59E+05	5.55E+06	606.84	HW Evidence - Scour	606.69	0.15	606.58	0.26	606.50	0.34	606.84	Dry
1094	Survey_Photo_55	Ecoscape	6.59E+05	5.55E+06	607.73	HW Evidence - Rafted Debris	607.22	0.51	607.11	0.62	607.02	0.71	606.89	0.84
1095	Survey_Photo_56	Ecoscape	6.59E+05	5.55E+06	607.13	HW Evidence - Scour	607.13	Dry	607.13	Dry	607.13	Dry	607.13	Dry
1106	Survey_Photo_57	Ecoscape	6.59E+05	5.55E+06	607.97	GRD	607.72	0.25	607.58	0.39	607.48	0.48	607.38	0.59
1107	Survey_Photo_58	Ecoscape	6.59E+05	5.55E+06	609.21	GRD	609.17	0.04	608.96	0.24	608.85	0.35	608.73	0.48
1108	Survey_Photo_59	Ecoscape	6.59E+05	5.55E+06	608.99	GRD	608.99	Dry	608.99	Dry	608.99	Dry	608.99	Dry
1109	Survey_Photo_60	Ecoscape	6.59E+05	5.55E+06	601.83	HW Evidence - Rafted Debris	602.24	-0.41	601.72	0.11	601.44	0.39	601.83	Dry
1110	Survey_Photo_61	Ecoscape	6.58E+05	5.55E+06	600.81	HW Evidence - Scour	600.76	0.04	600.81	Dry	600.81	Dry	600.81	Dry
1188	Survey_Photo_62	Ecoscape	6.59E+05	5.55E+06	599.80	HW Evidence - Sediment Deposit	599.77	0.02	599.51	0.28	599.32	0.47	599.80	Dry
1344	Survey_Photo_63	Ecoscape	6.58E+05	5.55E+06	599.90	HW Evidence - Sediment Deposit	599.90	Dry	599.90	Dry	599.90	Dry	599.90	Dry
1377	Survey_Photo_64	Ecoscape	6.58E+05	5.55E+06	596.84	HW Evidence - Scour	596.84	Dry	596.84	Dry	596.84	Dry	596.84	Dry
1523	Survey_Photo_65	Ecoscape	6.57E+05	5.55E+06	593.79	HW Evidence - Rafted Debris	593.29	0.49	593.22	0.57	593.14	0.65	592.92	0.86
1524	Survey_Photo_66	Ecoscape	6.57E+05	5.55E+06	593.39	HW Evidence - Scour	593.39	Dry	593.39	Dry	593.39	Dry	593.39	Dry
1723	Survey_Photo_67	Ecoscape	6.57E+05	5.55E+06	590.06	HW Evidence - Fence Debris	589.43	0.63	589.35	0.71	590.06	Dry	590.06	Dry
1724	Survey_Photo_68	Ecoscape	6.57E+05	5.55E+06	590.06	HW Evidence - Fence Debris	589.42	0.64	589.34	0.72	589.19	0.88	590.06	Dry
1725	Survey_Photo_69	Ecoscape	6.57E+05	5.55E+06	589.74	HW Evidence - Sediment Stain	589.74	Dry	589.74	Dry	589.74	Dry	589.74	Dry
1726	Survey_Photo_70	Ecoscape	6.57E+05	5.55E+06	589.31	HW Evidence - Fence Debris	589.31	Dry	589.31	Dry	589.31	Dry	589.31	Dry
1727	Survey_Photo_71	Ecoscape	6.57E+05	5.55E+06	587.96	HW Evidence - Fence Debris	587.21	0.75	587.96	Dry	587.96	Dry	587.96	Dry
1728	Survey_Photo_72	Ecoscape	6.57E+05	5.55E+06	590.32	HW Evidence - Fence Debris	590.32	Dry	590.32	Dry	590.32	Dry	590.32	Dry
1729	Survey_Photo_73	Ecoscape	6.57E+05	5.55E+06	590.11	HW Evidence - Sediment Deposit	590.11	Dry	590.11	Dry	590.11	Dry	590.11	Dry
1730	Survey_Photo_73	Ecoscape	6.57E+05	5.55E+06	590.13	HW Evidence - Sediment Deposit	590.13	Dry	590.13	Dry	590.13	Dry	590.13	Dry
1731	Survey_Photo_73	Ecoscape	6.57E+05	5.55E+06	590.13	HW Evidence - Sediment Deposit	590.13	Dry	590.13	Dry	590.13	Dry	590.13	Dry
1732	Survey_Photo_74	Ecoscape	6.57E+05	5.55E+06	590.75	HW Evidence - Sediment Stain	590.75	Dry	590.75	Dry	590.75	Dry	590.75	Dry
1733	Survey_Photo_75	Ecoscape	6.57E+05	5.55E+06	591.42	HW Evidence - Fence Debris	590.88	0.55	590.77	0.65	591.42	Dry	591.42	Dry

Survey Point	Photo_Name	Source	Easting	Northing	Elevation	Code	400 m³/s Run		300 m³/s Run		250 m³/s Run		200 m³/s Run	
							Modelled Elevation (m)	Offset (m)	Modelled Elevation (m)	Offset (m)	Modelled Elevation (m)	Offset (m)	Modelled Elevation (m)	Offset (m)
1734	Survey_Photo_76	Ecoscape	6.57E+05	5.55E+06	591.67	HW Evidence - Fence Debris	591.38	0.29	591.67	Dry	591.67	Dry	591.67	Dry
1735	Survey_Photo_77	Ecoscape	6.57E+05	5.55E+06	591.93	HW Evidence - Fence Debris	591.48	0.45	591.43	0.51	591.93	Dry	591.93	Dry
1736	Survey_Photo_78	Ecoscape	6.57E+05	5.55E+06	592.33	HW Evidence - Sediment Stain	591.99	0.34	591.90	0.43	591.78	0.55	592.33	Dry
1737	Survey_Photo_79	Ecoscape	6.57E+05	5.55E+06	592.00	HW Evidence - Fence Debris	591.82	0.18	591.73	0.27	592.00	Dry	592.00	Dry
1738	Survey_Photo_80	Ecoscape	6.57E+05	5.55E+06	592.86	HW Evidence - Fence Debris	592.35	0.51	592.86	Dry	592.86	Dry	592.86	Dry
1739	Survey_Photo_81	Ecoscape	6.57E+05	5.55E+06	593.38	HW Evidence - Sediment Deposit	593.38	Dry	593.38	Dry	593.38	Dry	593.38	Dry
1740	Survey_Photo_82	Ecoscape	6.57E+05	5.55E+06	591.62	HW Evidence - Sediment Stain	591.43	0.19	591.62	Dry	591.62	Dry	591.62	Dry
1741	Survey_Photo_83	Ecoscape	6.57E+05	5.55E+06	588.85	HW Evidence - Fence Debris	588.82	0.04	588.78	0.07	588.76	0.09	588.72	0.13
1742	Survey_Photo_84	Ecoscape	6.57E+05	5.55E+06	589.92	HW Evidence - Fence Debris	590.03	-0.11	589.96	-0.04	589.91	0.01	589.83	0.09
1743	Survey_Photo_85	Ecoscape	6.57E+05	5.55E+06	589.73	HW Evidence - Fence Debris	589.67	0.07	589.61	0.12	589.56	0.17	589.50	0.24
1744	Survey_Photo_86	Ecoscape	6.57E+05	5.55E+06	590.28	HW Evidence - Fence Debris	590.23	0.05	590.15	0.13	590.08	0.20	589.97	0.31
1745	Survey_Photo_87	Ecoscape	6.57E+05	5.55E+06	590.17	HW Evidence - Fence Debris	590.08	0.10	590.17	Dry	590.17	Dry	590.17	Dry
1746	Survey_Photo_88	Ecoscape	6.58E+05	5.55E+06	589.70	HW Evidence - Rafted Debris	589.48	0.22	589.70	Dry	589.70	Dry	589.70	Dry
1747	Survey_Photo_89	Ecoscape	6.58E+05	5.55E+06	590.35	HW Evidence - Sediment Stain	590.42	-0.06	590.25	0.10	590.15	0.20	590.35	Dry
1748	Survey_Photo_90	Ecoscape	6.58E+05	5.55E+06	590.59	HW Evidence - Fence Debris	590.52	0.07	590.39	0.20	590.26	0.33	590.59	Dry
1749	Survey_Photo_91	Ecoscape	6.58E+05	5.55E+06	591.17	HW Evidence - Fence Debris	590.93	0.24	590.78	0.39	590.65	0.52	590.51	0.66
1750	Survey_Photo_92	Ecoscape	6.58E+05	5.55E+06	591.60	HW Evidence - Fence Debris	591.60	Dry	591.60	Dry	591.60	Dry	591.60	Dry
1751	Survey_Photo_93	Ecoscape	6.58E+05	5.55E+06	591.29	HW Evidence - Fence Debris	591.07	0.22	591.29	Dry	591.29	Dry	591.29	Dry
1752	Survey_Photo_94	Ecoscape	6.58E+05	5.55E+06	590.86	HW Evidence - Fence Debris	590.82	0.04	590.86	Dry	590.86	Dry	590.86	Dry
1753	Survey_Photo_95	Ecoscape	6.57E+05	5.55E+06	589.14	HW Evidence - Rafted Debris	589.30	-0.16	589.13	0.02	589.01	0.14	588.85	0.29
1754	Survey_Photo_96	Ecoscape	6.57E+05	5.55E+06	590.60	HW Evidence - Fence Debris	590.53	0.07	590.43	0.16	590.35	0.25	590.24	0.36
1755	Survey_Photo_97	Ecoscape	6.57E+05	5.55E+06	592.01	HW Evidence - Fence Debris	590.89	1.12	590.76	1.25	590.65	1.36	590.47	1.54
1756	Survey_Photo_98	Ecoscape	6.57E+05	5.55E+06	591.56	HW Evidence - Fence Debris	591.56	0.01	591.37	0.19	591.22	0.35	591.02	0.55
1757	Survey_Photo_99	Ecoscape	6.57E+05	5.55E+06	591.57	HW Evidence - Fence Debris	591.59	-0.02	591.39	0.18	591.23	0.34	591.02	0.55
1758	Survey_Photo_100	Ecoscape	6.57E+05	5.55E+06	591.37	HW Evidence - Fence Debris	591.38	-0.01	591.21	0.16	591.07	0.29	590.89	0.47
1759	Survey_Photo_101	Ecoscape	6.57E+05	5.55E+06	591.59	HW Evidence - Fence Debris	591.43	0.16	591.25	0.34	591.10	0.49	591.59	Dry
1761	Survey_Photo_102	Ecoscape	6.57E+05	5.55E+06	591.48	HW Evidence - Fence Debris	591.58	-0.10	591.36	0.12	591.20	0.28	591.00	0.48
1762	Survey_Photo_103	Ecoscape	6.58E+05	5.55E+06	592.61	HW Evidence - Fence Debris	592.07	0.54	592.61	Dry	592.61	Dry	592.61	Dry

Survey Point	Photo_Name	Source	Easting	Northing	Elevation	Code	400 m^3/s Run		300 m^3/s Run		250 m^3/s Run		200 m^3/s Run	
							Modelled Elevation (m)	Offset (m)	Modelled Elevation (m)	Offset (m)	Modelled Elevation (m)	Offset (m)	Modelled Elevation (m)	Offset (m)
1763	Survey_Photo_105	Ecoscape	6.58E+05	5.55E+06	592.17	HW Evidence - Fence Debris	591.98	0.19	591.84	0.33	591.75	0.41	592.17	Dry
1764	Survey_Photo_104	Ecoscape	6.58E+05	5.55E+06	592.20	HW Evidence - Fence Debris	592.02	0.18	591.91	0.29	591.85	0.35	591.77	0.43
1785	Survey_Photo_106	Ecoscape	6.58E+05	5.55E+06	596.91	HW Evidence - Scour	596.91	Dry	596.91	Dry	596.91	Dry	596.91	Dry
1786	Survey_Photo_107	Ecoscape	6.58E+05	5.55E+06	597.12	HW Evidence - Scour	596.91	0.21	597.12	Dry	597.12	Dry	597.12	Dry
1787	Survey_Photo_108	Ecoscape	6.58E+05	5.55E+06	597.57	HW Evidence - Scour	597.57	Dry	597.57	Dry	597.57	Dry	597.57	Dry
1788	Survey_Photo_109	Ecoscape	6.58E+05	5.55E+06	597.65	HW Evidence - Scour	597.65	0.00	597.65	Dry	597.65	Dry	597.65	Dry
1789	Survey_Photo_110	Ecoscape	6.58E+05	5.55E+06	597.95	HW Evidence - Scour	597.95	Dry	597.95	Dry	597.95	Dry	597.95	Dry
1790	Survey_Photo_111	Ecoscape	6.58E+05	5.55E+06	597.97	HW Evidence - Scour	598.15	-0.18	597.97	Dry	597.97	Dry	597.97	Dry
1791	Survey_Photo_112	Ecoscape	6.58E+05	5.55E+06	598.54	HW Evidence - Scour	598.59	-0.04	598.54	Dry	598.54	Dry	598.54	Dry
1792	Survey_between 112 and 113	Ecoscape	6.58E+05	5.55E+06	599.03	HW Evidence - Scour	599.03	Dry	599.03	Dry	599.03	Dry	599.03	Dry
1793	Survey_between 112 and 113	Ecoscape	6.58E+05	5.55E+06	599.02	HW Evidence - Scour	599.02	Dry	599.02	Dry	599.02	Dry	599.02	Dry
1794	Survey_between 112 and 113	Ecoscape	6.58E+05	5.55E+06	599.21	HW Evidence - Scour	599.21	Dry	599.21	Dry	599.21	Dry	599.21	Dry
1795	Survey_Photo_113	Ecoscape	6.58E+05	5.55E+06	599.22	HW Evidence - Scour	599.22	Dry	599.22	Dry	599.22	Dry	599.22	Dry
1796	Survey_Photo_114	Ecoscape	6.58E+05	5.55E+06	599.31	HW Evidence - Scour	599.31	Dry	599.31	Dry	599.31	Dry	599.31	Dry
1797	Survey_Photo_115	Ecoscape	6.58E+05	5.55E+06	599.44	HW Evidence - Scour	599.44	Dry	599.44	Dry	599.44	Dry	599.44	Dry
1798	Survey_Photo_116	Ecoscape	6.58E+05	5.55E+06	599.98	HW Evidence - Rafted Debris	599.98	Dry	599.98	Dry	599.98	Dry	599.98	Dry
1799	Survey_Photo_117	Ecoscape	6.58E+05	5.55E+06	600.20	HW Evidence - Scour	600.20	Dry	600.20	Dry	600.20	Dry	600.20	Dry
1800	Survey_Adjacent to photo 117	Ecoscape	6.58E+05	5.55E+06	600.65	HW Evidence - Scour	600.65	Dry	600.65	Dry	600.65	Dry	600.65	Dry
1801	Survey_Photo_118	Ecoscape	6.59E+05	5.55E+06	603.35	HW Evidence - Scour	603.90	-0.56	603.35	Dry	603.35	Dry	603.35	Dry
1802	Survey_Photo_119	Ecoscape	6.59E+05	5.55E+06	604.63	HW Evidence - Fence Debris	604.62	0.01	604.28	0.35	604.09	0.54	604.63	Dry
1803	Survey_Photo_120	Ecoscape	6.59E+05	5.55E+06	603.41	HW Evidence - Fence Debris	603.91	-0.50	603.28	0.14	603.41	Dry	603.41	Dry
1804	Survey_Photo_121	Ecoscape	6.59E+05	5.55E+06	602.23	HW Evidence - Rafted Debris	602.12	0.12	602.23	Dry	602.23	Dry	602.23	Dry
1805	Survey_Photo_123	Ecoscape	6.57E+05	5.55E+06	588.95	HW Evidence - Sediment Deposit	589.02	-0.07	588.95	Dry	588.95	Dry	588.95	Dry
1806	Survey_Photo_124	Ecoscape	6.57E+05	5.55E+06	588.91	HW Evidence - Fence Debris	588.76	0.15	588.62	0.28	588.91	Dry	588.91	Dry
1807	Survey_Photo_125	Ecoscape	6.57E+05	5.55E+06	588.23	HW Evidence - Rafted Debris	588.37	-0.14	588.15	0.09	588.02	0.21	587.89	0.34
1808	Survey_Photo_126	Ecoscape	6.57E+05	5.55E+06	588.31	HW Evidence - Sediment Deposit	588.40	-0.09	588.31	Dry	588.31	Dry	588.31	Dry
1809	Survey_Photo_127	Ecoscape	6.57E+05	5.55E+06	588.49	HW Evidence - Fence Debris	588.24	0.25	587.99	0.50	587.90	0.59	587.77	0.72

Survey Point	Photo_Name	Source	Easting	Northing	Elevation	Code	400 m^3/s Run		300 m^3/s Run		250 m^3/s Run		200 m^3/s Run	
							Modelled Elevation (m)	Offset (m)	Modelled Elevation (m)	Offset (m)	Modelled Elevation (m)	Offset (m)	Modelled Elevation (m)	Offset (m)
1810	Survey_Photo_128	Ecoscape	6.57E+05	5.55E+06	588.33	HW Evidence - Rafted Debris	587.74	0.58	587.51	0.82	587.41	0.92	587.32	1.01
1811	Survey_Photo_129	Ecoscape	6.57E+05	5.55E+06	587.82	HW Evidence - Fence Debris	587.62	0.20	587.82	Dry	587.82	Dry	587.82	Dry
1812	Survey_Photo_130	Ecoscape	6.57E+05	5.55E+06	587.32	HW Evidence - Fence Debris	587.34	-0.02	587.16	0.17	587.01	0.32	586.77	0.55
1813	Survey_Photo_131	Ecoscape	6.57E+05	5.55E+06	587.75	HW Evidence - Fence Debris	587.67	0.09	587.42	0.33	587.28	0.48	587.21	0.55
5326	Survey_Photo_1	Ecoscape	6.57E+05	5.55E+06	589.47	HW Evidence - Fence Debris	589.46	0.01	589.41	0.06	589.39	0.08	589.35	0.12
5327	Survey_Photo_2	Ecoscape	6.57E+05	5.55E+06	589.97	HW Evidence - Fence Debris	590.23	-0.26	590.14	-0.17	590.07	-0.10	589.95	0.01
5328	Survey_Photo_3	Ecoscape	6.57E+05	5.55E+06	590.01	HW Evidence - Fence Debris	590.43	-0.42	590.32	-0.31	590.22	-0.22	590.08	-0.07
5329	Survey_Photo_4	Ecoscape	6.57E+05	5.55E+06	590.90	HW Evidence - Fence Debris	591.12	-0.22	590.96	-0.06	590.84	0.06	590.66	0.24
5330	Survey_Photo_5	Ecoscape	6.58E+05	5.55E+06	591.55	HW Evidence - Fence Debris	591.56	-0.01	591.42	0.13	591.37	0.18	591.30	0.25
5331	Survey_Photo_6	Ecoscape	6.58E+05	5.55E+06	591.92	HW Evidence - Fence Debris	591.81	0.11	591.68	0.24	591.62	0.31	591.92	Dry
5332	Survey_Photo_7	Ecoscape	6.58E+05	5.55E+06	592.21	HW Evidence - Fence Debris	592.02	0.18	591.92	0.29	591.86	0.35	591.79	0.42
5333	Survey_Photo_8	Ecoscape	6.58E+05	5.55E+06	593.24	HW Evidence - Fence Debris	593.17	0.07	593.01	0.24	592.89	0.35	592.78	0.46
5334	Survey_Photo_9	Ecoscape	6.58E+05	5.55E+06	593.33	HW Evidence - Fence Debris	593.60	-0.27	593.44	-0.11	593.32	0.01	593.18	0.14
5335	Survey_Photo_10	Ecoscape	6.58E+05	5.55E+06	594.02	HW Evidence - Fence Debris	593.86	0.17	593.74	0.28	593.67	0.35	594.02	Dry
5336	Survey_Photo_11	Ecoscape	6.58E+05	5.55E+06	594.71	HW Evidence - Fence Debris	594.43	0.28	594.71	Dry	594.71	Dry	594.71	Dry
5337	Survey_Photo_12	Ecoscape	6.58E+05	5.55E+06	595.04	HW Evidence - Fence Debris	594.77	0.27	594.68	0.36	594.64	0.41	595.04	Dry
5338	Survey_Photo_13	Ecoscape	6.58E+05	5.55E+06	594.48	HW Evidence - Fence Debris	594.15	0.33	594.48	Dry	594.48	Dry	594.48	Dry
5339	Survey_Photo_14	Ecoscape	6.58E+05	5.55E+06	594.14	HW Evidence - Fence Debris	594.14	Dry	594.14	Dry	594.14	Dry	594.14	Dry
5340	Survey_Photo_15	Ecoscape	6.58E+05	5.55E+06	595.89	HW Evidence - Fence Debris	595.79	0.09	595.61	0.27	595.49	0.40	595.31	0.57
5341	Survey_Photo_16	Ecoscape	6.58E+05	5.55E+06	595.01	HW Evidence - Fence Debris	594.72	0.29	594.62	0.39	594.56	0.44	594.53	0.48
5342	Survey_Photo_17	Ecoscape	6.58E+05	5.55E+06	595.47	HW Evidence - Fence Debris	595.39	0.08	595.22	0.25	595.10	0.38	594.96	0.51
5343	Survey_Photo_18	Ecoscape	6.58E+05	5.55E+06	595.25	HW Evidence - Fence Debris	595.34	-0.08	595.18	0.07	595.07	0.18	594.94	0.32
5344	Survey_Photo_19	Ecoscape	6.58E+05	5.55E+06	595.30	HW Evidence - Fence Debris	595.27	0.03	595.13	0.17	595.04	0.26	594.92	0.38
5345	Survey_Photo_20	Ecoscape	6.58E+05	5.55E+06	595.94	HW Evidence - Fence Debris	595.85	0.09	595.66	0.29	595.94	Dry	595.94	Dry
5346	Survey_Photo_21	Ecoscape	6.58E+05	5.55E+06	596.38	HW Evidence - Fence Debris	596.35	0.03	596.16	0.22	596.02	0.35	596.38	Dry
5347	Survey_Photo_22	Ecoscape	6.58E+05	5.55E+06	596.60	HW Evidence - Fence Debris	596.60	0.01	596.40	0.20	596.29	0.31	596.23	0.38
5348	Survey_Photo_23	Ecoscape	6.58E+05	5.55E+06	596.70	HW Evidence - Fence Debris	596.71	-0.01	596.47	0.23	596.36	0.34	596.22	0.48
5349	Survey_Photo_24	Ecoscape	6.58E+05	5.55E+06	597.47	HW Evidence - Sediment Stain	597.34	0.13	597.47	Dry	597.47	Dry	597.47	Dry

Survey Point	Photo_Name	Source	Easting	Northing	Elevation	Code	400 m^3/s Run		300 m^3/s Run		250 m^3/s Run		200 m^3/s Run	
							Modelled Elevation (m)	Offset (m)	Modelled Elevation (m)	Offset (m)	Modelled Elevation (m)	Offset (m)	Modelled Elevation (m)	Offset (m)
5350	Survey_Photo_25	Ecoscape	6.58E+05	5.55E+06	596.85	HW Evidence - Sediment Stain	596.85	Dry	596.85	Dry	596.85	Dry	596.85	Dry
5351	Survey_Photo_26	Ecoscape	6.58E+05	5.55E+06	595.72	HW Evidence - Fence Debris	595.58	0.14	595.42	0.31	595.34	0.39	595.27	0.45
5352	Survey_Photo_27	Ecoscape	6.59E+05	5.55E+06	607.91	HW Evidence - Fence Debris	607.79	0.12	607.62	0.29	607.91	Dry	607.91	Dry
5353	Survey_Photo_28	Ecoscape	6.59E+05	5.55E+06	603.71	HW Evidence - Fence Debris	604.16	-0.45	603.73	-0.02	603.33	0.38	603.71	Dry
5354	Survey_Photo_29	Ecoscape	6.59E+05	5.55E+06	603.97	HW Evidence - Sediment Stain	604.20	-0.23	603.81	0.16	603.55	0.42	603.97	Dry
5355	Survey_Photo_30	Ecoscape	6.59E+05	5.55E+06	604.09	HW Evidence - Sediment Stain	604.36	-0.27	604.00	0.09	604.09	Dry	604.09	Dry
5356	Survey_Photo_31	Ecoscape	6.59E+05	5.55E+06	604.68	HW Evidence - Fence Debris	604.84	-0.16	604.58	0.10	604.68	Dry	604.68	Dry
5357	Survey_Photo_32	Ecoscape	6.59E+05	5.55E+06	606.97	HW Evidence - Sediment Deposit	606.97	Dry	606.97	Dry	606.97	Dry	606.97	Dry
5358	Survey_Photo_33	Ecoscape	6.59E+05	5.55E+06	606.89	HW Evidence - Sediment Deposit	606.89	Dry	606.89	Dry	606.89	Dry	606.89	Dry
5359	Survey_Photo_34	Ecoscape	6.59E+05	5.55E+06	604.95	HW Evidence - Sediment Deposit	604.95	Dry	604.95	Dry	604.95	Dry	604.95	Dry
5360	Survey_Photo_35	Ecoscape	6.59E+05	5.55E+06	603.88	HW Evidence - Fence Debris	604.16	-0.28	603.88	Dry	603.88	Dry	603.88	Dry
5361	Survey_Photo_36	Ecoscape	6.59E+05	5.55E+06	603.52	HW Evidence - Sediment Stain	603.75	-0.23	603.52	Dry	603.52	Dry	603.52	Dry
5362	Survey_Photo_37	Ecoscape	6.59E+05	5.55E+06	603.28	HW Evidence - Fence Debris	603.40	-0.12	603.28	Dry	603.28	Dry	603.28	Dry
5363	Survey_Photo_38	Ecoscape	6.59E+05	5.55E+06	602.65	HW Evidence - Fence Debris	602.65	0.01	602.65	Dry	602.65	Dry	602.65	Dry
5364	Survey_Photo_39	Ecoscape	6.58E+05	5.55E+06	596.68	HW Evidence - Sediment Stain	596.77	-0.09	596.62	0.06	596.52	0.15	596.38	0.30
5365	Survey_Photo_40	Ecoscape	6.58E+05	5.55E+06	596.62	HW Evidence - Fence Debris	597.57	-0.95	597.27	-0.65	597.04	-0.42	596.79	-0.16
5366	Survey_Photo_41	Ecoscape	6.58E+05	5.55E+06	597.81	HW Evidence - Sediment Deposit	598.03	-0.22	597.81	Dry	597.81	Dry	597.81	Dry
5367	Survey_Photo_42	Ecoscape	6.58E+05	5.55E+06	598.49	HW Evidence - Sediment Deposit	598.96	-0.47	598.46	0.03	598.49	Dry	598.49	Dry
5368	Survey_Photo_43	Ecoscape	6.59E+05	5.55E+06	599.28	HW Evidence - Sediment Deposit	599.78	-0.50	599.54	-0.25	599.36	-0.07	599.15	0.13
5369	Survey_Photo_44	Ecoscape	6.58E+05	5.55E+06	600.17	HW Evidence - Sediment Deposit	600.10	0.07	599.87	0.30	599.72	0.45	599.55	0.62
5370	Survey_Photo_45	Ecoscape	6.58E+05	5.55E+06	601.86	HW Evidence - Sediment Deposit	602.44	-0.58	601.89	-0.03	601.86	Dry	601.86	Dry
5371	Survey_Photo_46	Ecoscape	6.59E+05	5.55E+06	601.96	HW Evidence - Sediment Deposit	602.49	-0.52	602.04	-0.08	601.80	0.16	601.96	Dry
5372	Survey_Photo_47	Ecoscape	6.59E+05	5.55E+06	602.66	HW Evidence - Sediment Deposit	602.52	0.14	602.66	Dry	602.66	Dry	602.66	Dry
5373	Survey_Photo_48	Ecoscape	6.59E+05	5.55E+06	602.64	HW Evidence - Sediment Deposit	603.79	-1.15	603.16	-0.52	602.79	-0.15	602.50	0.14
5374	Survey_Photo_49	Ecoscape	6.59E+05	5.55E+06	603.04	HW Evidence - Sediment Deposit	604.66	-1.62	604.33	-1.29	604.11	-1.06	603.75	-0.71
5375	Survey_Photo_50	Ecoscape	6.59E+05	5.55E+06	604.59	HW Evidence - Sediment Deposit	604.88	-0.29	604.52	0.07	604.28	0.31	603.95	0.64
n/a	Photo_1	FLNRO	657159.066	5553680.32	n/a	HW Evidence - Fence Debris	n/a	0	n/a	-0.03	n/a	-0.06	n/a	-0.11
n/a	Photo_2	BGC	657018.826	5553186.559	n/a	HW Evidence - Sediment Deposit	n/a	0.01	n/a	-0.22	n/a	-0.72	n/a	n/a[*2]

Survey Point	Photo_Name	Source	Easting	Northing	Elevation	Code	400 m^3/s Run		300 m^3/s Run		250 m^3/s Run		200 m^3/s Run	
							Modelled Elevation (m)	Offset (m)	Modelled Elevation (m)	Offset (m)	Modelled Elevation (m)	Offset (m)	Modelled Elevation (m)	Offset (m)
n/a	Photo_3	FLNRO	657026.523	5553163.069	n/a	HW Evidence - Sediment Deposit	n/a	-0.1	n/a	-0.4	n/a	-0.55	n/a	n/a[*2]
n/a	Photo_4	BGC	657498.975	5553444.881	n/a	HW Evidence - Fence Debris	n/a	-0.03	n/a	-0.16	n/a	-0.26	n/a	-0.36
n/a	Photo_5	BGC	657463.039	5553382.932	n/a	HW Evidence - Rafted Debris	n/a	-0.01	n/a	-0.1	n/a	-0.2	n/a	-0.38
n/a	Photo_6	BGC	657452.799	5553366.249	n/a	HW Evidence - Fence Debris	n/a	-0.04	n/a	-0.14	n/a	-0.24	n/a	-0.42
n/a	Photo_7	BGC	657775.657	5552832.729	n/a	HW Evidence - Fence Debris	n/a	-0.04	n/a	-0.16	n/a	-0.2	n/a	-0.27
n/a	Photo_8	BGC	657815.794	5552806.407	n/a	HW Evidence - Fence Debris	n/a	-0.08	n/a	-0.2	n/a	-0.24	n/a	-0.31
n/a	Photo_9	FLNRO	657792.869	5552697.49	n/a	HW Evidence - Fence Debris	n/a	-0.04	n/a	-0.11	n/a	-0.16	n/a	-0.24
n/a	Photo_10	FLNRO	657911.889	5552777.953	n/a	HW Evidence - Fence Debris	n/a	-0.03	n/a	-0.2	n/a	-0.32	n/a	-0.45
n/a	Photo_11	BGC	657992.793	5552756.627	n/a	HW Evidence - Fence Debris	n/a	-0.37	n/a	-0.53	n/a	-0.62	n/a	-0.69
n/a	Photo_12	FLNRO	657959.607	5552599.242	n/a	HW Evidence - Fence Debris	n/a	0.14	n/a	-0.07	n/a	-0.023	n/a	-0.41
n/a	Photo_13	FLNRO	658181.611	5552565.315	n/a	HW Evidence - Fence Debris	n/a	0.04	n/a	-0.23	n/a	-0.23	n/a	-0.23

Table B-2 Summary of high-water marks (HWMs) and comparison with hydraulic modelling results.

Survey Point	Photo_Name	Source	Easting	Northing	Elevation	Code	500 m3/s Run		400 m3/s Run		300 m3/s Run		250 m3/s Run		200 m3/s Run	
							Modelled Elevation	Offset (m)	Modelled Elevation	Offset (m)	Modelled Elevation	Offset (m)	Modelled Elevation	Offset (m)	Modelled Elevation	Offset (m)
1042	Survey_Photo_51	Ecoscape	6.59E+05	5.55E+06	608.14	HW Evidence - Fence Debris	608.26	-0.12	608.18	-0.04	608.10	0.04	608.14	Dry	608.14	Dry
1066	Survey_Photo_52	Ecoscape	6.59E+05	5.55E+06	606.59	HW Evidence - Sediment Deposit	606.59	Dry	606.59	Dry	606.59	Dry	606.59	Dry	606.59	Dry
1092	Survey_Photo_53	Ecoscape	6.59E+05	5.55E+06	606.44	HW Evidence - Rafted Debris	606.26	0.19	606.17	0.27	606.10	0.35	605.77	0.68	605.61	0.83
1093	Survey_Photo_54	Ecoscape	6.59E+05	5.55E+06	606.84	HW Evidence - Scour	607.23	-0.39	607.17	-0.33	607.11	-0.27	606.89	-0.05	606.78	0.06
1094	Survey_Photo_55	Ecoscape	6.59E+05	5.55E+06	607.73	HW Evidence - Rafted Debris	607.40	0.32	607.34	0.39	607.28	0.44	607.05	0.68	606.94	0.78
1095	Survey_Photo_56	Ecoscape	6.59E+05	5.55E+06	607.13	HW Evidence - Scour	607.41	-0.28	607.35	-0.21	607.29	-0.16	607.13	Dry	607.13	Dry
1106	Survey_Photo_57	Ecoscape	6.59E+05	5.55E+06	607.97	GRD	608.06	-0.09	608.00	-0.03	607.94	0.03	607.70	0.27	607.58	0.39
1107	Survey_Photo_58	Ecoscape	6.59E+05	5.55E+06	609.21	GRD	609.32	-0.11	609.20	0.00	609.11	0.09	608.80	0.40	609.21	Dry

Survey Point	Photo_Name	Source	Easting	Northing	Elevation	Code	500 m3/s Run		400 m3/s Run		300 m3/s Run		250 m3/s Run		200 m3/s Run	
							Modelled Elevation	Offset (m)	Modelled Elevation	Offset (m)	Modelled Elevation	Offset (m)	Modelled Elevation	Offset (m)	Modelled Elevation	Offset (m)
1108	Survey_Photo_59	Ecoscape	6.59E+05	5.55E+06	608.99	GRD	609.26	-0.27	609.19	-0.20	609.11	-0.12	608.99	Dry	608.99	Dry
1109	Survey_Photo_60	Ecoscape	6.59E+05	5.55E+06	601.83	HW Evidence - Rafted Debris	601.83	Dry	601.83	Dry	601.83	Dry	601.83	Dry	601.83	Dry
1110	Survey_Photo_61	Ecoscape	6.58E+05	5.55E+06	600.81	HW Evidence - Scour	600.81	Dry	600.81	Dry	600.81	Dry	600.81	Dry	600.81	Dry
1188	Survey_Photo_62	Ecoscape	6.59E+05	5.55E+06	599.80	HW Evidence - Sediment Deposit	599.80	Dry	599.80	Dry	599.80	Dry	599.80	Dry	599.80	Dry
1344	Survey_Photo_63	Ecoscape	6.58E+05	5.55E+06	599.90	HW Evidence - Sediment Deposit	599.90	Dry	599.90	Dry	599.90	Dry	599.90	Dry	599.90	Dry
1377	Survey_Photo_64	Ecoscape	6.58E+05	5.55E+06	596.84	HW Evidence - Scour	596.84	Dry	596.84	Dry	596.84	Dry	596.84	Dry	596.84	Dry
1523	Survey_Photo_65	Ecoscape	6.57E+05	5.55E+06	593.79	HW Evidence - Rafted Debris	593.79	Dry	593.79	Dry	593.79	Dry	593.79	Dry	593.79	Dry
1524	Survey_Photo_66	Ecoscape	6.57E+05	5.55E+06	593.39	HW Evidence - Scour	593.39	Dry	593.39	Dry	593.39	Dry	593.39	Dry	593.39	Dry
1723	Survey_Photo_67	Ecoscape	6.57E+05	5.55E+06	590.06	HW Evidence - Fence Debris	589.73	0.33	589.69	0.37	589.65	0.41	590.06	Dry	590.06	Dry
1724	Survey_Photo_68	Ecoscape	6.57E+05	5.55E+06	590.06	HW Evidence - Fence Debris	589.72	0.34	589.68	0.38	589.65	0.41	589.47	0.59	589.41	0.65
1725	Survey_Photo_69	Ecoscape	6.57E+05	5.55E+06	589.74	HW Evidence - Sediment Stain	589.60	0.13	589.74	Dry	589.74	Dry	589.74	Dry	589.74	Dry
1726	Survey_Photo_70	Ecoscape	6.57E+05	5.55E+06	589.31	HW Evidence - Fence Debris	589.21	0.10	589.20	0.11	589.31	Dry	589.31	Dry	589.31	Dry
1727	Survey_Photo_71	Ecoscape	6.57E+05	5.55E+06	587.96	HW Evidence - Fence Debris	587.52	0.44	587.39	0.57	587.30	0.66	587.96	Dry	587.96	Dry
1728	Survey_Photo_72	Ecoscape	6.57E+05	5.55E+06	590.32	HW Evidence - Fence Debris	590.17	0.15	590.15	0.18	590.32	Dry	590.32	Dry	590.32	Dry
1729	Survey_Photo_73	Ecoscape	6.57E+05	5.55E+06	590.11	HW Evidence - Sediment Deposit	590.11	Dry	590.11	Dry	590.11	Dry	590.11	Dry	590.11	Dry
1730	Survey_Photo_73	Ecoscape	6.57E+05	5.55E+06	590.13	HW Evidence -	590.13	Dry	590.13	Dry	590.13	Dry	590.13	Dry	590.13	Dry

Survey Point	Photo_Name	Source	Easting	Northing	Elevation	Code	500 m3/s Run		400 m3/s Run		300 m3/s Run		250 m3/s Run		200 m3/s Run	
							Modelled Elevation	Offset (m)	Modelled Elevation	Offset (m)	Modelled Elevation	Offset (m)	Modelled Elevation	Offset (m)	Modelled Elevation	Offset (m)
						Sediment Deposit										
1731	Survey_Photo_73	Ecoscape	6.57E+05	5.55E+06	590.13	HW Evidence - Sediment Deposit	590.13	Dry	590.13	Dry	590.13	Dry	590.13	Dry	590.13	Dry
1732	Survey_Photo_74	Ecoscape	6.57E+05	5.55E+06	590.75	HW Evidence - Sediment Stain	590.75	Dry	590.75	Dry	590.75	Dry	590.75	Dry	590.75	Dry
1733	Survey_Photo_75	Ecoscape	6.57E+05	5.55E+06	591.42	HW Evidence - Fence Debris	590.93	0.50	591.42	Dry	591.42	Dry	591.42	Dry	591.42	Dry
1734	Survey_Photo_76	Ecoscape	6.57E+05	5.55E+06	591.67	HW Evidence - Fence Debris	591.67	Dry	591.67	Dry	591.67	Dry	591.67	Dry	591.67	Dry
1735	Survey_Photo_77	Ecoscape	6.57E+05	5.55E+06	591.93	HW Evidence - Fence Debris	591.61	0.33	591.57	0.36	591.54	0.39	591.93	Dry	591.93	Dry
1736	Survey_Photo_78	Ecoscape	6.57E+05	5.55E+06	592.33	HW Evidence - Sediment Stain	592.00	0.33	591.95	0.38	591.89	0.43	592.33	Dry	592.33	Dry
1737	Survey_Photo_79	Ecoscape	6.57E+05	5.55E+06	592.00	HW Evidence - Fence Debris	591.84	0.16	592.00	Dry	592.00	Dry	592.00	Dry	592.00	Dry
1738	Survey_Photo_80	Ecoscape	6.57E+05	5.55E+06	592.86	HW Evidence - Fence Debris	592.86	Dry	592.86	Dry	592.86	Dry	592.86	Dry	592.86	Dry
1739	Survey_Photo_81	Ecoscape	6.57E+05	5.55E+06	593.38	HW Evidence - Sediment Deposit	593.38	Dry	593.38	Dry	593.38	Dry	593.38	Dry	593.38	Dry
1740	Survey_Photo_82	Ecoscape	6.57E+05	5.55E+06	591.62	HW Evidence - Sediment Stain	591.62	Dry	591.62	Dry	591.62	Dry	591.62	Dry	591.62	Dry
1741	Survey_Photo_83	Ecoscape	6.57E+05	5.55E+06	588.85	HW Evidence - Fence Debris	589.05	-0.20	588.97	-0.11	588.93	-0.08	588.86	0.00	588.81	0.04
1742	Survey_Photo_84	Ecoscape	6.57E+05	5.55E+06	589.92	HW Evidence - Fence Debris	589.97	-0.05	589.95	-0.03	589.93	-0.01	589.85	0.08	589.78	0.14
1743	Survey_Photo_85	Ecoscape	6.57E+05	5.55E+06	589.73	HW Evidence - Fence Debris	589.73	0.00	589.71	0.03	589.69	0.05	589.59	0.15	589.54	0.20
1744	Survey_Photo_86	Ecoscape	6.57E+05	5.55E+06	590.28	HW Evidence	590.16	0.12	590.13	0.15	590.11	0.17	589.99	0.29	589.88	0.40

Survey Point	Photo_Name	Source	Easting	Northing	Elevation	Code	500 m3/s Run		400 m3/s Run		300 m3/s Run		250 m3/s Run		200 m3/s Run	
							Modelled Elevation	Offset (m)	Modelled Elevation	Offset (m)	Modelled Elevation	Offset (m)	Modelled Elevation	Offset (m)	Modelled Elevation	Offset (m)
						- Fence Debris										
1745	Survey_Photo_87	Ecoscape	6.57E+05	5.55E+06	590.17	HW Evidence - Fence Debris	590.19	-0.02	590.14	0.04	590.07	0.10	590.17	Dry	590.17	Dry
1746	Survey_Photo_88	Ecoscape	6.58E+05	5.55E+06	589.70	HW Evidence - Rafted Debris	589.65	0.05	589.52	0.18	589.70	Dry	589.70	Dry	589.70	Dry
1747	Survey_Photo_89	Ecoscape	6.58E+05	5.55E+06	590.35	HW Evidence - Sediment Stain	590.59	-0.23	590.52	-0.17	590.46	-0.10	590.20	0.15	590.35	Dry
1748	Survey_Photo_90	Ecoscape	6.58E+05	5.55E+06	590.59	HW Evidence - Fence Debris	590.61	-0.02	590.56	0.03	590.50	0.09	590.25	0.34	590.59	Dry
1749	Survey_Photo_91	Ecoscape	6.58E+05	5.55E+06	591.17	HW Evidence - Fence Debris	591.10	0.07	591.06	0.11	591.01	0.16	590.74	0.43	590.63	0.55
1750	Survey_Photo_92	Ecoscape	6.58E+05	5.55E+06	591.60	HW Evidence - Fence Debris	591.43	0.16	591.60	Dry	591.60	Dry	591.60	Dry	591.60	Dry
1751	Survey_Photo_93	Ecoscape	6.58E+05	5.55E+06	591.29	HW Evidence - Fence Debris	591.16	0.13	591.29	Dry	591.29	Dry	591.29	Dry	591.29	Dry
1752	Survey_Photo_94	Ecoscape	6.58E+05	5.55E+06	590.86	HW Evidence - Fence Debris	590.93	-0.07	590.89	-0.03	590.86	Dry	590.86	Dry	590.86	Dry
1753	Survey_Photo_95	Ecoscape	6.57E+05	5.55E+06	589.14	HW Evidence - Rafted Debris	589.48	-0.34	589.43	-0.28	589.37	-0.23	589.11	0.03	589.04	0.10
1754	Survey_Photo_96	Ecoscape	6.57E+05	5.55E+06	590.60	HW Evidence - Fence Debris	590.49	0.11	590.44	0.16	590.35	0.25	590.60	Dry	590.60	Dry
1755	Survey_Photo_97	Ecoscape	6.57E+05	5.55E+06	592.01	HW Evidence - Fence Debris	591.10	0.91	591.06	0.95	591.02	0.99	590.78	1.23	590.66	1.35
1756	Survey_Photo_98	Ecoscape	6.57E+05	5.55E+06	591.56	HW Evidence - Fence Debris	591.71	-0.14	591.65	-0.09	591.60	-0.03	591.35	0.22	591.23	0.34
1757	Survey_Photo_99	Ecoscape	6.57E+05	5.55E+06	591.57	HW Evidence - Fence Debris	591.70	-0.12	591.64	-0.07	591.58	-0.01	591.32	0.25	591.21	0.37
1758	Survey_Photo_100	Ecoscape	6.57E+05	5.55E+06	591.37	HW Evidence - Fence Debris	591.51	-0.14	591.46	-0.09	591.40	-0.04	591.17	0.20	591.07	0.30
1759	Survey_Photo_101	Ecoscape	6.57E+05	5.55E+06	591.59	HW Evidence	591.68	-0.09	591.62	-0.03	591.55	0.04	591.25	0.35	591.59	Dry

Survey Point	Photo_Name	Source	Easting	Northing	Elevation	Code	500 m3/s Run		400 m3/s Run		300 m3/s Run		250 m3/s Run		200 m3/s Run	
							Modelled Elevation	Offset (m)	Modelled Elevation	Offset (m)	Modelled Elevation	Offset (m)	Modelled Elevation	Offset (m)	Modelled Elevation	Offset (m)
						- Fence Debris										
1761	Survey_Photo_102	Ecoscape	6.57E+05	5.55E+06	591.48	HW Evidence - Fence Debris	591.86	-0.38	591.80	-0.32	591.73	-0.25	591.45	0.03	591.32	0.16
1762	Survey_Photo_103	Ecoscape	6.58E+05	5.55E+06	592.61	HW Evidence - Fence Debris	592.33	0.28	592.27	0.34	592.22	0.39	592.61	Dry	592.61	Dry
1763	Survey_Photo_105	Ecoscape	6.58E+05	5.55E+06	592.17	HW Evidence - Fence Debris	592.17	0.00	592.11	0.06	592.05	0.12	591.82	0.35	592.17	Dry
1764	Survey_Photo_104	Ecoscape	6.58E+05	5.55E+06	592.20	HW Evidence - Fence Debris	592.10	0.10	592.07	0.13	592.03	0.17	591.90	0.30	591.85	0.35
1785	Survey_Photo_106	Ecoscape	6.58E+05	5.55E+06	596.91	HW Evidence - Scour	596.91	Dry	596.91	Dry	596.91	Dry	596.91	Dry	596.91	Dry
1786	Survey_Photo_107	Ecoscape	6.58E+05	5.55E+06	597.12	HW Evidence - Scour	597.12	Dry	597.12	Dry	597.12	Dry	597.12	Dry	597.12	Dry
1787	Survey_Photo_108	Ecoscape	6.58E+05	5.55E+06	597.57	HW Evidence - Scour	597.57	Dry	597.57	Dry	597.57	Dry	597.57	Dry	597.57	Dry
1788	Survey_Photo_109	Ecoscape	6.58E+05	5.55E+06	597.65	HW Evidence - Scour	597.65	Dry	597.65	Dry	597.65	Dry	597.65	Dry	597.65	Dry
1789	Survey_Photo_110	Ecoscape	6.58E+05	5.55E+06	597.95	HW Evidence - Scour	597.95	Dry	597.95	Dry	597.95	Dry	597.95	Dry	597.95	Dry
1790	Survey_Photo_111	Ecoscape	6.58E+05	5.55E+06	597.97	HW Evidence - Scour	598.04	-0.07	597.96	0.01	597.97	Dry	597.97	Dry	597.97	Dry
1791	Survey_Photo_112	Ecoscape	6.58E+05	5.55E+06	598.54	HW Evidence - Scour	598.69	-0.14	598.65	-0.11	598.65	-0.11	598.54	Dry	598.54	Dry
1792	Survey_between 112 and 113	Ecoscape	6.58E+05	5.55E+06	599.03	HW Evidence - Scour	599.03	Dry	599.03	Dry	599.03	Dry	599.03	Dry	599.03	Dry
1793	Survey_between 112 and 113	Ecoscape	6.58E+05	5.55E+06	599.02	HW Evidence - Scour	599.02	Dry	599.02	Dry	599.02	Dry	599.02	Dry	599.02	Dry
1794	Survey_between 112 and 113	Ecoscape	6.58E+05	5.55E+06	599.21	HW Evidence - Scour	599.21	Dry	599.21	Dry	599.21	Dry	599.21	Dry	599.21	Dry
1795	Survey_Photo_113	Ecoscape	6.58E+05	5.55E+06	599.22	HW Evidence - Scour	599.22	Dry	599.22	Dry	599.22	Dry	599.22	Dry	599.22	Dry
1796	Survey_Photo_114	Ecoscape	6.58E+05	5.55E+06	599.31	HW Evidence - Scour	599.31	Dry	599.31	Dry	599.31	Dry	599.31	Dry	599.31	Dry
1797	Survey_Photo_115	Ecoscape	6.58E+05	5.55E+06	599.44	HW Evidence - Scour	599.69	-0.26	599.65	-0.22	599.61	-0.18	599.46	-0.02	599.44	Dry
1798	Survey_Photo_116	Ecoscape	6.58E+05	5.55E+06	599.98	HW Evidence - Rafted Debris	599.98	Dry	599.98	Dry	599.98	Dry	599.98	Dry	599.98	Dry

Survey Point	Photo_Name	Source	Easting	Northing	Elevation	Code	500 m3/s Run		400 m3/s Run		300 m3/s Run		250 m3/s Run		200 m3/s Run	
							Modelled Elevation	Offset (m)	Modelled Elevation	Offset (m)	Modelled Elevation	Offset (m)	Modelled Elevation	Offset (m)	Modelled Elevation	Offset (m)
1799	Survey_Photo_117	Ecoscape	6.58E+05	5.55E+06	600.20	HW Evidence - Scour	600.20	Dry	600.20	Dry	600.20	Dry	600.20	Dry	600.20	Dry
1800	Survey_Adjacent to photo 117	Ecoscape	6.58E+05	5.55E+06	600.65	HW Evidence - Scour	600.65	Dry	600.65	Dry	600.65	Dry	600.65	Dry	600.65	Dry
1801	Survey_Photo_118	Ecoscape	6.59E+05	5.55E+06	603.35	HW Evidence - Scour	604.05	-0.71	603.86	-0.51	603.67	-0.32	603.39	-0.04	603.35	Dry
1802	Survey_Photo_119	Ecoscape	6.59E+05	5.55E+06	604.63	HW Evidence - Fence Debris	605.01	-0.38	604.81	-0.18	604.60	0.03	604.63	Dry	604.63	Dry
1803	Survey_Photo_120	Ecoscape	6.59E+05	5.55E+06	603.41	HW Evidence - Fence Debris	604.05	-0.64	603.84	-0.42	603.60	-0.19	603.41	Dry	603.41	Dry
1804	Survey_Photo_121	Ecoscape	6.59E+05	5.55E+06	602.23	HW Evidence - Rafted Debris	602.37	-0.14	602.27	-0.04	602.06	0.17	602.23	Dry	602.23	Dry
1805	Survey_Photo_123	Ecoscape	6.57E+05	5.55E+06	588.95	HW Evidence - Sediment Deposit	589.31	-0.36	589.25	-0.30	589.19	-0.24	589.02	-0.07	588.95	Dry
1806	Survey_Photo_124	Ecoscape	6.57E+05	5.55E+06	588.91	HW Evidence - Fence Debris	589.02	-0.11	588.95	-0.04	588.89	0.02	588.91	Dry	588.91	Dry
1807	Survey_Photo_125	Ecoscape	6.57E+05	5.55E+06	588.23	HW Evidence - Rafted Debris	588.84	-0.61	588.72	-0.49	588.61	-0.38	588.18	0.05	587.95	0.28
1808	Survey_Photo_126	Ecoscape	6.57E+05	5.55E+06	588.31	HW Evidence - Sediment Deposit	588.90	-0.60	588.74	-0.43	588.59	-0.28	588.34	-0.03	588.33	-0.02
1809	Survey_Photo_127	Ecoscape	6.57E+05	5.55E+06	588.49	HW Evidence - Fence Debris	588.55	-0.06	588.47	0.02	588.37	0.12	588.49	Dry	588.49	Dry
1810	Survey_Photo_128	Ecoscape	6.57E+05	5.55E+06	588.33	HW Evidence - Rafted Debris	588.03	0.30	587.94	0.39	587.86	0.47	587.45	0.88	588.33	Dry
1811	Survey_Photo_129	Ecoscape	6.57E+05	5.55E+06	587.82	HW Evidence - Fence Debris	588.00	-0.18	587.92	-0.10	587.83	-0.01	587.82	Dry	587.82	Dry
1812	Survey_Photo_130	Ecoscape	6.57E+05	5.55E+06	587.32	HW Evidence - Fence Debris	587.61	-0.29	587.54	-0.22	587.48	-0.15	587.12	0.21	587.32	Dry
1813	Survey_Photo_131	Ecoscape	6.57E+05	5.55E+06	587.75	HW Evidence - Fence Debris	587.96	-0.21	587.89	-0.13	587.81	-0.05	587.40	0.35	587.75	Dry
5326	Survey_Photo_1	Ecoscape	6.57E+05	5.55E+06	589.47	HW Evidence	589.59	-0.12	589.57	-0.10	589.55	-0.08	589.45	0.02	589.40	0.07

Survey Point	Photo_Name	Source	Easting	Northing	Elevation	Code	500 m3/s Run		400 m3/s Run		300 m3/s Run		250 m3/s Run		200 m3/s Run	
							Modelled Elevation	Offset (m)	Modelled Elevation	Offset (m)	Modelled Elevation	Offset (m)	Modelled Elevation	Offset (m)	Modelled Elevation	Offset (m)
						- Fence Debris										
5327	Survey_Photo_2	Ecoscape	6.57E+05	5.55E+06	589.97	HW Evidence - Fence Debris	590.35	-0.38	590.32	-0.35	590.28	-0.31	590.12	-0.15	590.02	-0.05
5328	Survey_Photo_3	Ecoscape	6.57E+05	5.55E+06	590.01	HW Evidence - Fence Debris	590.63	-0.62	590.58	-0.58	590.53	-0.52	590.30	-0.29	590.15	-0.14
5329	Survey_Photo_4	Ecoscape	6.57E+05	5.55E+06	590.90	HW Evidence - Fence Debris	591.32	-0.42	591.27	-0.37	591.22	-0.32	590.98	-0.08	590.86	0.04
5330	Survey_Photo_5	Ecoscape	6.58E+05	5.55E+06	591.55	HW Evidence - Fence Debris	591.74	-0.19	591.69	-0.14	591.64	-0.09	591.41	0.14	591.55	Dry
5331	Survey_Photo_6	Ecoscape	6.58E+05	5.55E+06	591.92	HW Evidence - Fence Debris	591.98	-0.05	591.93	0.00	591.87	0.05	591.64	0.28	591.92	Dry
5332	Survey_Photo_7	Ecoscape	6.58E+05	5.55E+06	592.21	HW Evidence - Fence Debris	592.16	0.05	592.12	0.09	592.09	0.12	591.95	0.26	591.87	0.34
5333	Survey_Photo_8	Ecoscape	6.58E+05	5.55E+06	593.24	HW Evidence - Fence Debris	593.38	-0.14	593.31	-0.07	593.25	0.00	592.93	0.31	592.75	0.50
5334	Survey_Photo_9	Ecoscape	6.58E+05	5.55E+06	593.33	HW Evidence - Fence Debris	593.74	-0.41	593.68	-0.35	593.63	-0.30	593.37	-0.04	593.28	0.04
5335	Survey_Photo_10	Ecoscape	6.58E+05	5.55E+06	594.02	HW Evidence - Fence Debris	594.03	-0.01	593.99	0.03	593.94	0.08	593.67	0.35	594.02	Dry
5336	Survey_Photo_11	Ecoscape	6.58E+05	5.55E+06	594.71	HW Evidence - Fence Debris	594.89	-0.17	594.78	-0.07	594.69	0.03	594.71	Dry	594.71	Dry
5337	Survey_Photo_12	Ecoscape	6.58E+05	5.55E+06	595.04	HW Evidence - Fence Debris	594.97	0.08	594.92	0.12	594.88	0.16	594.74	0.31	595.04	Dry
5338	Survey_Photo_13	Ecoscape	6.58E+05	5.55E+06	594.48	HW Evidence - Fence Debris	594.35	0.13	594.31	0.17	594.27	0.21	594.48	Dry	594.48	Dry
5339	Survey_Photo_14	Ecoscape	6.58E+05	5.55E+06	594.14	HW Evidence - Fence Debris	593.79	0.36	593.77	0.38	593.74	0.41	594.14	Dry	594.14	Dry
5340	Survey_Photo_15	Ecoscape	6.58E+05	5.55E+06	595.89	HW Evidence - Fence Debris	595.88	0.01	595.84	0.05	595.79	0.10	595.52	0.36	595.89	Dry
5341	Survey_Photo_16	Ecoscape	6.58E+05	5.55E+06	595.01	HW Evidence	594.88	0.13	594.86	0.15	594.84	0.17	594.75	0.25	595.01	Dry

Survey Point	Photo_Name	Source	Easting	Northing	Elevation	Code	500 m3/s Run		400 m3/s Run		300 m3/s Run		250 m3/s Run		200 m3/s Run	
							Modelled Elevation	Offset (m)	Modelled Elevation	Offset (m)	Modelled Elevation	Offset (m)	Modelled Elevation	Offset (m)	Modelled Elevation	Offset (m)
						- Fence Debris										
5342	Survey_Photo_17	Ecoscape	6.58E+05	5.55E+06	595.47	HW Evidence - Fence Debris	595.58	-0.11	595.51	-0.04	595.44	0.04	595.13	0.34	594.99	0.49
5343	Survey_Photo_18	Ecoscape	6.58E+05	5.55E+06	595.25	HW Evidence - Fence Debris	595.51	-0.25	595.44	-0.18	595.37	-0.11	595.10	0.15	594.98	0.27
5344	Survey_Photo_19	Ecoscape	6.58E+05	5.55E+06	595.30	HW Evidence - Fence Debris	595.35	-0.05	595.29	0.02	595.22	0.08	595.00	0.30	594.89	0.41
5345	Survey_Photo_20	Ecoscape	6.58E+05	5.55E+06	595.94	HW Evidence - Fence Debris	595.98	-0.04	595.90	0.04	595.83	0.12	595.94	Dry	595.94	Dry
5346	Survey_Photo_21	Ecoscape	6.58E+05	5.55E+06	596.38	HW Evidence - Fence Debris	596.42	-0.05	596.37	0.01	596.31	0.06	596.05	0.32	596.38	Dry
5347	Survey_Photo_22	Ecoscape	6.58E+05	5.55E+06	596.60	HW Evidence - Fence Debris	596.65	-0.05	596.58	0.03	596.50	0.10	596.18	0.42	596.60	Dry
5348	Survey_Photo_23	Ecoscape	6.58E+05	5.55E+06	596.70	HW Evidence - Fence Debris	596.81	-0.12	596.75	-0.05	596.67	0.02	596.70	Dry	596.70	Dry
5349	Survey_Photo_24	Ecoscape	6.58E+05	5.55E+06	597.47	HW Evidence - Sediment Stain	597.42	0.04	597.37	0.10	597.47	Dry	597.47	Dry	597.47	Dry
5350	Survey_Photo_25	Ecoscape	6.58E+05	5.55E+06	596.85	HW Evidence - Sediment Stain	596.86	-0.01	596.82	0.03	596.85	Dry	596.85	Dry	596.85	Dry
5351	Survey_Photo_26	Ecoscape	6.58E+05	5.55E+06	595.72	HW Evidence - Fence Debris	595.81	-0.09	595.73	0.00	595.64	0.08	595.72	Dry	595.72	Dry
5352	Survey_Photo_27	Ecoscape	6.59E+05	5.55E+06	607.91	HW Evidence - Fence Debris	608.11	-0.20	608.03	-0.12	607.97	-0.06	607.91	Dry	607.91	Dry
5353	Survey_Photo_28	Ecoscape	6.59E+05	5.55E+06	603.71	HW Evidence - Fence Debris	604.36	-0.65	604.18	-0.47	604.00	-0.29	603.56	0.15	603.71	Dry
5354	Survey_Photo_29	Ecoscape	6.59E+05	5.55E+06	603.97	HW Evidence - Sediment Stain	604.39	-0.42	604.22	-0.25	604.05	-0.08	603.65	0.32	603.97	Dry
5355	Survey_Photo_30	Ecoscape	6.59E+05	5.55E+06	604.09	HW Evidence -	604.59	-0.50	604.38	-0.29	604.17	-0.08	604.09	Dry	604.09	Dry

Survey Point	Photo_Name	Source	Easting	Northing	Elevation	Code	500 m3/s Run		400 m3/s Run		300 m3/s Run		250 m3/s Run		200 m3/s Run	
							Modelled Elevation	Offset (m)	Modelled Elevation	Offset (m)	Modelled Elevation	Offset (m)	Modelled Elevation	Offset (m)	Modelled Elevation	Offset (m)
						Sediment Stain										
5356	Survey_Photo_31	Ecoscape	6.59E+05	5.55E+06	604.68	HW Evidence - Fence Debris	605.02	-0.34	604.88	-0.19	604.73	-0.05	604.68	Dry	604.68	Dry
5357	Survey_Photo_32	Ecoscape	6.59E+05	5.55E+06	606.97	HW Evidence - Sediment Deposit	606.97	Dry	606.97	Dry	606.97	Dry	606.97	Dry	606.97	Dry
5358	Survey_Photo_33	Ecoscape	6.59E+05	5.55E+06	606.89	HW Evidence - Sediment Deposit	606.89	Dry	606.89	Dry	606.89	Dry	606.89	Dry	606.89	Dry
5359	Survey_Photo_34	Ecoscape	6.59E+05	5.55E+06	604.95	HW Evidence - Sediment Deposit	604.95	Dry	604.95	Dry	604.95	Dry	604.95	Dry	604.95	Dry
5360	Survey_Photo_35	Ecoscape	6.59E+05	5.55E+06	603.88	HW Evidence - Fence Debris	604.36	-0.48	604.20	-0.33	604.04	-0.17	603.88	Dry	603.88	Dry
5361	Survey_Photo_36	Ecoscape	6.59E+05	5.55E+06	603.52	HW Evidence - Sediment Stain	603.99	-0.47	603.81	-0.29	603.56	-0.05	603.52	Dry	603.52	Dry
5362	Survey_Photo_37	Ecoscape	6.59E+05	5.55E+06	603.28	HW Evidence - Fence Debris	603.64	-0.36	603.52	-0.24	603.28	Dry	603.28	Dry	603.28	Dry
5363	Survey_Photo_38	Ecoscape	6.59E+05	5.55E+06	602.65	HW Evidence - Fence Debris	603.00	-0.34	602.77	-0.12	602.56	0.10	602.65	Dry	602.65	Dry
5364	Survey_Photo_39	Ecoscape	6.58E+05	5.55E+06	596.68	HW Evidence - Sediment Stain	597.07	-0.39	596.94	-0.26	596.80	-0.12	596.46	0.22	596.68	Dry
5365	Survey_Photo_40	Ecoscape	6.58E+05	5.55E+06	596.62	HW Evidence - Fence Debris	597.41	-0.79	597.32	-0.70	597.23	-0.60	596.74	-0.12	596.52	0.10
5366	Survey_Photo_41	Ecoscape	6.58E+05	5.55E+06	597.81	HW Evidence - Sediment Deposit	597.99	-0.18	597.81	Dry	597.81	Dry	597.81	Dry	597.81	Dry
5367	Survey_Photo_42	Ecoscape	6.58E+05	5.55E+06	598.49	HW Evidence - Sediment Deposit	599.23	-0.75	599.12	-0.63	598.97	-0.49	598.49	Dry	598.49	Dry
5368	Survey_Photo_43	Ecoscape	6.59E+05	5.55E+06	599.28	HW Evidence -	599.55	-0.26	599.47	-0.19	599.40	-0.11	599.28	Dry	599.28	Dry

Survey Point	Photo_Name	Source	Easting	Northing	Elevation	Code	500 m3/s Run		400 m3/s Run		300 m3/s Run		250 m3/s Run		200 m3/s Run	
							Modelled Elevation	Offset (m)	Modelled Elevation	Offset (m)	Modelled Elevation	Offset (m)	Modelled Elevation	Offset (m)	Modelled Elevation	Offset (m)
						Sediment Deposit										
5369	Survey_Photo_44	Ecoscape	6.58E+05	5.55E+06	600.17	HW Evidence - Sediment Deposit	599.72	0.45	599.70	0.47	599.68	0.49	599.59	0.57	600.17	Dry
5370	Survey_Photo_45	Ecoscape	6.58E+05	5.55E+06	601.86	HW Evidence - Sediment Deposit	602.36	-0.50	602.20	-0.34	602.00	-0.14	601.86	Dry	601.86	Dry
5371	Survey_Photo_46	Ecoscape	6.59E+05	5.55E+06	601.96	HW Evidence - Sediment Deposit	602.38	-0.42	602.26	-0.29	602.12	-0.15	601.96	Dry	601.96	Dry
5372	Survey_Photo_47	Ecoscape	6.59E+05	5.55E+06	602.66	HW Evidence - Sediment Deposit	602.66	Dry	602.66	Dry	602.66	Dry	602.66	Dry	602.66	Dry
5373	Survey_Photo_48	Ecoscape	6.59E+05	5.55E+06	602.64	HW Evidence - Sediment Deposit	603.95	-1.31	603.74	-1.09	603.50	-0.86	602.68	-0.03	602.39	0.26
5374	Survey_Photo_49	Ecoscape	6.59E+05	5.55E+06	603.04	HW Evidence - Sediment Deposit	604.87	-1.83	604.69	-1.65	604.51	-1.46	603.66	-0.62	603.30	-0.25
5375	Survey_Photo_50	Ecoscape	6.59E+05	5.55E+06	604.59	HW Evidence - Sediment Deposit	605.03	-0.44	604.86	-0.27	604.68	-0.09	603.94	0.65	604.59	Dry

DRAWING

THIS BAR MEASURES 100 mm AT FULL SIZE. ALL SCALES REFERENCED TO FULL SIZE.

NOTES:

1. ALL DIMENSIONS ARE IN METRES UNLESS OTHERWISE NOTED.
2. THIS DRAWING MUST BE READ IN CONJUNCTION WITH BGC'S REPORT TITLED "DESIGN FLOOD FOR THE COLDWATER RIVER AT MERRITT", AND DATED MAY 2022.
3. COORDINATE SYSTEM IS NAD 1983 UTM ZONE 10N. VERTICAL DATUM IS CGVD2013.
4. UNLESS BGC AGREES OTHERWISE IN WRITING, THIS DRAWING SHALL NOT BE MODIFIED OR USED FOR ANY PURPOSE OTHER THAN THE PURPOSE FOR WHICH BGC GENERATED IT. BGC SHALL HAVE NO LIABILITY FOR ANY DAMAGES OR LOSS ARISING IN ANY WAY FROM ANY USE OR MODIFICATION OF THIS DOCUMENT NOT AUTHORIZED BY BGC. ANY USE OF OR RELIANCE UPON THIS DOCUMENT OR ITS CONTENT BY THIRD PARTIES SHALL BE AT SUCH THIRD PARTIES' SOLE RISK.

DRAFT

SCALE:	1:10,000
DATE:	MAY 2022
DRAWN:	LL
REVIEW:	KL
APPROVED:	PG

CLIENT: Fraser Basin Council

BGC

PROJECT: Design Flood for the Coldwater River at Merritt

TITLE: Overview of Modelling Results

PROJECT No.: 0407 004

DWG No.: 01

X:\Projects\0704004\GIS\Production\Report\20220414_xxx01_Figure_for_Insert_D_SIZE_V4.mxd Date: Thursday, April 14, 2022 Time: 4:12 PM